From the

Lung Repair and Regeneration Unit from the

Comprehensive Pneumology Center Munich of the

Helmholtz Zentrum München

Director: Prof. Dr. Dr. med. Melanie Königshoff

The role of WNT ligand secretion in idiopathic pulmonary fibrosis

---

Dissertation

zum Erwerb des Doctor of Philosophy (Ph.D.)

an der Medizinischen Fakultät der

Ludwig-Maximilians-Universität München

submitted by

Aina Martin-Medina

from Mallorca, Spain

on

2020

Supervisor: Prof. Dr. Dr. med. Melanie Königshoff

Second evaluator: Prof. Dr. Oliver Eickelberg

Dean: Prof. Dr. med. Reinhard Hickel

Date of oral defense: 08.12.2020

A mi familia…

TABLE OF CONTENTS

LIST OF ABREVIATIONS

A

αSMA	Alpha Smooth Muscle Actin
ACTA2	smooth muscle aortic alpha-actin
ATII	Alveolar Type II
APS	Amonium Peroxodisulfate
AB	Antibody

B

Bleo	Bleomycin
BSA	Bovine Serum Albumin
BALF	Bronchoalveolar Lavage Fluid

C

CCND1	Cyclin D1
CL	Cell Lysates
COL1A1	Colagen 1A1
pBALF	pure Broncheoalveolar Lavage Fluid
CLD	Chronic Lung Disease
COP	Cryptogenic Organizing Pneumonia
COPD	Chronic Obstructive Pulmonary Disease

D

DLCO	Diffusing capaticty of the Lung for Carbon monoxide
DLS	Dynamic Light Scattering
DMEM	Dulbecco's Modified Eagle's Medium
DMSO	Dimethyl Sulfoxide
DTT	Dithiothreitol

E

ECM	Extracelullar Matrix
ER	Endoplasmatic Reticulum
EMT	Epithelial-to-Mesenchymal-Transition
eurIPFreg	European IPF registry
Exo	Exosomes
EV	Extracellular Vesicle
EV-free-SN	EV-free-Supernatant

F

F-12	Nutrient mixture F12 medium
FBS	Fetal Bovine Serum
FCS	Fetal Calf Serum
FN1	Fibronectin 1
FVC	Forced Vital Capacity
Fzd	Frizzled

G

GAPDH	Gliceraldehide-2-phosphat deshidrogenase
GPR177	G Protein-coupled Receptor 177

H

HEPES	N-2-hydroxyethilpiperazine-N-2-ethane sulfonic acid
HP	Hypersensitivity Pneumonitis
HRP	Horseradish Peroxidase

I

IgG	Imnumoglobulin G
ILD	Interstitial Lung Disease
IPF	Idiopathic Pulmonary Fibrosis
IWP2	Inhibitor of Wnt production molecule 2

J

JNK	c-Jun-N-terminal Kinase

K

Kg	kilogram
kDa	Kilodalton

L

LMU	Ludwig-Maximilian-Universität
Lrp	Low-density lipoprotein receptor-related proteins
LFs	Lung Fibroblasts

N

nm	Nanometers
NTA	Nanoparticle Tracking Analysis

M

µl	microliters
mg	miligrams
ml	mililiters
MSC	Mesenchymal Stem Cell
MV	Microvesicle
MVB	Multivesicular Body

P

PBS	Phosphatate Buffered Saline
PCR	Polymerase Chain Reaction
phLFs	primary human Lung Fibroblasts
Porcn	Porcupine

Q

qPCR	quantitative PCR

R

RIPA	Radio-Immunoprecipitation Assay

S

Scr	Scramble
SDS	Sodium Doecyl Sulphate
SDS-PAGE	SDS Polyacryolamide Gel Electrophoresis
siRNA	small interference RNA
SN	Supernatant

T

TBS	Tris-Buffered Saline
TBS-T	TBS with TWEEN®20
TEM	Transmission Electron Microscopy
TGF-β	Transforming Growth Factor Beta
TNFα	Tumor Necrosis Factor Alpha

U

UCSF	University of California San Francisco

W

Wg	Wingless
WISP-1	WNT-Inducible Signaling Protein 1
Wls	Wntless
WNT	Wingless/Integrated

ZUSAMMENFASSUNG

Die idiopathische Lungenfibrose (IPF) ist eine chronische interstitielle Lungenerkrankung mit bisher unbekannter Ätiologie, die durch eine fortschreitende Abnahme der Atemkapazität und einer sehr schlechten Prognose gekennzeichnet ist. Kennzeichenend fuer die IPF ist die wiederholt auftretende epitheliale Zellschädigung, die zu aberranten Aktivität von Entwicklungssignalwegen wie dem WNT-Signalweg und der Aktivierung von Myofibroblasten führen, die infolgedessen vermehrt extrazelluläre Matrixkomponenten sekretieren. Extrazelluläre Vesikel (EVs) sind sekretierte Vesikel, die verschiedene Signalmoleküle wie Proteine, Nukleinsäuren und Lipide über weite Strecken transportieren und so die interzelluläre Kommunikation fördern. Es wurde festgestellt, dass der nicht-kanonische WNT-5A-Ligand in der IPF hochreguliert ist, insbesondere bei Lungenfibroblasten von IPF Patienten im Vergleich zu gesunden Spendern. Vor Kurzem wurde entdeckt, dass WNT-Liganden durch EVs transportiert werden und in der Lage sind, die WNT-Signalübertragung in den Rezeptorzellen zu aktivieren. Die Rolle von EVs und die Sekretion von WNT-Liganden in EVs ist in der IPF jedoch unbekannt. Die vorliegende Arbeit basiert auf der Hypothese, dass die EV-Sekretion in IPF erhöht ist und dass WNT-5A vermehrt in EVs sekretiert wird was zu einem profibrotischen Phänotyp der Lungenfibroblasten beiträgt. Um das EV-Sekretionsprofil in IPF zu charakterisieren und den Beitrag von EV-gebundenem WNT-5A zur Entwicklung und Fortschreiten der Krankheit aufzuklären, wurden EVs aus bronchoalveolarer Lavageflüssigkeit (BALF) von experimenteller Lungenfibrose sowie von IPF , nicht IPF-ILD und nicht ILD sowie Gesunden Proben aus zwei unterschiedlichen Kohorten, isoliert. Die EVs wurden dann durch Transmissionselektronenmikroskopie, Nanopartikel-Tracking-Analyse und Western Blot (WB) charakterisiert. Primäre humane Lungenfibroblasten (phLFs) wurden zur EV-Isolierung verwendet und durch Stoffwechselaktivitätstests, qPCR und WB nach WNT-5A-Funktionsverlust- und WNT-5A-Stimulationsstudien analysiert. Diese Experimente zeigen eine hochregulierte EV-Sekretion in BALF von sowohl experimenteller als auch humaner Lungenfibrose mit einem Anstieg des WNT-Liganden WNT-5A-. Zusätzlich wurde die WNT-5A-Sekretion auf EVs in primären menschlichen Lungenfibroblasten

(phLFs) nach fibrotischer Stimulation durch TGF-β induziert. Darüber hinaus konnten die von phLF sekretierten EVs die Proliferation von phLF fördern, die durch WNT-5A-Inhibierung durch siRNA oder Antikörper Behandlung abgeschwächt wurde. In ähnlicher Weise waren EVs aus IPF-BALF in der Lage, eine PhLF-Proliferation zu induzieren, die vom EV-gebundenen WNT-5A-Liganden abhängig war.

In dieser Doktorarbeit konnte gezeiget werden, dass eine erhöhte Sekretion von EVs im BALF von IPF-Erkrankten die Signalübertragung von WNT-5A vermittelt, die durch Erhöhung der Proliferation von Lungenfibroblasten zur Pathogenese der Erkrankung beiträgt.

Zukünftige Studien zur Sekretion und Zusammensetzung von Evs, sowie deren Rolle bei der Pathogenese der IPF, könnten zu neuen Ansätzen für die Diagnose und Behandlung von Lungenfibrose führen.

SUMMARY

Idiopathic pulmonary fibrosis (IPF) is a lethal interstitial lung disease of yet unknown etiology characterized by a progressive decrease of lung function and poor prognosis. The cellular hallmarks of IPF are repetitive epithelial cell injury that leads to aberrant activity of developmental pathways, such as WNT signaling pathway, and activation of myofibroblasts which secrete extracellular matrix components in excess. Extracellular vesicles (EVs) are secreted membranous particles that transport diverse signaling mediators such as proteins, nucleic acids and lipids, over long distances thus mediating intercellular communication. The Non-canonical ligand WNT-5A is upregulated in IPF, especially in lung fibroblasts from patients in comparison to donors. Recently, it was discovered that WNT ligands are secreted on EVs which can activate WNT signaling in the receptor cells. However, the role of EVs and the secretion of WNT ligands through EVs in IPF remain largely unknown. The present work hypothesizes that EV secretion is increased in IPF and the WNT-ligand WNT-5A is transported on EVs which contributes to profibrotic lung fibroblast function. In order to characterize the EV secretion profile in IPF and elucidate the contribution of EV-bound WNT-5A to the disease, EVs were isolated from bronchoalveolar lavage fluid (BALF) from experimental lung fibrosis as well as from IPF, non IPF-ILD, non-ILD and healthy volunteer samples from two independent cohorts or from primary human lung fibroblasts (phLFs). EVs were then characterized by transmission electron microscopy, nanoparticle tracking analysis and Western Blotting (WB). These experiments reported an upregulated EV secretion in BALF from both experimental and human lung fibrosis samples with an increase in the content of the WNT-ligand WNT-5A. In addition, WNT-5A secretion on EVs was induced in primary human lung fibroblasts (phLFs) upon fibrotic stimulation by TGF-β. For functional studies, phLFs were used for EV stimulation and analysed by metabolic activity assays, qPCR and WB upon WNT-5A loss-of-function and WNT-5A stimulation studies. The phLF-derived EVs were able to promote phLF proliferation, which was attenuated by WNT-5A silencing and antibody-mediated WNT-5A inhibition. Similarly, EVs from IPF-BALF were capable of inducing phLF proliferation which was dependent on the EV-bound WNT-5A ligand. Taken together, this thesis showed that increased secretion of EVs in the IPF lung mediates WNT-5A signaling, which contributes to disease pathogenesis by increasing lung fibroblast proliferation. Future studies of EV secretion and composition, as well as their role in disease pathogenesis may lead to novel approaches for the diagnosis and treatment of pulmonary fibrosis.

1. INTRODUCTION

1.1. Chronic Lung Diseases

Chronic lung disease (CLD) is a broad term describing a variety of persistent lung disorders. CLDs are one of the leading causes of death worldwide (Lozano, Naghavi et al. 2012, Sauleda, Nunez et al. 2018) and include a series of complex lung diseases that are usually caused by genetic and environmental factors that harm the lung epithelium and architecture (Dela Cruz, Kang et al. 2011, Ley and Collard 2013).

CLDs are subclassified as obstructive or restrictive lung disease. In obstructive lung disease (i.e. chronic obstructive lung disease (COPD), asthma, cystic fibrosis), patients suffer from a reduced breath due to a narrowing of the airways that causes deficient exhalation of air from the lungs, whereas in restrictive lung disease (i.e. idiopathic pulmonary fibrosis (IPF), sarcoidosis, tuberculosis), patients are not able to fully fill their lungs due to an increased stiffness of their lung insterstitium (World-Health-Organization 2007).

Currently, there is a lack of treatment for most of the CLDs to reverse their pathology and the therapeutic options to relief their symptoms are very limited (Barnes 2017, Galli, Pandya et al. 2017). Therefore, there is a big need of research to better understand the mechanisms underlying the disease pathology in order to develop more effective therapies.

1.2. Interstitial Lung Disease

Interstitial lung disease (ILD) comprises a large group of lung diseases that share common clinical and pathological features but vary among the etiologies and pathophysiologies (Eickelberg and Selman 2010). ILDs are caused by the inhalation of harmful substances such as cigarette smoke or air pollutants as well as by infectious agents or radiation exposure. All ILDs are associated with high mortality and morbidity rates and affect the interstitium of the lung, therefore concerning the epithelium, endothelium, the perivascular and perilymphatic tissues of the lung and the basal membrane (Antoniou, Margaritopoulos et al. 2014).

1.3. Idiopathic Pulmonary Fibrosis

Idiopathic Pulmonary Fibrosis (IPF) is the most common form of ILD with a yet unknown etiology that carries a high mortality rate with a life expectancy of 2-3 years and an estimated prevalence of 14-63 cases per 100,000 in the United States and 1.25-23.4 per 100,000 in Europe (Nalysnyk, Cid-Ruzafa et al. 2012). IPF is mainly characterized by a progressive and irreversible injury of the lung epithelium that leads to abnormal wound healing (Strieter and Mehrad 2009, Meiners, Eickelberg et al. 2015). The dysfunctional wound repair results in a massive myofibroblast activation and excessive extracellular matrix deposition ultimately causing lung failure and death (White, Lazar et al. 2003, Chambers and Mercer 2015). The risk factors that contribute to disease progression include cigarette smoke, exposure to air pollutants or gastroesophageal reflux and genetical predisposition (Raghu, Collard et al. 2011). The therapeutic options for those patients are nowadays very limited. There are currently two FDA-approved drugs; Nintedanib (Ofev®) and Pirfenidone (Esbrit®), which have a positive effect on disease progression by improving lung function and survival rates (Fisher, Nathan et al. 2017, Fleetwood, McCool et al. 2017, Nathan, Albera et al. 2017). However, the mechanisms of action of these agents are not fully understood and, althought, they might slow the progression, the positive effects are only modest and do not allow to reverse the disease course. Furthermore, these treatments are only recommended for patients with mild-to-moderate IPF leaving the lung transplantation as only option for those patients that suffer from severe lung fibrosis (Raghu 2017). Therefore, it is important the search for new targets to develop future therapies.

1.4. Clinical features of IPF

Patients with IPF commonly present a dry, non-productive cough with dyspnoea that rapidly progresses to decreased lung function (Flaherty and Martinez 2000).

The histopathological features of IFP are classically described by varying degrees of peripheral fibrosis, patchy damaged epithelium, mild inflammation, dysfunctional proliferation of mesenchymal cells, excessive extracellular matrix (ECM) deposition and honeycomb structures underlined by hyperplastic alveolar type II cells (White, Lazar et al. 2003, King, Pardo et al. 2011, Jones, Fabre et al. 2016). Fibroblasts foci are a hallmark in IPF pathology described as abnormal accumulation of fibroblasts (and myofibroblasts) within an ECM highly rich in collagen (Chambers and Mercer 2015, Jones, Fabre et al. 2016).

Besides the disease-specific features, 5-10% of patients with IPF also suffer from acute exacerbations which are additional respiratory difficulties of unknown cause that worsen the dyspnoea in less than 30 days and lead to a drastic drop of lung function and life quality together with a decrease in life expectancy (Johannson, Vittinghoff et al. 2014, Papiris, Kagouridis et al. 2015, Collard, Richeldi et al. 2017, King and Nathan 2017).

1.5. Pathomechanisms of IPF

The continuous inhalation of harmful environmental factors such as cigarette smoke or air pollutants causes repetitive injury of the lung epithelium which leads to (re)activation of developmental pathways, such as WNT (Wingless/Integrated) pathway, and an aberrant wound healing response (Magro, Allen et al. 2003, White, Lazar et al. 2003, Kottmann, Hogan et al. 2009, Strieter and Mehrad 2009, Wolters, Collard et al. 2014). The aberrant response is perpetuated by an impaired epithelial-to-mesenchymal crosstalk that drives, fibroblasts proliferation, epithelial-to-mesenchymal transition (EMT) and myofibroblast activation thus ending in an excessive ECM deposition (Figure 1) (Selman and Pardo 2002, Chapman 2011, Marmai, Sutherland et al. 2011, Chapman 2012). Among the cellular mechanisms implicated in the impaired cellular communication in IPF, fibrogenic factors (e.g. transforming growth factor β [TGF-β]) are known to be upregulated and they usually act through an autocrine and paracrine fashion (White, Lazar et al. 2003, Fernandez and Eickelberg 2012). In addition, aging is a potent risk factor due to a number of hallmarks related to aging that predispose to the disease, such as cellular senescence which is a mechanism of cell cycle arrest that compromises tissue repair therefore contributing to the progression of IPF (Chilosi, Carloni et al. 2013, Spagnolo, Grunewald et al. 2014, Lehmann, Baarsma et al. 2016, Schafer, White et al. 2017). Recent evidence is also pointing to a strong genetic factor including polymorphisms or mutations in genes linked to epithelial injury, host defence, wound healing and cellular repair, which convey susceptibility to IPF (Selman, Pardo et al. 2008, Spagnolo, Grunewald et al. 2014).

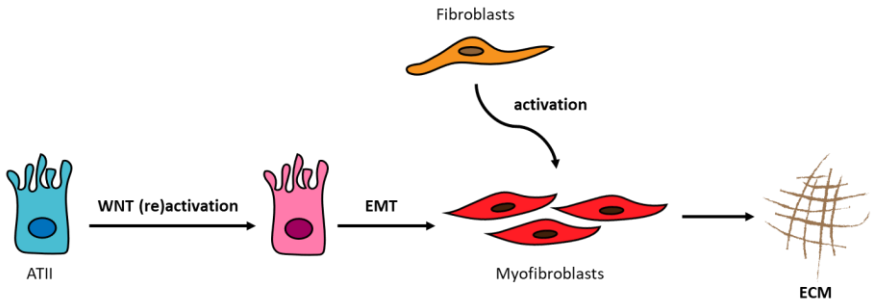

Figure. 1 Pathomechanisms in IPF. Repetitive lung injury leads to (re)activation of developmental pathways such as WNT pathway and drives EMT in epithelial cells and fibroblasts proliferation that differentiate into myofibroblasts and secrete excessive extracellular matrix (ECM) components.

1.5.1. Lung fibroblast plasticity in IPF

Fibroblasts are cells of the connective tissue that possess high plasticity and can gain different phenotypes which are key attributes to response to tissue injury. The phases of tissue repair include coagulation, inflammation, fibroblast proliferation and remodelling/restorin of the normal tissue. Fibroblasts, and their activated phenotype (myofibroblasts), are main players in these repair and regeneration processes in the lung and their main function is to secrete ECM components that provide a tissue scaffold that allow repair events to happen and eventually dissolves restoring the normal tissue architecture (Lorena, Uchio et al. 2002).

During the repair process, secreted factors such as TGF-β, tumor necrosis factor alpha (TNFα) and interleukins (e.g. IL-1), promote an activated fibroblast phenotype called myofibroblasts that first synthetize and secrete ECM components, growth factors and cytokines during the inflammation phase and later promote the contraction of the wound to restore the damaged tissue. Myofibroblasts can be recruited from mesenchymal cells, bone marrow fibrocytes and from epithelial cells through the EMT process (Kuhn and McDonald 1991, White, Lazar et al. 2003, Fernandez and Eickelberg 2012).

In lung fibrosis, the damage is persistent, and the repair process becomes dysregulated when the tissue scaffold is not resolved contributing to a scar formation (Chapman 2011, Chambers and Mercer 2015). In this scenario, proliferation and activation of lung fibroblasts become key ongoing events that facilitate IPF pathogenesis.

1.6. WNT pathway

The WNT pathway is a developmental pathway that regulates both normal developmental and repair processes in the organism. Dysregulation of the WNT pathway and its secreted factors has been reported in CLD such as lung cancer, COPD or IPF (Chilosi, Poletti et al. 2003, Konigshoff, Balsara et al. 2008, Baarsma and Konigshoff 2017). The WNT signalling consists of two different pathways (Figure 2): 1. The canonical, or β-catenin-dependent pathway, and 2. the non-canonical, or β-catenin-independent pathway. In the canonical pathway, the activation of specific membrane receptors named frizzled (Fzd) or low-density lipoprotein receptor-related proteins (Lrp) by canonical WNT ligands (i.e. WNT3A) leads to a phosphorylation cascade that recruits Axin, thereby preventing the constitutive degradation of β-catenin which translocates into the nucleus to regulate the expression of certain genes. The non-canonical pathway is activated by the binding of non-canonical WNT ligands (i.e. WNT-5A) to specific Fzd receptors allowing the downstream activation of c-Jun-N-terminal kinase (JNK)-dependent or Calcium-dependent signaling pathways that are involved in the rearrangement of the cytoskeleton and the organization of the cell polarity during development (Baarsma, Konigshoff et al. 2013).

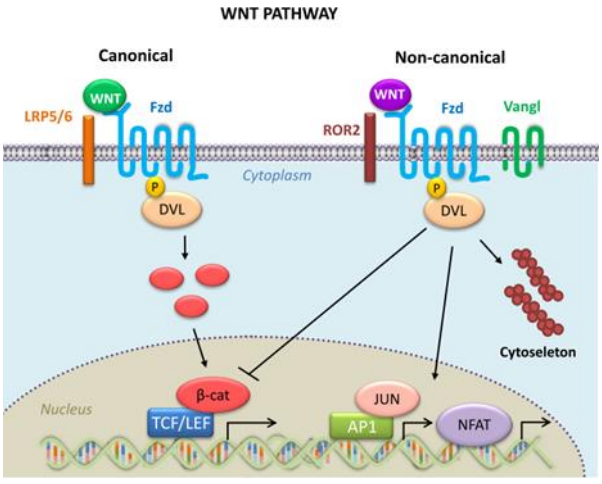

Figure. 2. Schematic representation of the canonical and non-canonical WNT pathway.

1.7. WNT ligand secretory pathway

WNT ligands are essential for the activation of the canonical and non-canonical pathways upon binding to their specific membrane receptors. This WNT ligand family is composed of 19 different secreted glycoproteins that are defined by their aminoacid sequence (Baarsma, Konigshoff et al. 2013). The WNT ligand structure includes an N-terminal sequence for its secretion, several glycosylation sites and a cysteine-rich domain that contributes to ligand folding (Nakatani, Masudo et al. 2002, Mikels and Nusse 2006). The regulation of the WNT ligand secretion is an important step in the activation of WNT signaling.

The first step of the WNT secretory process takes part in the endoplasmatic reticulum (ER) where immature WNT ligands are postranslationally modified by the O-acyl transferase Porcupine (Porcn) (Tanaka, Okabayashi et al. 2000). Palmitoylated WNT ligands are subsequently transferred to the Golgi where they bind to the G protein-coupled receptor 177 (GPR177), also named Evi/Wls (Wntless), that facilitates their secretion (Bartscherer, Pelte et al. 2006). Because of the lipid modifications, WNT ligands are highly hydrophobic, therefore they need additional support to travel through the extracellular matrix (Willert and Nusse 2012). Different, but not mutually exclusive, proposed mechanisms provide a solution to allow lipid-modified WNT proteins to travel in the extracellular space: 1. Short-range interaction between WNT ligands and extracellular carbohydrate chains such as heparan sulfates (Port and Basler 2010), 2. binding to carrier particles that make WNT ligands soluble such as the lipoprotein Lipophorin or the fly lipocalin Swim (Panakova, Sprong et al. 2005), and, 3. packaging into extracellular vesicles (i.e. exosomes) which have recently emerged as potent vehicles that allow WNT ligands to travel long distances (Figure 3) (Gross and Boutros 2013, Routledge and Scholpp 2019).

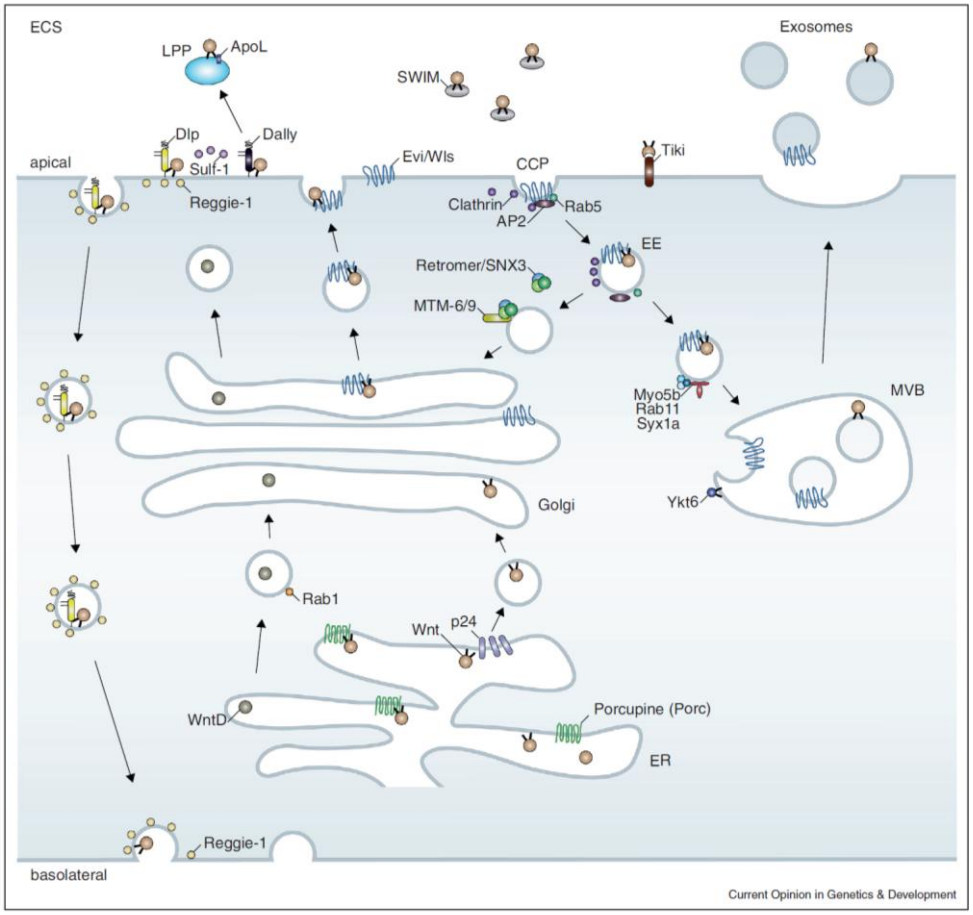

Fig. 3. Schematic representation of the WNT secretory pathway(Gross and Boutros 2013). WNT proteins are first palmitoylated by Porcupine in the endoplasmatic reticle (ER) and then go to the golgi were they bind to the WNT shuttle protein GPR177 (Evi/Wls) that allows their secretion into EVs.

1.8. WNT pathway in IPF

The aberrant activation of wound-healing and developmental pathways is known to contribute to IPF pathogenesis. The (re)activated WNT signaling pathway and upregulation of certain WNT ligands are currently considered as a common signature in IPF (Chilosi, Poletti et al. 2003, Konigshoff, Balsara et al. 2008). Most of the attention has been paid to the canonical/β-catenin WNT pathway which has been found to be upregulated in alveolar type II (ATII) cells from both bleomycin-induced mouse lung fibrosis and patients with IPF (Aumiller, Balsara et al. 2013). The WNT target gene, WNT1-inducible signaling protein-1 (WISP-1) was found to induce proliferation and expression of EMT components in mouse ATII cells (Konigshoff, Kramer et al. 2009, Konigshoff and Eickelberg 2010) and proliferation in mouse and human lung fibroblasts (Klee, Lehmann et al. 2016). Furthermore, WISP-1 neutralization decreased fibrotic burden in bleomycin-treated mice (Konigshoff, Kramer et al. 2009). In addition, the canonical ligand WNT-10A has been found to be upregulated in experimental mouse lung fibrosis and correlated with poor prognosis in IPF patients (Oda, Yatera et al. 2016). The non-canonical WNT pathway, although much less explored, has also been linked to IPF through its ligand WNT-5A. The expression of the non-canonical ligand WNT-5A is upregulated in lung fibroblasts and myofibroblasts from IPF patients (Vuga, Ben-Yehudah et al. 2009, Newman, Sills et al. 2016). In addition, treatment with WNT-5A increased proliferation and induced resistance to apoptosis in normal lung fibroblasts and in lung fibroblasts from IPF patients (Vuga, Ben-Yehudah et al. 2009). This data suggests that there is an important effect of non-canonical WNT signaling in IPF for lung fibroblast expansion in the disease.

1.9. Extracellular Vesicles

Active intercellular communication is required to maintain the homeostasis within the organisms. To facilitate this process, a series of mechanisms, such as extracellular vesicle (EV) secretion, have evolved to safely transport secreted factors from sending to receiving cells.

EVs were first observed 50 years ago as membrane-enclosed vesicles from tumor cells and platelets by P. Wolf who referred to them as "platelet dust" (Wolf 1967). At the beginning, EVs were thought to be released only by simple budding of the cellular plasma membrane, however, in the 80s a more complex secretion pathway for EVs was described. It includes a pre-step where vesicles are formed within a multivesicular body (MVB) which later fuses with the plasma membrane thus releasing the EVs (Harding and Stahl 1983, Pan and Johnstone 1983). A decade later, EVs were found to be biologically active by presenting antigens to induce T-cell response (Raposo, Nijman et al. 1996) and to contain cellular mediators such as RNAs, miRNA, lipids and proteins (Ratajczak, Miekus et al. 2006, Valadi, Ekstrom et al. 2007). Since then, increasing evidence has accumulated towards a potent role of EVs in the cell-to-cell communication. Currently, EVs are defined as highly heterogeneous membranous vesicles that carry specific components depending on the cellular source, state and environment (Colombo, Raposo et al. 2014, Kowal, Tkach et al. 2014, Yanez-Mo, Siljander et al. 2015). Two main groups of EVs have been defined (Figure 4, (Gould and Raposo 2013, Nana-Sinkam, Acunzo et al. 2017): (a) microvesicles (MV) from around 150-2000 nm that are formed by outward budding directly from the plasma membrane, and (b) exosomes from around 30-150 nm that are formed in endosomal compartments (MVBs) which then fuse with the plasma membrane.

The composition of EVs is cell type specific and thus varies depending on the cellular environment. In particular, exosomes carry different proteins, lipids and nucleic acids (DNA, mRNAs and miRNAs) that are sorted and encapsulated during exosome biogenesis (Kowal, Tkach et al. 2014, Hessvik and Llorente 2018). Therefore, EVs play a crucial role in mediating the intercellular communication under physiological as well as pathological conditions. EVs can be found in a large variety of biological fluids, including bronchoalveolar lavage fluid (BALF) which is often used to diagnose lung diseases such as IPF.

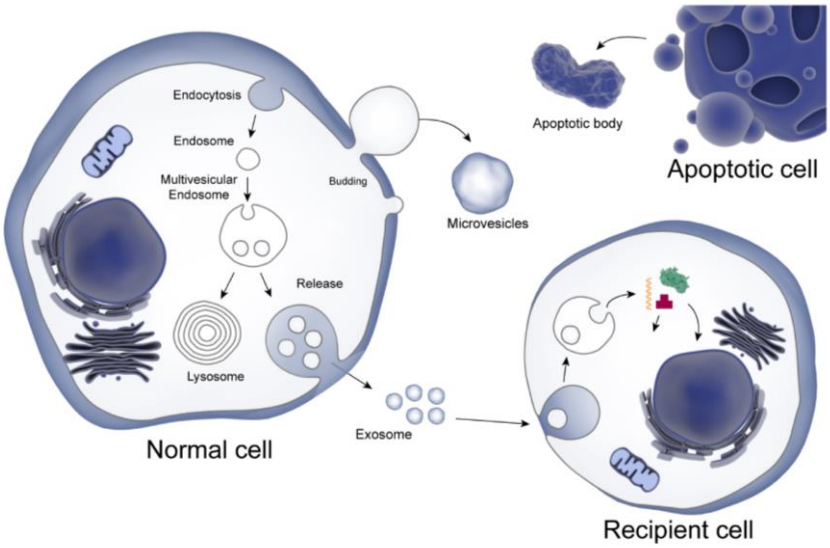

Figure 4. Extracellular vesicle biogenesis (Nana-Sinkam, Acunzo et al. 2017). Microvesicles are larger vesicles that bud out from the membrane whereas exosomes are smaller concave vesicles that are pre-encapsulated in a multivesicular endosome (MVB) which then fuses with the membrane.

1.10. Extracellular vesicles and WNT ligands

WNT ligands are produced and secreted to the extracellular space to drive the activation of the pathway at the neighbouring/distant cells upon binding to their receptors. To travel in the extracellular space, WNT ligands need the assistance of soluble vehicles such as EVs. The first evidence that involved EVs in the WNT ligand secretion was described by Greco et al. who proposed that Wingless (Wg), the Wnt homologue in *Drosophila*, was found in the so called "argosome", vesicles in the wing imaginal discs (Greco, Hannus et al. 2001). Diverse studies found later that Wg/WNT and the WNT shuttle protein GPR177 were in EVs in multiple systems as demonstrated by electron microscopy and proteomics (Korkut and Budnik 2009, Koles, Nunnari et al. 2012, Gross and Boutros 2013). In fact, active WNT ligands were found to localize on the surface of EVs due to their binding with the transmembrane protein GPR177 which allows them to interact directly with the cell membrane receptors (Gross and Boutros 2013). Colocalization of WNT with EV proteins were further observed within and outside of the producing cell, thus highlighting a complex WNT secretory pathway that is connected to EVs and facilitated by GPR177 (Lakkaraju, Mary et al. 2008, Luga, Zhang et al. 2012).

1.11. EVs and chronic lung diseases

Several cell types in the lung, such as fibroblasts, epithelial cells and immune cells, are known to release EVs which are key mediators of intracellular communication (Nana-Sinkam, Acunzo et al. 2017, Kubo 2018). Importantly, the EV secretion in the lung appears to be modified under disease conditions (Figure 5, (Fujita, Kosaka et al. 2015). Circulating EVs were found increased in plasma from patients with chronic obstructive pulmonary disease (COPD) and correlated with worse lung function when compared to ex-smokers (Takahashi, Kobayashi et al. 2012). Cigarette smoke extract stimulation of human lung bronchial epithelial cells induced release of EVs that, in turn, promoted myofibroblast differentiation (Fujita, Araya et al. 2015). In Sarcoidosis and in asthma, EVs from BALF of patients have been suggested to contribute to the inflammatory process (Qazi, Torregrosa Paredes et al. 2010, Torregrosa Paredes, Esser et al. 2012). In addition, the inhibition of EV secretion by the compound GW4869 was reported to ameliorate the disease in the murine asthma model (Kulshreshtha, Ahmad et al. 2013). In lung cancer, EVs have been implicated with malignant processes such as EMT, angiogenesis, metastasis and drug resistance (Janowska-Wieczorek, Wysoczynski et al. 2005, Li, Liu et al. 2016, Rahman, Barger et al. 2016, Deng, Rong et al. 2017). Despite the increasing knowledge of EV involvement in CLDs, there is little known about the EV role in IPF. Currently, there is only one observational study published that found increased miR-21-5p expression in EVs from serum of bleomycin-treated and patients with IPF which correlated with disease progression (Makiguchi, Yamada et al. 2016). In conclusion, several evidences point to an increased profile of EV secretion in CLDs that contribute to specific pathomechanisms, therefore, investigating the EV secretion in IPF could provide new therapeutic targets.

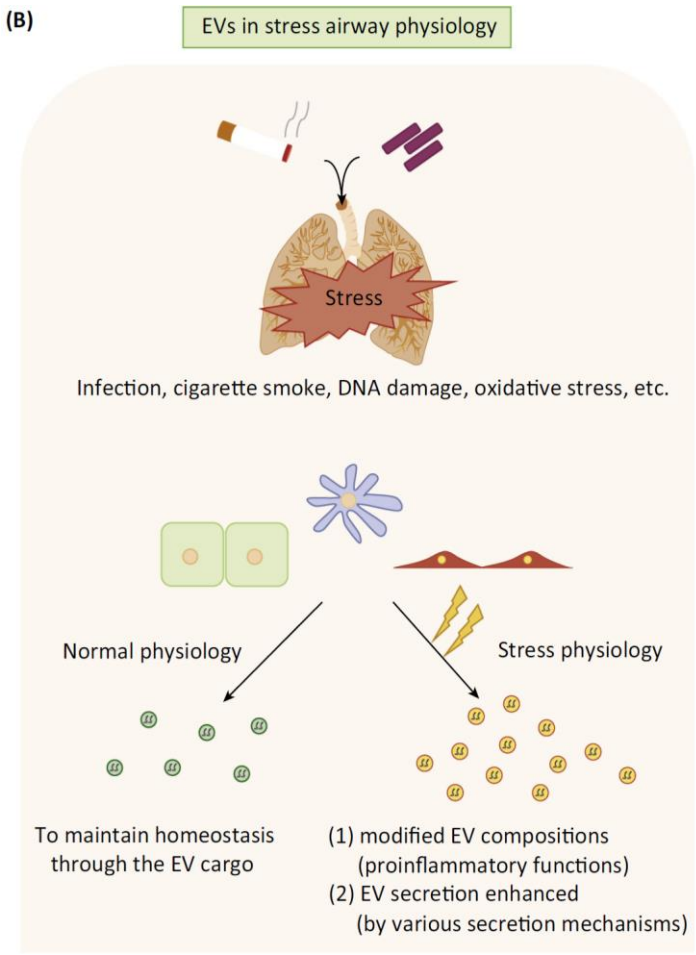

Figure. 5. EVs in stress airway physiology (Fujita, Kosaka et al. 2015). Repetitive damage of the lung epithelium leads to changes in the cell environment that modifies EV secretion and composition therefore compromising the normal cell-to-cell communication.

2. HYPOTHESIS AND OBJECTIVES

Idiopathic pulmonary fibrosis (IPF) is a lethal chronic lung disease of yet unknown etiology and with limited therapeutic options. Current evidence suggests that impaired epithelial to mesenchymal crosstalk is a hallmark of the disease that leads to myofibroblast activation and subsequently deposition of excessive extracellular matrix components (White, Lazar et al. 2003, Fernandez and Eickelberg 2012). Extracellular vesicles (EVs) are potent mediators of cell-to-cell communication under both physiological and disease conditions (Yanez-Mo, Siljander et al. 2015, Nana-Sinkam, Acunzo et al. 2017). Recently, the potential contribution of EVs to diverse chronic lung diseases like asthma, COPD and lung cancer has been investigated (Kubo 2018). However, the expression and role of EVs in the local lung environment in the context of lung fibrosis remains largely unexplored. Aberrant activity of the WNT signaling pathway is known to contribute to the IPF pathogenesis (Chilosi, Poletti et al. 2003, Konigshoff, Balsara et al. 2008) and it has been recently discovered that WNT ligands can be secreted on EVs to mediate intercellular communication (Gross and Boutros 2013). Most of the research has focused on the canonical WNT/β-catenin pathway thus reporting that canonical WNT ligands, like WNT3A, WNT7B and WNT10A, are mostly increased in the lung epithelium in both human and experimental mouse lung fibrosis. The non-canonical WNT pathway, however, is much less studied. Non-canonical WNT-5A ligand has been found upregulated and to promote proliferation in IPF lung fibroblasts (Vuga, Ben-Yehudah et al. 2009), however, its potential involvement in EV-mediated signaling has not been yet investigated. Therefore, this work aimed to test the hypothesis that **increased EVs in IPF carry WNT-5A that contributes to profibrotic lung fibroblast function**.

The present study had the following **objectives**:

1. To characterize the EV secretion profile in bronchoalveolar lavage in both experimental and human pulmonary fibrosis.
2. To investigate the secretion of WNT-5A on EVs in BALF from IPF compared to non-IPF patients (non-IPF-ILD/non-ILD as well as healthy volunteers) in two independent cohorts.
3. To identify the major cellular source of EV-bound WNT-5A using primary human cells (lung fibroblasts vs lung epithelial type II cells).
4. To study the potential effect of EV-bound WNT-5A on lung fibroblast function.

3. MATERIALS AND METHODS

3.1. Materials

3.1.1. Laboratory equipment and software

Table 1. Laboratory equipment

Product	Manufacturer
-80 ^{O}C freezer U570 HEF	New Brunswick; Hamburg, Germany
-20 ^{O}C freezer MediLine LGex	Liebherr; Biberach, Germany
Agarose gel running chamber	Biorad; Hercules, USA
Analytical scale XS20S Dual Range	Mettler Toledo; Gießen, Germany
Autoclave DX-45	Systec; Wettenberg, Germany
Cell culture bench Herasafe KS180	Thermo Fisher Scientific; Schwerte, Germany
Cell Incubator BBD6620	Thermo Fisher Scientific; Darmstadt, GE
Centrifuge MiniSpin plus	Eppendorf; Hamburg, Germany
Centrifuge Rotina 420R	Hettich; Tuttlingen, Germany
ChemiDoc XRS+ Gel imaging system	Biorad; Hessen, USA
Dry ice container Forma 8600 Series	Thermo Fisher Scientific; Darmstadt, GE
Dynamic Light Scattering Zetasizer Ultra	Malvern Panalytical; Malvern, UK
Electronic pipet	Eppendorf; Hamburg, Germany
Electrophoretic Transfer Cell, Mini Protean Tetra	Biorad; Hercules, USA
Fixed-angle rotor T635.5	Thermo Fisher Scientific; Massachusetts, USA
Fixed-angle rotor TFT80.2	Thermo Fisher Scientific; Massachusetts, USA
FlexiVent system	Scireq; Montreal, Canada
Fridge MediLine LKv 3912	Liebherr; Biberach, Germany
Ice device ZBE 110-35	Ziegra; Hannover, Germany
Light Cycler LC480II	Roche Diagnostics; Mannheim, Germany
Liquid nitrogen tank Apollo 200	Cryotherm; Kirchen-Sieg, Germany
Liquid nitrogen tank BioSafe 420SC	Cryotherm; Kirchen-Sieg, Germany
Magnetic stirrer KMO2	IKA; Staufen, Germany
Mastercycler gradient and Nexus	Eppendorf; Hamburg, Germany
Micro-Sprayer Aerosolizer, Model IA-1C	Penn-Century; Philadelphia, USA
Multipette stream	Eppendorf; Hamnurg, Germany
Incubator HERATherm IGS60	Thermo Fisher Scientific; Darmstadt, GE
Sartorius Micro-Dismembrator	Thermo Fisher Scientific; Darmstadt, GE
Nalgene Freezing Container	Omnilab; Munich, Germany
NanoDrop 1000	PeqLab; Erlangen, Germany
Nanosight NS300	Malvern Panalytical; Malvern, UK
Pipettes Research Plus	Eppendorf; Hamburg, Germany
Plate centrifuge 5430	Eppendorf; Hamburg, Germany
Roll mixer VWR	VWR International; Darmstadt, Germany
Scale XS400 2S	Mettler Toledo; Gießen, Germany
Shaker Duomax 1030	Heidolph; Schwabach, Germany
Thermo Scientific Bottle PC Ultra 75mL PK/	Thermo Fisher Scientific; Massachusetts, USA
Thermo Scientific Cap Al Sealing Tube 2mL EA	Thermo Fisher Scientific; Massachusetts, USA
Thermo Scientific Cap Sealing 75mL Ultra Tube	Thermo Fisher Scientific; Massachusetts, USA
Thermo Scientific Tube PA Thinwall 2mL PK/50	Thermo Fisher Scientific; Massachusetts, USA
Transmission Electron Microscope Zeiss Libra	Carl Zeiss NTS GmbH; Oberkochen, Germany
Ultracentrifuge Sorvall WX 80+	Thermo Fisher Scientific; Massachusetts, USA
Ultrapure water supply MilliQ Advantage A10	Merck Millipore; Darmstadt, Germany
Vortex Mixer	IKA; Staufen, Germany
Vacuum pump NO22AN.18	KNF; Freiburg, Germany
Water Barth Aqualine AL12	Lauda; Lauda-Königshofen, Germany

Table 2. Software

Software	Producer
Endnote X6	Thomson Reuters; San Francisco, USA
GaphPad Prism 5	GraphPad Software; La Jolla, USA
Image Lab 6.0	Biorad; Hercules, USA
LightCycler®480 software 1.5	Roche Diagnostics; Mannheim, Germany
WinTEM™ Libra®120	Carl Zeiss NTS GmbH; Oberkochen, Germany
NanoSiht NTA software 3.1	Malvern Panalytical; Malvern, UK
Zetasizer Xplorer software	Malvern Panalytical; Malvern, UK

3.1.2. Chemicals and consumables

Table 3. Chemicals and reagents

Product	Manfacturer
0.2% Trypsin – EDTA solution	Sigma-Aldrich; Taufkirchen, Germany
Ammonium peroxodisulfate (APS)	AppliChem; Darmstadt, Germany
Agarose	Sigma-Aldrich; Taufkirchen, Germany
Bleomycin	Almirall; Barcelona, Spain
Bovine serum albumin (BSA)	Sigma-Aldrich; Taufkirchen, Germany
BrdU cell proliferation kit	Cell Signaling, USA
Complete® Mini without EDTA (Protease-inhibitor)	Roche Diagnostics; Mannheim, Germany
Desoxyribonucleotides mix (dNTPs)	Thermo Fisher Scientific; Schwerte
Dimethyl sulfoxide (DMSO)	Carl Roth; Karlsruhe, Germany
Dithiothreitol (DTT)	AppliChem; Darmstadt, Germany
Exoquick exosome precipitation solution	System Bioscience; California, USA
Exosome-depleted FBS Media Supplement	System Bioscience; California, USA
Ethanol, p.a.	AppliChem; Darmstadt, Germany
Fetal bovine serum (FBS) GOLD, heat inactivated	GE Healthcare; Freiburg, Germany
GeneAMP PCR kit	Life Technologies; Carlsbad, USA
Glucose	AppliChem; Darmstadt, Germany
HEPES	PAA laboratories; Pasching, Austria
I-glutamine	Gibco, Life Technologies; Germany
Isopropanol, p.a.	AppliChem; Darmstadt, Germany
IWP-2 small molecule inhibitor	Sigma-Aldrich; Taufkirchen, Germany
Light Cycler 480 SybrGreen I Master Mix	Roche Diagnostics; Manheim, Germany
Lipofectamine LTX with PLUS reagent	Invitrogen, Life Technologies; Carlsbad
Lipofectamine RNAiMAX	Invitrogen, Life Technologies; Carlsbad
Methanol, p.a.	AppliChem; Darmstadt, Germany
N,N,N',N'-Tetramethylethylenediamine (TEMED)	AppliChem; Darmstadt, Germany
Non-fat dried milk powder	AppliChem; Darmstadt, Germany
Penicillin-Streptomycin (10.000 U/ml)	Gibco, Life Technologies; Carlsbad,
Ponceau S solution	Sigma-Aldrich; Taufkirchen, Germany
Poly-L-lysine (0.01% solution)	Sigma-Aldrich; Taufkirchen, Germany
Random hexamers	Life Technologies; Carlsbad, USA
Recombinant human TGF-β1 protein	R&D Systems; Minneapolis, USA
Recombinant human WNT-5A protein	R&D Systems; Minneapolis, USA
Roti®block Blocking solution	Carl Roth; Darmstadt, Germany
Rotiphorese Gel 30 (37,5:1)	Carl Roth; Darmstadt, Germany
Sodium doecyl sulphate (SDS)	Carl Roth; Darmstadt, Germany
Supersignal West Dura Extended Duration	Pierce, Thermo Fisher Scientific; Germany
Supersignal West Femto Substrate	Pierce, Thermo Fisher Scientific; Germany
Tris base, buffer grade	AppliChem; Darmstad, Germany
Triton X-100	AppliChem; Darmstad, Germany

Tween 20	AppliChem; Darmstad, Germany
Ultrapure DNase/RNase-Free Distilled Water	Invitrogen, Life Technologies; Carlsbad
WST-1 Cell Proliferation reagent	Abcam; Cambridge, UK

Table 4. Consumables

Product	**Manufacturer**
Amicon Ultra 3K-0.5mL centrifugal filters	Merck Milliore; Darmstadt, Germany
Carbon coated copper grids	Agar Scientific; Stansted, UK
CD45 microbeads	Miltenyi Biotec; Teterow, Germany
EpCAM microbeads	Miltenyi Biotec; Teterow, Germany
Cell culture dishes	Corning; Schwerte, Germany
Cell culture flasks	Nunc; Wiesbaden, Germany
Cell culture multi-well plates	TPP Techno Plastic Products, Switzerland
Cell scraper	Corning; Schwerte, Germany
Cryovials 1.5mL	Greiner Bio-One; Frikenhausen, Germany
Falcon tubes (5mL and 50mL)	BD Bioscience, Heidelberg, Germany
Filter tips	Biozym Scientific, Heissisch Oldendorf, GE
Glas Pasteur pipettes	VWR International; Darmstadt, Germany
Measuring sterile pipettes (2mL, 5mL, 10mL, 50mL)	VWR International; Darmstadt, Germany
PCR 96-well plates, white	Biozym Scientific; Hessisch Oldendorf, GE
Reaction tubes (0.5mL, 1.5mL)	Eppendorf; Hamburg, Germany
Whatman blotting paper 3mm	GE Healthcare; Freiburg, Germany

3.1.3. Buffers and solutions

Table 5. Buffers and solutions

Substance	**Concentration**
HEPES (N-2-hydroxyethilpiperazine-N-2-ethane sulfonic acid)	1M
Laemli loading buffer (4x)	
SDS	12% (w/v)
Glycerol (87%)	60% (v/v)
Bromophenol blue	0.06% (w/v)
Tris/HCl, ph 6.8	375 mM
DTT (dithiothreitol)	600 mM
PBS (Phosphatate buffered saline, pH 7.4, 10x)	
NaCl	1.37 M
KCl	27 M
Na_2HPO_4	100mM
KH_2PO_4	20 mM
RIPA (radio-immunoprecipitation assay)	
Tris-Cl, pH 7.4	50 mM
NaCl	150 mM
NP40	1% (v/v)
Na-deoxycholate	0.25% (v/v)
SDS (sodium dodecyl sulphate, 20%)	
SDS	200 g (w/v)
Millipore H_2O	1 L

SDS-PAGE (sodium dodecyl sulfate polyacryolamide gel electrophoresis) Running Buffer	
Tris/HCl, pH 7.4	250 mM
Glycine	1.92 M
SDS	1% (w/v)
SDS-PAGE Separation Gel (10%)	
Millipore H_2O	3.7 mL
1.5 M Tris/HCl pH 8.8	2.25 mL
SDS 20%	45 µL
Acrylamide	3 mL
APS 10%	30 µL
TEMED	6 µL
SDS-PAGE Stacking Gel (4%)	
Millipore H_2O	1.8 mL
0.5 M Tris/HCl pH 6.8	750 µL
SDS 20%	15 µL
Acrylamide	400 µL
APS 10%	15 µL
TEMED	3 µL
TBS (Tris-buffered saline) (10x)	
Tris/HCl pH 7.4	10 mM
NaCl	150 mM
TBS-T (TBS with TWEEN®20) (1x)	
TBS (10x)	10% (v/v)
Tween®20	0.1% (v/v)
Millipore H_2O	89.99% (v/v)
Transfer buffer (10x)	
Tris/HCl	250 mM
Glycine	1.92 M
Transfer buffer (1x)	
Transfer buffer (10x)	10% (v/v)
Methanol	10% (v/v)
Millipore H_2O	80% (v/v)

3.1.4. Standards and kits

Table 6. Standards

Product	Manufacturer
Protein marker V	Peqlab; Erlangen, Germany

Table 7. Kits

Product	Manufacturer
BCA Protein assay kit	Pierce, Thermo Fisher Scientific; Schwerte, Germany
PeqGold RNA kit	Peqlab; Erlangen, Germany
RNase-Free DNase set	Qiagen; Hilden, Germany
RNeasy Mini kit	Cell Signaling; Massachusetts, USA
BrdU cell proliferation kit	

3.1.5. Enzymes

Table 8. Enzymes

Product	Manufacturer
Collagenase I	Biochrom; Berlin, Germany
Dispase	BD Bioscience; Heidelberg, Germany
DNase I	AppliChem; Darmstadt, Germany
RNase inhibitor 20U/µL	Invitrogen, Life Technologies; Carlsbad, USA

3.1.6. SiRNA

The silencing RNAs were dissolved in sterile DNas/RNase-free water to obtain 100 µM stock solutions and stored at -80^{O}C. The siRNA solutions were used at 200 pmol.

Table 9. SiRNA

Product	Manufacturer
Non-silencing control siRNA (SC-37007)	Santa Cruz Biotechnology; California, USA
WNT-5A siRNA (SC-41112)	Santa Cruz Biotechnology; California, USA

3.1.7. Quantitative PCR

The primers for quantitative PCR (Polymerase Chain Reaction) were designed using the platform PrimerBLAST (http://www.ncbi.jlm.nih.gov/tools/primer-blast/). Primers were given an amplicon with a length of 80-150 bp (200 bp maximal).

Table 10. Human primers

Gene	Sequence
HPRT	5´AAGGACCCCACGAAGTGTTG3´ 3´GGCTTTGTATTTTGCTTTTCCA5´
WNT-5A	5´CCAAGGGCTCCTACGAGAGTGC3´ 3´CACATCAGCCAGGTTGTACACCG5´
CCND1	5´CCGAGAAGCTGTGCATCTACAC3´ 5´AGGTTCCACTTGAGCTTGTTCAC3´
FN1	5´GGATGTGTGGCAGATAGGATGTATT3´ 3´CAATGCGGTACATGACCCCT5´
ACTA2	5´CGAGATCTCACTGACTACCTCATGA3´ 3´AGAGCTACATAACACAGTTTCTCCTTGA5´
COL1A1	5'CAAGAGGAAGGCCAAGTCGAG'3 5'TTGTCGCAGACGCAGATCC'3
TNC	5´CCATCTATGGGGTGATCCGG3´ 3´TCGGTAGCCATCCAGGAGAG5´

Table 11. Murine primers

Gene	Sequence
HPRT	5´CCTAAGATGAGCGCAAGTTGAA3´ 5´CCACAGGACTAGAACACCTGCTAA3´
WNT-5A	5´GACTCCGCAGCCCTGCTTTG3´ 5´CCAATGGGCTTCTTCATGGCGAG3´

3.1.8. Antibodies for Western Blot

Primary antibodies were diluted 1:1000 in 10% Roti®block Blocking solution in TBS-T and secondary antibodies were diluted 1:4000 in 5% milk in TBS-T. Directly HRP-conjugated antibodies were diluted 1:50000 (β-actin) or 1:1000 (GAPDH) in 5% milk in TBS-T.

Table 12. Primary antibodies

Antigen	Source	Manufacturer
Calreticulin (2891S)	rabbit	Cell Signaling; Massachusetts, USA
CD81 (DLN-09707)	rabbit	Dianova; Hamburg, Germany
CCND1 (EPR2241)	rabbit	Abcam; Cambrige, UK
GPR177 (sc-13635)	rabbit	Santa Cruz Biotechnology; California, USA
TGS101 (HPA006161)	mouse	Sigma-Aldrich; Taufkirchen, Germany
WNT-5A (MAB645)	rat	R&D systems; Abingdon, UK

Table 13. Secondary antibodies, HRP-linked

Antigen	Source	Manufacturer
Mouse IgG (NA931V)	sheep	GE healthcare; Munich, Germany
Rabbit IgG (NA934V)	donkey	GE healthcare; Munich, Germany
Rat IgG (NA935V)	sheep	GE healthcare; Munich, Germany

Table 14. Directly HRP-conjugated antibodies

Antigen	Source	Manufacturer
β-actin (A3854)	mouse	Sigma-Aldrich; Taufkirchen, Germany
GAPDH (3683)	rabbit	Cell Signaling Technology; Boston, USA

3.1.9. Cell culture media

Primary human lung fibroblasts were cultured in Dulbecco's Modified Eagle's medium/Nutrient mixture F12 medium (DMEM/F-12) from Gibco (Life Technologies, Carlsbad, USA). Primary human ATII cells were cultured in DMEM medium supplemented with 10% fetal calf serum (FCS), 1% penicillin/streptomycin, 2mM I-glutamine (Life Technologies, Carlsbad, USA), 3.6 mg/ml glucose (Applichem, Darmstadt, Germany) and 10 mM HEPES (PAA Laboratories, Pasching, Austria). 3D-lung tissue cultures were cultured in DMEM/F-12 medium supplemented with 1% EV-depleted FCS, 1% penicillin/streptomycin and 2.5% amphotericin B (Sigma Aldrich, St Louis, MO). For starvation medium, DMEM/F12 medium was supplemented with 0.1% FCS and 1% penicillin/streptomycin. For EV-depleted medium, DMEM/F12 medium was supplemented with 1% EV-depleted FCS and 1% penicillin/streptomycin.

3.1.10. Human lung tissue samples

All lung tissue samples were collected from the Giessen site of the European IPF registry (eurIPFreg) and obtained as described in (Zuo, Kohls et al. 2010) by the UGMLC Giessen Biobank (member of the DZL Platform Biobanking, Ethics Approval No. 111/08 and 58/15) and the CPC Bioarchive CPC-M (University Hospital Grosshadern of the Ludwig Maximilian University, Ethics Approval No. 333-10, 455-12). The lung tissue specimens used for western blot were obtained from lung explants of healthy controls or patients with IPF (table 15). The diagnosis of IPF was based on the American Thoracic Society (ATS) criteria (Raghu, Collard et al. 2011, Raghu, Remy-Jardin et al. 2019). The primary human lung fibroblasts (phLFs) and primary human alveolar type II cells used for EV isolations were obtained from non-carcigenic lung cancer resections and explanted lungs.

Table 15. Lung tissue homogenates for western blot

Patient	Number	Mean age (years)	Male gender (%)
Sporadic IPF	13	50 (34-61)	40%
Healthy control	13	54 (42-62)	50%

3.1.11. Patient cohorts for broncheoalveolar lavage fluid (BALF) analysis

Two independent cohorts (Munich and UCSF) were used to obtain bronchoalveolar lavage fluid (BALF). The diagnoses were given in accordance with established criteria (Raghu, Collard et al. 2011, Raghu, Remy-Jardin et al. 2019). For Non-ILD patients, BALF was performed for diagnostic evaluation (unclear cough) and ILD was excluded. The diagnosis of non-IPF ILD and IPF was determined by a pathology core consisting of two pulmonary pathologists, a radiology core consisting of three pulmonary radiologists, and a clinical core consisting of five pulmonary physicians. Informed consent was obtained from every patient. The Munich study was approved by the ethics committee at the LMU (Ludwig-Maximilians Universität München, Germany, Ethics Approval 382-10) and patient characteristics are presented in Table 4.16. The UCSF study cohort was approved by the University of California San Francisco (UCSF) ethics committee (study #12-09662) and patient characteristics are presented in Table 4.17.

Table 16. Patients included in the Munich cohort.

Diagnosis	N	Male gender (%)	Age (years±SD)	FLV (L±SD)	DLCO (% pred ± SD)
Non-ILD*	12	3 (25%)	57.4 ± 14.3	4.9 ± 0.4	77.1 ± 10.7
COP	2	1 (50%)	73 ± 1.5	5.0 ± 0.8	82 ± 11
HP	5	3 (60%)	55.6 ± 5.9	4.2 ± 0.7	43.9 ± 7.16
IPF	16	10 (63%)	68.7 ± 11.0	3.4 ± 0.7	54.3 ± 12.6
All	35	17 (49%)	63.8 ± 12.3	3.8 ± 0.8	60.3 ± 18.5

Footnotes: *control non-ILD group: diagnostic evaluation of unclear cough (n=10), Previous breast cancer metastasis (n=1) and post-transplantation (n=1). All with no signs of ILD. Abbreviations; COP: Cryptogenic organizing pneumonia, HP: Hypersensitivity pneumonitis, FVC: Forced vital capacity, DLCO: diffusing capacity of the lung for carbon monoxide.

Table 17. Patients included in the UCSF cohort.

Diagnosis	N	Male gender (%)	Age (years±SD)	FLV (L±SD)	DLCO (% pred ± SD)
Healthy volunteers	8	4 (50%)	57.5 ± 6.7	4.3 ± 1.0	no data
IPF	9	9 (100%)	71.1 ± 3.3	3.6 ± 1.2	47.9 ± 12.9
All	17	13 (76%)	64.7 ± 8.6	4.0 ± 1.1	-

Footnotes: Abbreviations; FVC: Forced vital capacity, DLCO: diffusing capacity of the lung for carbon monoxide.

3.1.12. Animals

For experimental lung fibrosis, eight to ten weeks old female C57BL/6N mice free of pathogen were purchased from Charles River Laboratories (Sulzfeld, Germany). All animals were kept under governmental and international guidelines including access to water and rodent chow *ad libidum*. The studies performed in mice were approved by the local government for the administrative region of Upper Bavaria (Project 55.2-1-54-2532-88-12). To induce lung fibrosis, mice were instilled intratracheally with 2U of Bleomycin (Almirall, Barcelona, Spain) per kg body weight dissolved in 50 µl of sterile PBS applied as a single dose per animal using the Micro-Sprayer Aerosolizer, Model IA-1C (Penn-Century, Wyndmoor, PA). PBS alone was instilled as control. At day 14 post-instillation, mice were sacrificed for the extraction of BALF and lung lobes.

3.1.13. 3D-Lung Tissue Cultures

The 3D-Lung Tissue Cultures were generated from bleomycin- or PBS-treated mice (day 14 post-instillation) as described in (Lehmann, Korfei et al. 2017) and kept in culture for 72 hours in EV-depleted medium supplemented with 2.5% amphotericin B (Sigma Aldrich, St Louis, MO) for subsequent EVs isolation.

3.2. Methods

3.2.1. Extracellular Vesicle isolation and characterization

3.2.1.1. Isolation of extracellular vesicles (EVs)

Isolation of EVs from murine and human BALF samples, as well as from primary human cell cultures (primary human lung fibroblasts [phLFs] and primary human alveolar type II cells [phATIIs]) were performed for characterization, protein analysis and functionality studies using the state-of-the-art method of ultracentrifugation (Thery, Witwer et al. 2018). First, BALF or cell culture supernatants were centrifugated at 2000 xg for 5 min to remove remaining cells. Cell-free fluids were subsequently subjected to 10.000 xg centrifugation for 30 min and the resulting supernatants were transferred to a new tube and further ultracentrifuged at 100.000 xg for 120 min. The resulting pellets containing EVs were washed in sterile PBS and subjected to a second ultracentrifugation step at 100.000 xg for 120 min. Finally, the EV pellets were resuspended in 30-100 µl of sterile PBS and stored at -80^{O}C until use. For protein characterization of EVs from small sample sizes (such as 3D lung tissue cultures and murine BALF-EVs) the isolations were performed using the precipitation reagent ExoQuick© (Systems Bioscience, California, USA). For that, the reagent was added to the cell-free BALF and culture supernatants at the concentrations indicated by the manufacturer and samples were incubated overnight at 4^{O}C. The next day, EVs were precipitated by centrifugation at 1500 xg for 30 min and the resulting EV pellets were resuspended in 30-100µl of sterile PBS and stored at -80^{O}C until use. All experiments were performed under sterile conditions. All centrifugations were performed at 4^{O}C. The rotors used for ultracentrifugation were fixed-angle T635.5 and TFT80 (both from Thermofisher, Sorvall, Massachusetts, USA).

3.2.1.2. Characterization of EVs

Nanoparticle tracking analysis

Nanoparticle tracking analysis (NTA) by NanoSight NS300 system (Malvern Panalytical, Malvern, UK) was performed to quantify and determine the size and distribution of the particles present in the different EV samples. To that end, EV samples were diluted in 500 µl of sterile PBS and injected through a single syringe into the fluidic chip at a constant flow. The vesicle movements were tracked by a fast video capture for 5 records of 30 sec each and the dedicated software (NTA 3.1, Malvern Panalytical, Malvern, UK) reported a particle concentration and size distribution for each measurement. The values are presented as calculations from 3 (mouse BALF) or 5 (human BALF and phLF) replicates and expressed as number of EVs per ml of initial sample.

Dynamic light scattering

The size distribution of the EVs that were isolated from murine BALF by ExoQuick© was determined using the dynamic light scattering (DLS) system with DLS Zetasizer Ultra (Malvern Panalythical, Malvern, UK). Briefly, EV samples were diluted serially in sterile PBS to fit the range of sensitivity and 70 µl of each preparation was disposed into the cubette. Measurements of the particles in suspension were done in triplicates and the software Zetasizer Xplorer calculated an average particle size and presented the size distribution as a curve for each measurement. The images were obtained by the software WinTEM Libra120.

Transmission electron microscopy (TEM)

Negative staining was used to visualize the EVs by the transmission electron microscope Zeiss Libra 120 Plus (Carl Zeiss, Oberkochen, Germany). Electromicroscopy grids were glow-discharged with carbon at 20mA for 20 seconds prior to sample preparation. Samples containing EVs were first vortexed for 20 seconds and serially diluted to fit the microscope range of sensitivity. Subsequently, 5 µl of each sample was added on a carbon-coated grid followed by a washing step with sterile water for 5 seconds. Then, the grid was incubated with uranyl acetate for 1 minute and washed twice for 5 seconds with sterile water. The grids were dried by blotting from the edge on filter paper and kept for visualization. The images were obtained by the software WinTEM Libra120.

3.2.2. Animal experiments

To induce lung fibrosis, eight to ten old mice were first anasthesized intraperitoneally with 0.2 mg/ml medetomidin (Orion Pharma, Hamburg, Germany), 2.0 mg/ml midazolam (Roche Pharma, Mannheim, Germany) and 0.02 mg/ml fentanyl (Janssen-Cliag, Neuss, Germany) per kg of body weight. Next, 2 Units of bleomycin (Sigma Aldrich, Taufkirchen, Germany) per kg of body weight dissolved in 200 µl saline solution (B. Braun, Melsungen, Germany) was instilled intratracheally as a single dose using a Micro Sprayer (Penn Century; Wyndmoor, USA) via a 20 G INTROCAN cannula. Afterwards, mice were awakened by subcutaneous administration of 0.29 mg/ml atipamezole (Orion Pharma, Hamburg), 0.059 mg/ml flumazenil (Hexal, Holzkirchen, Germany) and 0.14 mg/ml Naloxon (Actavis, Munich, Germany) per kg of body weight. 14 days post-instillation, mice were anasthesized intraperitoneally with 100 mg/ml ketamine and 0.7 mg/ml Rompun (both from Bela Pharm; Vechta, Germany) per kg of body weight. Following the cutting of the Vena cava, the trachea was exposed, and the mice were intubated intratracheally to proceed with 2 times lavage with 500 µl sterile PBS containing Protease inhibitor to collect broncheoalveolar lavage fluid (BALF). BALF was then centrifuged at 500 xg for 5 min and frozen for subsequent EV isolation. The lung was rinsed with 0.9 % saline solution through the right ventricle of the heart and shock-frozen in liquid nitrogen prior to protein isolation. The development of lung fibrosis was confirmed by lung function measurements before BALF collection using the flexiVent system (Scireq, Montreal, Canada) with a tidal volume of 10 ml per kg of body weight at 150 breaths per minute. All surgical instruments were obtained from Fine Science Tools (Heidelberg, Germany) and the cannulas from B. Braun (Melsungen, Germany).

3.2.3. Patient cohorts for broncheoalveolar lavage fluid (BALF) analysis

Bronchoscopy procedure was performed in a single sub-segment of the right middle lobe and 100mL of sterile saline was used to collect BAL fluid (BALF) according to a standardized protocol (Goldstein, Rohatgi et al. 1990). The BALF was kept on ice and then frozen at –80^{O}C until EV isolation.

3.2.4. Cell biology

3.2.4.1. Isolation of primary human lung fibroblasts (phLFs)

Primary human lung fibroblasts (phLFs) were isolated as previously described(Staab-Weijnitz, Fernandez et al. 2015). Human lung tissue was first dissected with a sterile scalpel blade and then digested with 1 mg/ml of collagenase I (Biochrom, Cambridge, UK) for 2h at 37^{O}C. Samples were then filtered through a 70 µm pore nylon filter (BD Falcon, NJ, USA). and centrifuged at 400 xg at 4^{O}C for 5 min. The resulting pellets were resuspended in DMEM/F-12 medium supplemented with 20% FBS and 1 % penicillin/streptomycin and seeded on cell culture dishes. All experiments were performed on phLFs at early passages (passages 2-6), to avoid any effects of replicative senescence in later passages.

3.2.4.2. Isolation of primary human alveolar type II cells (phATII)

Primary human ATII cells (phATII) were isolated as previously described (Konigshoff, Kramer et al. 2009, Mutze, Vierkotten et al. 2015, Ota, Ng-Blichfeldt et al. 2018) with slight modifications. Briefly, human lung tissue was mechanically minced and enzymatically digested using a mix of dispase/collagenase and the cell suspension recovered after filtration through nylon filters 100 µm and 20 µm. Cells were then subjected to a Percoll gradient (Sigma-Aldrich, Taufkirchen, Germany). After collection from the Percoll interphase, red blood cells were lysed (Red blood cell lysis buffer, Sigma, USA) and phATII were sorted by negative selection using a magnetic activated cell sorting-based method using the CD45 marker (human CD45 MicroBeads, Miltenyi, USA). The collected cells were resuspended in Dulbecco's Modified Eagle's medium/Nutrient mixture F12 medium (DMEM/F-12) (Gibco, Carlsbad, Germany) supplemented with 20% FCS (GE Healthcare, Freiburg, Germany) and 1% penicillin/streptomycin and cultured for 48h before being used for experiment.

3.2.4.3. Culturing and cryopreservation of mammalian cells

Culturing of phATII was performed in 10cm dishes with Dulbecco's Modified Eagle's medium/Nutrient mixture F-12 medium (DMEM/F-12) medium supplemented with 10% (v/v) FCS (GE Healthcare, Freiburg, Germany), and 1% (v/v) antibiotics (100 µg/ml streptomycin and 100 U/ml penicillin (Gibco, Carlsbad, Germany). After 2 days of culturing, phATII were washed twice with PBS and cultured for 48 h in extracellular vesicle (EV)-depleted medium. The phLFs were cultured in DMEM/F-12 supplemented with 20% (v/v) FCS and 1% (v/v) antibiotics until 80% confluence and then starved for 24 h in DMEM/F-12 supplemented with 0.1% FCS and 1% antibiotics. Afterwards, cells were kept or treated in EV-depleted medium for 48 h prior to EV isolation. All the EV treatments performed on phLFs were done in EV-depleted medium as well. When passage was lower than 3, phLFs were eventually cryopreserved for future experiments. The cells were first detached by incubation with trypsin/EDTA solution for 5 min at 37^{O}C, followed by resuspension in complete medium and centrifugation at 500 rpm for 5 min. The cell pellets containing approximately 2-3x10^{6} cells/ml were then resuspended in freezing medium (90% complete medium, 10% DMSO) and transferred into cryovials that were frozen at -80^{O}C. The next day, the cryovials were transferred into liquid nitrogen tanks for long-term storage.

3.2.4.4. Generation and culturing of murine 3D-lung tissue cultures (3D-LTCs)

Mouse 3D-LTCs were obtained from healthy and bleomycin-treated mice using the procedure described in (Uhl, Vierkotten et al. 2015). Briefly, once the mice were anaesthetised and intubated, the lungs were flushed via the right ventricle of the heart with PBS and subsequently a syringe pump was used to inject liquid agarose (2% in DMEM/F-12 medium supplemented with 1% streptomycin/penicillin). The trachea was then ligated, and the lung was transferred into a tube with culture medium that was kept on ice, to allow the agarose to solidify. Afterwards, the lobes were cut with a vibratome device (Hyraz V55; Zeiss, Jena, Germany) to a thickness of 300 µm using a speed of 10–12 µm·s–1, a frequency of 80 Hz and an amplitude of 1 mm. The resulting 3D-LTCs were cultivated in DMEM/F-12 medium supplemented with 1% EV-depleted FCS for 48 h before EV isolation from cell culture supernatants.

3.2.4.5. Treatments on EVs

WNT-5A neutralization

WNT-5A was inhibited on EVs using a WNT-5A neutralizing antibody. EV-Pellets isolated from phLFs or BALF from IPF patients were diluted in EV-depleted medium and incubated with 1µg of either αWNT-5A antibody (RND systems: MAB645) or control IgG antibody (RND systems: MAB006) for 30 min before stimulation of phLFs for functional analysis.

Disruption of EV membrane by detergent

EV-Pellets isolated from phLFs or BALF from IPF patients were first incubated with 0.075% triton (diluted in EV-depleted medium) for 30 minutes. Afterwards, mixtures were vortexed for 15 seconds and then used to treat donor phLFs.

3.2.4.6. Cell treatments

All cells were grown to 80% confluence and then starved in starvation medium for 24 h. Afterwards, all treatments were performed in EV-depleted medium.

TGF-β treatments

phLFs were grown in 75 cm^3 flasks, starved for 24 h, and then treated with TGF-β (2ng/ml) or 0.01% BSA as a control for 48 h. Afterwards, 50ml (pool of 5 flasks) of the supernatants from each condition were used for EV isolation.

IWP-2 treatments

phLFs were grown in 75 cm^3 flasks and starved for 24 h. Depletion of WNT ligand secretion was then performed by treatment with 100nM of IWP2 (Sigma-Aldrichs, Taufkirchen, Germany) or DMSO as vehicle control. Treatments were refreshed once after 24 h by adding IWP2 or DMSO to the supernatants. After 48 h, 1ml of the supernatants was collected to confirm WNT-5A depletion, and the remaining volume was subjected to EV isolation.

WNT-5A knock down transfections

phLFs were grown in 75 cm^3 flasks (for EV isolation) or in 6-well plates (for protein analysis) to 80% confluency and transiently transfected with siRNA against WNT-5A (SC-41112; Santa Cruz Biotechnology, California, USA). Transfection was performed on cells using 5 ml per flask or 1 ml per well of serum-free Opti-MEM medium (Life Technologies, Carlsbad, Germany) containing 200 pmol per ml of WNT-5A siRNA or non-silencing control combined with Lipofectamine 2000 transfection reagent (Life Technologies, Carlsbad, Germany). After 6 h, the medium was changed to complete medium and kept O/N. For EV isolations, cells were kept in EV-depleted medium for 48 h. To analyse Cyclin-D1 expression, cells were further starved in starvation medium for 24 h.

EV stimulations for proliferation analysis

Donor phLFs were seeded in a 96-well plate at 5.000 cells per well and put on starvation for 24 h. The protein concentration of the different EV-Pellets was quantified using Pierce™ BCA Protein Assay Kit (Thermofisher Scientific), according to manufacturer´s instructions. EV-Pellets were then diluted at concentrations of 0.01, 0.5 or 1.5 µg protein/ml in EV-depleted medium and used to stimulate the donor phLFs for 48 h. Neutralized WNT-5A EVs or IgG-treated EVs were used at the concentration of 0.5 µg protein/ml. EV-depleted medium alone was used as control. EVs alone or treated with detergent were used at the concentration of 0.5 µg protein/ml and EV-depleted medium with same concentration of detergent without EVs was used as control. Afterwards, proliferation was assessed by cell counting, WST-1 Cell Proliferation Reagent (ab155902, Abcam, Cambridge, UK) and BrdU cell proliferation kit (#6813, Cell Signaling, Massachusetts, USA). For cell counting, cells were detached by incubation with trypsine for 5 min at 37 ^{O}C and then stained with Trypan Blue (Sigma-Aldrich) at 1:1 concentration and counted with a Neubauer chamber. Proliferation assessment by WST-1 or BrdU were performed according to manufacturer's guidelines. For WST-1 assay, 10 µl of WST-1 solution (Abcam, Cambridge, UK) was added to each well and the plate was incubated at 37^{O}C for 2 h, subsequently, the absorbance was read at 460 nm wavelength. For BrdU assay, 10 µl of 10x BrdU solution was added to each well and the plate was then incubated at 37^{O}C for 4 h, the plate was then incubated with fixing/denaturating solution at RT for 30 min followed by incubation with 1X detection antibody solution at RT for 1 h. The plate was then washed 3 times with 1X washing buffer and incubated with 1X HPR-conjugated secondary antibody at RT for 1h. Afterwards, the plate was washed 3 times and absorbance was read at 460 nm wavelength.

EV stimulations for protein analysis

Donor phLFs were seeded in a 12-well plate at 100.000 cells per well and put on starvation for 24 h. Next, protein concentration of the EV-Pellets obtained from phLFs secreted under baseline conditions was quantified by Pierce™ BCA Protein Assay Kit (Biochrom, Berlin, Germany). EV-Pellets were then diluted at 0.5 µg protein/ml in EV-depleted medium and used to stimulate the donor phLFs for 48 h. EV-depleted medium alone was used as control.

3.2.5. Molecular biology

3.2.5.1. RNA analysis

mRNA isolation

The murine lung tissue was first homogenised into a cryotube with a grinding ball using a microdismembrator at 3000 rpm for 30 seconds. The tissue powder was lysed by incubation in 700 µl QIAzol for 15 min at RT and the tubes were agitated again into the microdismembrator. The tubes were then vortexed for 30 seconds and incubated at RT for 5 min. 140 µl of chloroform per 700 µl QIAzol was added to each sample followed by vortex and incubation at RT for 3 min and further centrifugation for 15 min at 12000 xg at RT. The upper aqueous phase was transferred into a column provided by the kit. For the human cell cultures, 600 µl Qiazol was added into each well of a six-well plate and incubated for 2 min at RT. The lysing procedure was facilitated by scratching and the mixture was transferred into a column provided by the kit. From there, total RNA isolation was performed using the PeqGold RNA kit (Peqlab, Erlangen, Germany) according to the manufacturer's guidelines. The concentration of the isolated RNA was quantified spectrophotometrically at 260 nm wavelength (NanoDrop 1000).

cDNA synthesis, Real-time PCR (RT-PCR)

The GeneAMP PCR kit (Applied Biosystems, Carlsbad, USA) was used to obtain cDNA from the isolated RNA. 1 µg of isolated RNA was diluted in RNAse-free water to a final volume of 20 µl. Samples were first denaturated and then complemented with the reagents for the reverse transcription as described in table 4.18. The denaturation and reverse transcription were performed in an Eppendorf Mastercycler according to the settings in table 4.19.

Table 18. Reverse transcription reagents

Reagent	**Stock concentration**	**Volume**	**Final concentration (in 40 µl)**
10x Buffer II	100 mM	4 µl	10 mM
$MgCl_2$	25 mM	8 µl	5 nM
dNTPs	10 mM	2 µl	0.5 nM
Random hexamers	50 mM	2 µl	2.5 µM
RNAse inhibitor	5 µM	1 µl	0.25 U/µl
Reverse transcriptase	5 U/µl	2 µl	2.5 U/µl
H_2O	50 U//µl	1 µl	-
Denat. RNA	50 ng/µl	18 µl	-

Table 19. Settings for RT-PCR

Reaction	temperature	duration
(1) Denaturation	90 ^{O}C	10 min
(2) Annealing	20 ^{O}C	10 min
(3) Reverse transcription	43 ^{O}C	75 min
(4) heat inactivation	99 ^{O}C	5 min

Quantitative PCR (qPCR)

For qPCR, all primers were designed with the platform NCBI PrimerBLAST and tested for efficiency by checking their melting temperatures and the melting curves in the reactions containing serial dilutions of the primers. The primers were diluted in DNAse/RNAse-free water to a concentration of 2.5 µM. The cDNA was mixed with the master mix and primers according to table 4.20. The reactions were performed in duplicates for 45 cycles in a LightCycler 480 (Roche Diagnostics; Mannheim, Germany) with the conditions listed in table 4.21. All target genes were normalized to HPRT.

Table 20. Reaction scheme for qPCR

Reagent	Stock concentration	Volume	Final concentration (in 10 µl)
SybrGreen I Master Mix	2x	5 µl	1x
Primer mix (fw/rv)	10 µM	0.5 µl	0.5 µM
H_2O	-	2 µl	-
cDNA	5 ng/µl	2.5 µl	12.5 ng

Table 21. Settings for qPCR

Reaction	temperature	duration
(1) Denaturation	95 ^{O}C	5 min
(2) Annealing	59 ^{O}C	5 sec
(3) Elongation	72 ^{O}C	20 sec
(4) Melting curve	60-95 ^{O}C	1 min

3.2.6. Protein biochemistry

3.2.6.1. Protein isolation and quantification

For murine and human lung tissue, the specimens were first homogenised into a cryotube containing a grinding ball using a microdismembrator at 3000 rpm for 30 sec. The tissue powder was lysed with 100-500 µl RIPA buffer (supplemented with 1x Roche complete mini protease inhibitor cocktail). Culture plates containing the cells for analysis were kept on ice and 100 µl RIPA buffer was added per well of a 6-well plate. The lysis was facilitated by scratching with a cell lifter and the lysates were transferred to a 1.5 ml tube and incubated on ice for 20 min which was interrupted for vortexing of the sample for several times. Protein extracts were purified by centrifugation at 12000 xg at 4 ^{O}C. The supernatants were transferred to a new tube and protein concentration was determined by BCA assay kit (Biochrom, Berlin, Germany) according to manufacturer's instructions by measuring absorbance at 563 nm wavelength with Tecan Sunrise multiplate reader. Samples were pre-diluted to fit the standard curve and reactions were performed in duplicates.

3.2.6.2. Sodium dodecyl sulphate polyacrylamide gel electrophoresis (SDS-PAGE) and Western blotting

The supernatants and BALF or EV-free samples were concentrated if necessary with Amicon Ultra-0.5 centrifugal filters (Merck Millipore, Amsterdam, The Netherlands) from 500 µl to 50 µl. Reducing conditions (4x Laemmli loading buffer: 150 mM Tris HCl, 275 mM SDS, 400 mM dithiothreitol, 116 3.5% (w/v) glycerol, 0.02% bromophenol blue) were used for the detection of GPR177 and non-reducing (without dithiothreitol) for all other proteins. For murine BALF-EVs, whole EV-Pellet lysates were loaded into the gel, whereas a constant protein amount (10 µg) was used for comparison of EVs obtained from 3D-LTCs, human BALF and phLFs or phATII cell culture supernatants. Samples were loaded into a 10% SDS PAGE gel and proteins were separated at 120 V until the running front reached the end of the gel. Separated proteins were then transferred to a nitrocellulose membrane (Millipore) at 350 mA for 60 min prior to blocking in 1x RotiBlock in TBS-T (Carl Roth, Darmstadt, Germany) for 30 min. Blocked membranes were incubated O/N at 4^{O}C with primary antibodies. Finally, membranes were incubated with HRP-conjugated secondary antibodies for 1 h at RT. The signal was detected by enhanced chemiluminescence reagents (Pierce ECL, Thermo Scientific, Darmstadt Germany) and imaged at ChemiDoc™ XRS+ system (Biorad, Hessen, Germany). B-Actin and GAPDH were used as loading controls for lung

homogenates. Ponceau S staining (Sigma-Aldrich, Taufkirchen, Germany) was used as loading control for samples containing EVs.

3.2.7. Statistical analysis

All data was analyzed with GraphPad Prism 5 software (La Jolla, CA, USA) and is expressed as mean±SD. Student's *t* test was used for comparison between PBS and bleomycin groups, whereas paired Student's *t* test was applied to experiments involving phLFs. For comparison of more than 2 groups, One-way ANOVA was used followed by Dunnett´s or Bonferroni post-hoc test. Normal distribution of the data distribution was determined by Kolmogorov-Smirnov testing with Lilliefors' correction before applying unpaired Student's *t* test.

4. RESULTS

4.1 Extracellular vesicle (EV) characterization in experimental and human IPF

The first aim of this study was to characterize the EV secretion in the context of pulmonary fibrosis. For that, EVs were isolated from bronchoalveolar lavage fluid (BALF) from experimental and human lung fibrosis and controls. In mice, experimental lung fibrosis was induced by intratracheal administration of bleomycin whereas PBS was used as vehicle and BALF was collected after 14 days when the fibrosis was well established. To study the disease in humans, BALF was collected from IPF, non-IPF-ILD and non-ILD patients as well as from healthy volunteers. Isolation of EVs from mouse and human samples were performed as described in figure 6 and the EVs were characterized by size, concentration and protein content. ExoQuick® precipitation reagent was used to isolate EVs from mouse BALF and 3D-lung cell cultures for protein characterization purposes, whereas the state-of-the-art method of serial ultracentrifugation was used to isolate EVs from mouse and human BALF, as well as from primary cell cultures for quantification and functionality experiments.

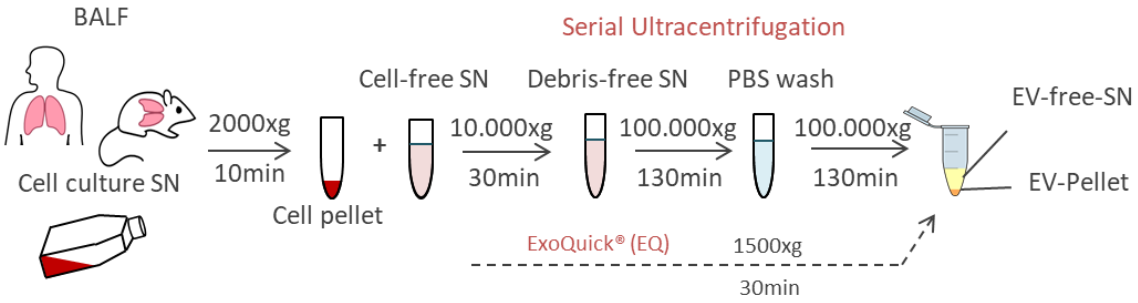

Figure 6. Schematic representation for the protocol used for the isolation of EVs in bronchoalveolar lavage fluid (BALF) and cell culture supernatant (SN). Abbreviations: broncheoalveolar lavage fluid (BALF), supernatant (SN), extracellular vesicle pellet (EV-Pellet), extracellular vesicle-free supernatant (EV-free-SN).

4.1.1. EV secretion is upregulated in experimental lung fibrosis

To study the EV secretion in experimental lung fibrosis, BALF was collected from bleomycin- or PBS (vehicle)-treated mice at day 14. BALF was then subjected to EV isolation by ultracentrifugation for the analysis of EV size and concentration, or by precipitation with ExoQuick® for protein characterization. Morphological assessment of EVs by transmission electron microscopy (TEM) revealed the presence of (i) large amounts of exosomes as smaller concave vesicles between 30 and 200 nm (Fig. 7A for ultracentrifugation and Fig. 7B for ExoQuick®; arrows), and (ii) a smaller fraction of microvesicles as irregular membranous vesicles between 200 and 1000 nm (Fig. 7A for ultracentrifugation and Fig. 7B for ExoQuick®; arrow heads). There were no particles found larger than 1000 nm, indicating no contamination by apoptotic bodies or cell debris in the samples.

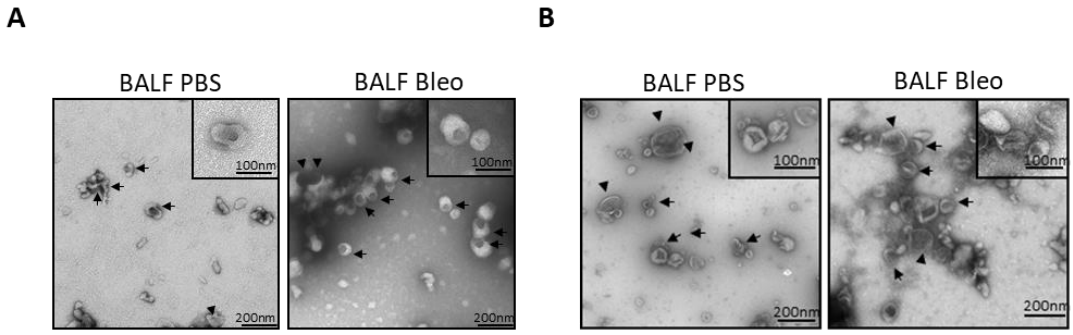

Figure 7. Characterization of EV morphology by transmission electron microscopy (TEM). Representative TEM image of EVs from BALF of mice treated with PBS as vehicle control (BALF PBS) or bleomycin (BALF Bleo) isolated by (A) ultracentrifugation or (B) ExoQuick®. BALF was collected at day 14 post-instillation. Arrows indicate exosomes and arrowheads indicate microvesicles.

Tumor susceptibility gene 101 (TSG101) is an endosomal sorting complex that regulates the sorting of cargos into the multivesicular bodies where the vesicles are formed, therefore it is commonly used to identify EVs (Yoshioka, Konishi et al. 2013). TSG101 was found enriched in the EV-Pellets, demonstrating the purity of the EV isolations (Fig. 8). Furthermore, TSG101 was increased in BALF-EVs from fibrotic lungs compared to BALF-EVs from control (Fig. 8A), suggesting a potential increase in EVs under fibrotic conditions. Of note, significantly increased amount of protein content was found in BALF-EVs from fibrotic compared to healthy mice (Fig. 8B, EV total µg protein/mL: PBS 51.3±25.32, Bleo 266.2±114.8, P=0.0001).

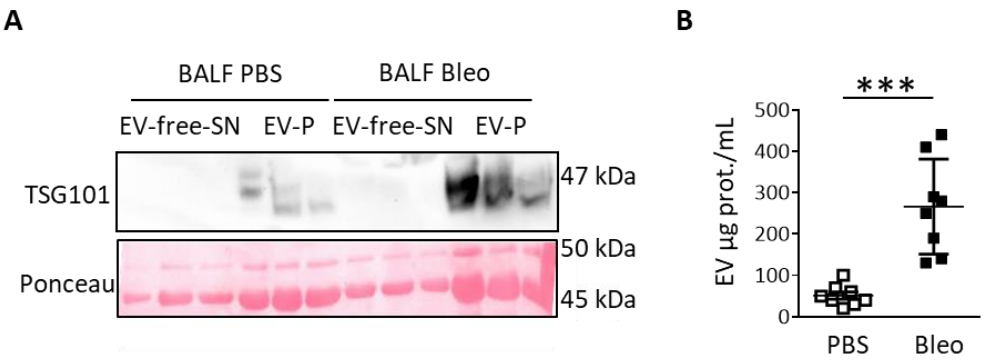

Figure 8. Increase of EV-associated proteins in BALF from bleomycin-treated mice. (A) Analysis of the expression of the EV-enriched protein TSG101 in EV-free-supernatants (EV-free-SN) and EV-Pellets (EV-P) from BALF from PBS- and bleomycin-treated mice. EVs were isolated by ExoQuick®. Pool of 2 mouse BALFs per n; n=3 per group. (B) Total protein quantification in BALF-EVs from PBS- and bleomycin-treated mice (n=8 per group). EVs were isolated by ultracentrifugation. Student's *t*-test; *p<0.05, ***p<0.001.

To obtain an accurate comparison of BALF-EVs between PBS- and bleomycin-treated mice, the EV numbers and size distribution were determined by nanoparticle tracking analysis (NTA); an accurate technique that records the Brownian motion of the individual vesicles (Fig. 9, left panel). An increased number of EVs, in particular exosomes, was found in the BALF from fibrotic mouse lungs compared to controls indicating a change in number and size distribution of EVs upon fibrosis development (Fig. 9, middle panel). Moreover, the number of exosomes was significantly higher in the fibrotic BALF when compared to control (Fig. 9, right panel, exosome particles/ml: PBS $1.93x10^8 \pm 6x10^6$, Bleo $4.3x10^8 \pm 1.9x10^8$, P=0.049). Taken together, these results demonstrate that EV secretion is increased in BALF in experimental lung fibrosis.

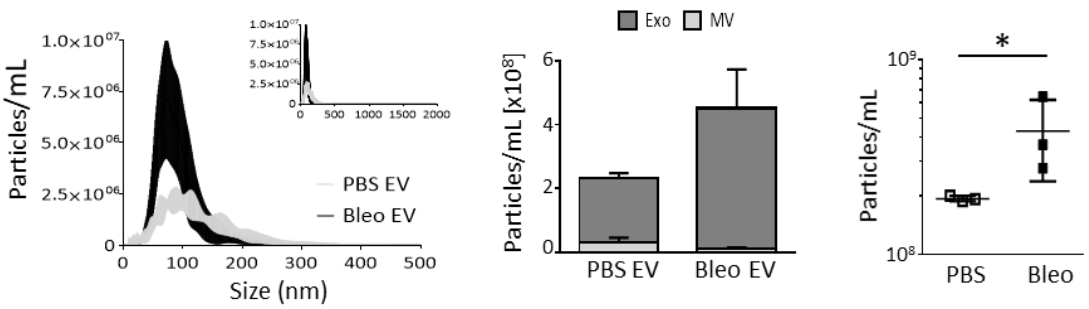

Figure 9. EV concentration is increased in BALF from bleomycin-treated mice. (Left) Histogram showing the results of nanoparticle tracking analysis (NTA) performed on same samples as in Fig. 5.2 (measurements in triplicates; n=3 per group). (Middle) graph of the vesicles grouped in exosomes (Exo; 30-200nm) or microvesicles (MV; 200-1000nm). (Right) statistics for the exosome fraction. Data is represented as particles/mL of EV fraction.

4.1.2. EV secretion is upregulated in IPF patients

To further investigate if EVs are also increased in the human disease, the presence of EVs was explored in human BALF. Two independent cohorts were studied: (i) non-ILD, non-IPF ILD and IPF patients (Table 1, Munich Cohort,) and (ii) IPF patients and healthy volunteers (Table 2, UCSF cohort). The isolated EVs were first characterized by morphology and protein expression. TEM images showed intact EVs and, similar to mouse BALF-EVs, a higher fraction of exosomes was found towards a smaller fraction of microvesicles (Fig. 10A exosomes; arrows, microvesicles; arrowheads). The purity of BALF-EVs was further validated by the expression of the EV-enriched protein TSG101, and the absence of Calreticulin (an ER marker which is absent in EVs) (Fig. 10B).

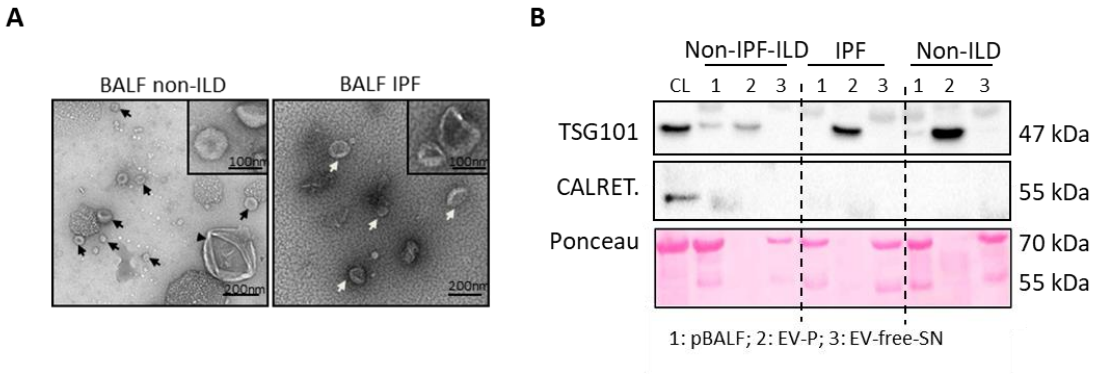

Figure 10. Characterization of EVs from human BALF. (A) Representative transmission electron microscopy images of EVs isolated from BALF from non-ILD or IPF patients. (B) Protein analysis of the ER-marker Calreticulin and the EV-enriched protein TSG101 in cell lysates (CL), pure BALF (pBALF), EV-Pellets (EV-P) and EV-free-BALF-supernatants (EV-free-SN) of human BALF sample from patients with non-IPF ILD, IPF or non-ILD. EVs were isolated by ultracentrifugation. Ponceau S staining was used as loading confirmation.

When investigating the EV-Pellets from the Munich cohort, a significant upregulation of EV protein content was observed in BALF from IPF patients compared to non-ILD/non-IPF-ILD (Fig. 11, EV total µg protein/mL: non-ILD/non-IPF-ILD (n=12/7) 251.6±166.6, IPF (n=16) 552.3±427.3, P=0.0212), indicating an increased EV secretion in the BALF from IPF

NTA was then performed on BALF-EVs to precisely quantify the number of particles. A significant increase in EVs, mainly attributed to exosomes (Fig. 12 left and middle panel), was found in BALF from IPF patients in comparison to non-ILD/non-IPF-ILD (Fig. 12, right panel, particles/mL of initial sample: non-ILD (n=7) $2.2x10^8±1.8x10^8$, non-IPF-ILD (n=6) $3.3x10^8±2.5x10^8$, and IPF (n=4) $6.0x10^8±3.8x10^8$; non-ILD *vs*. IPF, P=0.0438; and for combined non-IPF groups *vs*. IPF, P=0.0387).

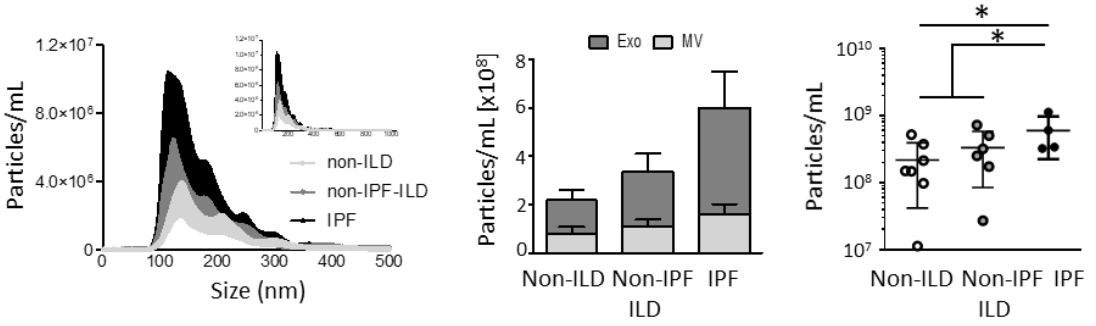

Figure 12. EV concentration is increased in BALF from IPF patients compared to non-IPF. Total protein quantification in EV-pellets isolated from BALF from non-ILD/non-IPF-ILD (n=12/7) and IPF (n=16) patients. EVs were isolated by ultracentrifugation.

Importantly, the increase of EVs in IPF was confirmed in a second independent cohort of IPF patients and healthy volunteers, although this analysis did not reach statistical significance (Fig. 13A, particles/mL of initial sample: healthy (n=8) $5.7x10^7±2.5x10^7$, IPF (n=9) $3.0x10^8±3.4x10^8$, P=0.0633). Further analysis of this cohort indicated that EV numbers negatively correlate with lung function (Fig. 13B), suggesting that increased EVs correlate with increased disease severity.

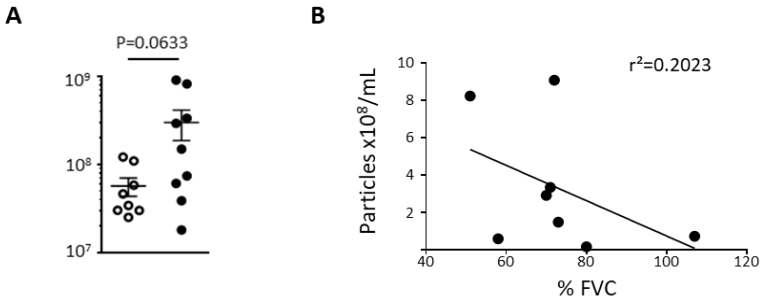

Figure 13. EV concentration correlates with lung function in IPF patients compared to healthy. Quantification of EVs isolated from BALF of healthy volunteers or patients with IPF from a second cohort of patients (Table 2). Data is represented as particle/mL related to initial sample. All EVs were isolated by ultracentrifugation. Student's *t*-test; *p<0.05, ***p<0.001. (B) Correlation of lung function parameter (%FVC) with EV amount isolated from BALF of patients with IPF (UCSF Cohort, Fig 5.6). Dots represent single patient values; correlation coefficient is indicated.

Notably, when combining both cohorts, EVs were significantly increased in IPF compared to non-IPF (Fig. 14 for combined analysis, P=0.0428), suggesting an enhanced EV secretion in human IPF. Altogether, these results strongly support the notion of enhanced secretion of EVs into the BALF, in both experimental lung fibrosis and human IPF.

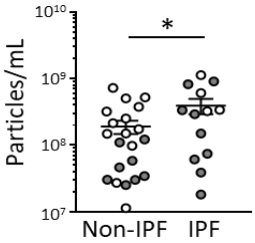

Figure 14. EV concentration is upregulated in IPF compared to non-IPF. Comparison of EV amount secreted in BALF from non-IPF and IPF patients. Quantification by nanoparticle tracking analysis of EV amount in BALF from non-IPF (n=21) and IPF (n=13) patients. The data of 2 different cohorts was combined (white; Munich cohort, grey; UCSF cohort). Measurements were done in 5 replicates. Unpaired Student's *t* test, *P<0.05.

4.2. EV-bound WNT-5A is upregulated in IPF

EVs exert their function by transporting a variety of mediators, including WNT proteins (Gross and Boutros 2013) which are known to be upregulated in IPF (Konigshoff, Balsara et al. 2008, Burgy and Konigshoff 2018). The protein WNT-5A, which is a major player in the non-canonical WNT pathway, has been linked to lung fibroblast proliferation which is a

main hallmark of IPF (Vuga, Ben-Yehudah et al. 2009). Therefore, the secretion of WNT ligands, specifically WNT-5A, through EVs was next studied in the context of lung fibrosis.

4.2.1. WNT-5A is increased in fibrotic lung tissue

First, the expression of WNT-5A was analysed in lung homogenates in both experimental and human lung fibrosis. Significant upregulation of WNT-5A was observed in lung homogenates from bleomycin- compared to PBS-treated mice at both mRNA and protein levels (Fig. 15A and 15B respectively) and upregulated WNT-5A protein was also found in lung homogenates from IPF compared to donor tissue specimens (Fig. 15C).

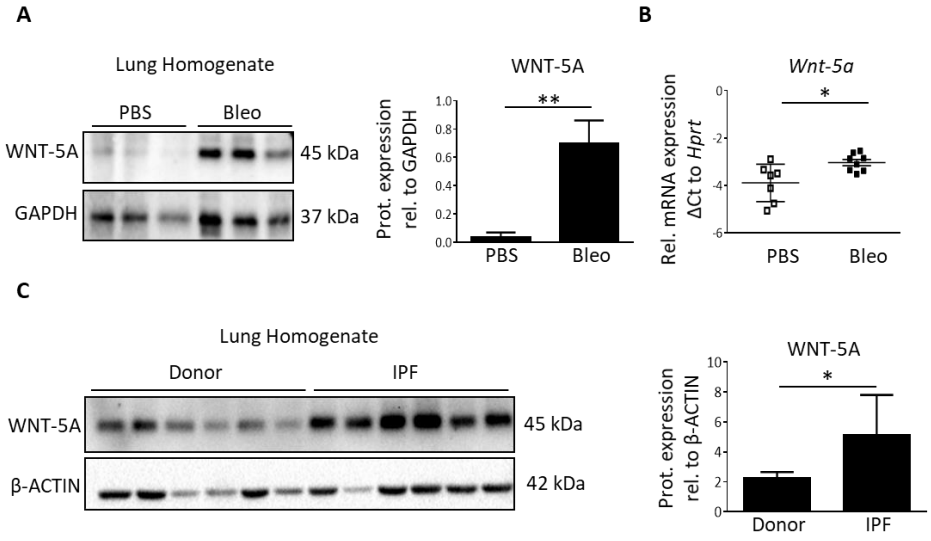

Figure 15. WNT-5A is upregulated in lung homogenates from experimental and human lung fibrosis. (A-B) Expression of WNT-5A (A) protein and (B) mRNA level in lung homogenates from PBS- or bleomycin-treated mice (n=3-8 mice per group). (C) Protein analysis of WNT-5A expression in lung homogenates from donors and IPF patients and subsequent densitometry analysis (n=6 per group).

4.2.2. The WNT shuttle protein GPR177 is upregulated in IPF

The WNT shuttle protein G protein-coupled receptor 177 (GPR177) is a key component of the WNT secretory pathway and is necessary for the shuttling of WNT ligands to the cellular membrane and the anchoring to EVs (Koles, Nunnari et al. 2012). To study whether the machinery required for the secretion of WNT ligands on EVs is increased in lung fibrosis,

the expression of GPR177 was investigated in lung homogenates from bleomycin-treated mice compared to PBS-treated controls. GPR177 was significantly increased in the fibrotic tissue at protein levels (Fig. 16A). Notably, the secretion of GPR177 was also found increased in BALF from bleomycin-treated mice (Fig. 16B). Upregulation of GPR177 was further confirmed in lung homogenates from IPF patients compared to donors (Fig. 16C, GPR177 protein: donors 0.35±0.25, IPF 0.48±0.16, P=0.0262). These results suggest that WNT ligand secretion through EVs is upregulated in lung fibrosis.

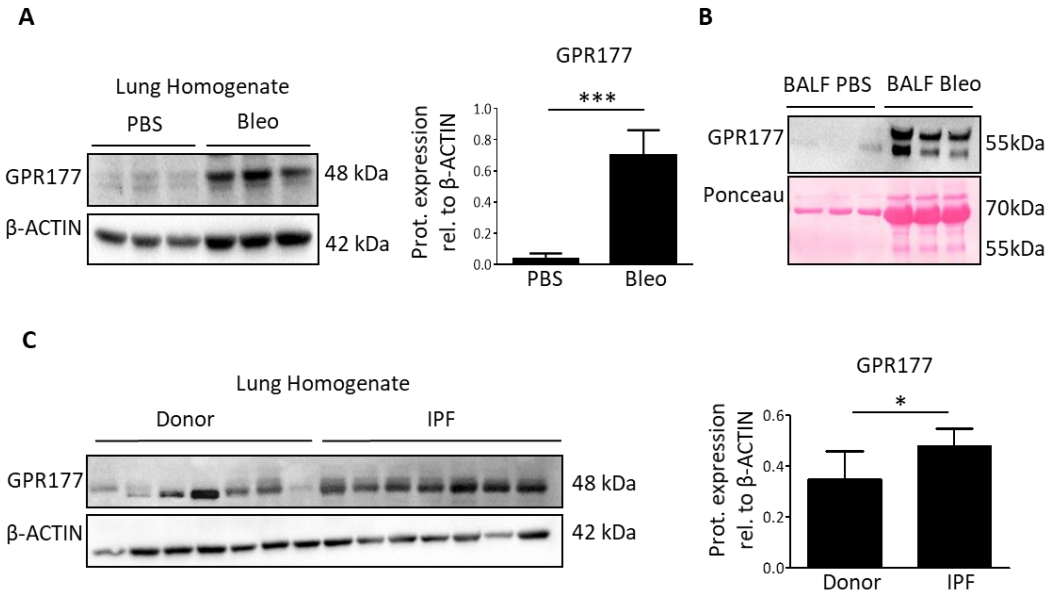

Figure 16. The WNT shuttle protein GPR177 is upregulated in experimental and human lung fibrosis. (A-B) Expression of the WNT shuttle protein GPR177 in (A) lung homogenates and (B) BALF from PBS- or bleomycin-treated mice (n=3 per group). Ponceau S staining was used as loading confirmation. (C) Protein expression of GPR177 in lung homogenates from donors (n=7) and IPF (n=7) patients and subsequent densitometry. Student´s *t* test was used in all statistics; *p<0.05, **p<0.01, ***p<0.001.

4.2.2. EVs transport increased WNT-5A in experimental lung fibrosis

As WNT-5A has been linked to IPF, its secretion on EVs was studied next. For that, the expression of WNT-5A was analysed in EVs and EV-free supernatants. WNT-5A was found in the EV fraction particularly enriched in EVs from BALF of fibrotic mouse lungs compared to controls (Fig. 17).

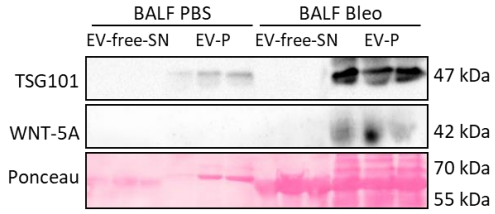

Figure 17. WNT-5A is enriched in EVs from BALF of bleomycin-treated mice. Analysis of TSG101 and WNT-5A in whole EV-Pellets from BALF (n=3 per group) from PBS- and bleomycin-treated mice by ExoQuick® (n=4 per group).

In addition, the EV-bound secretion of WNT-5A was also studied in supernatants of 3D-lung tissue cultures (3D-LTCs), which closely represent the *in vivo* lung microenvironment and allow the analysis of EVs including those from distal areas of the lung, in contrast to BALF which may be restricted to more proximal regions. Importantly, WNT-5A was highly enriched in EVs from fibrotic 3D-LTCs compared to controls, indicating that these EVs carry WNT-5A under fibrotic conditions and can originate from distal areas of lung tissue (Fig. 18, WNT-5A expression relative to TSG101: PBS 0.3±0.4, Bleo 3.7±0.9, p=0.0011). These results strongly indicate that increased WNT-5A is predominantly transported by EVs in experimental and human lung fibrosis.

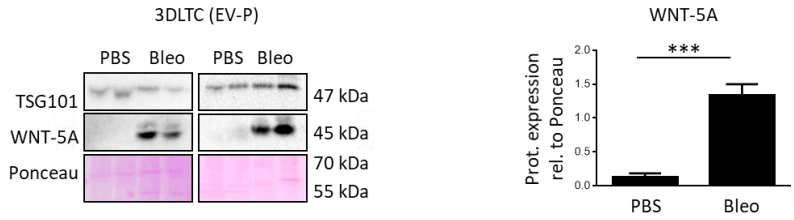

Figure 18. WNT-5A is enriched in EVs from fibrotic 3D-lung tissue cultures. Analysis of TSG101 and WNT-5A in EV-Pellets from 3D-lung slices culture supernatants derived from PBS- and bleomycin-treated mice by ExoQuick® (n=4 per group). Equal amount of EV pellets was loaded (10ug). Densitometry analysis of WNT-5A expression relative to Ponceau (right panel), Student's *t* test.

4.2.3. EV-bound WNT-5A is increased in BALF from IPF patients

To elucidate the potential clinical relevance of EV-mediated WNT-5A signaling in IPF, the expression of WNT-5A was studied in EVs isolated from BALF of non-ILD, non-IPF-ILD, or IPF patients. For that, WNT-5A was analysed along with the EV-enriched proteins TSG101 and CD81, the latter being a tetraspanin involved in EV biogenesis (Andreu and Yanez-Mo

2014). Increased levels of WNT-5A were found in EVs from IPF patients when compared to non-IPF EVs (Fig. 19, WNT-5A expression: non-IPF (n=5) 24.98±9.51, IPF (n=7) 72.09±43.56, P=0.0408).

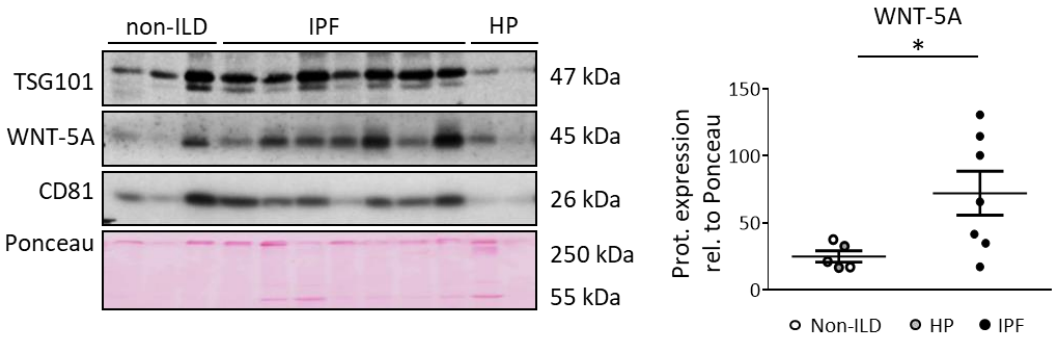

Figure 19. EVs from BALF of IPF patients are enriched in WNT-5A. Protein analysis of EV-enriched proteins TSG101 and CD81, as well as WNT-5A in EV-P isolated by ultracentrifugation in BALF from non-ILD (n=3), IPF (n=7) and Hypersensitivity Pneumonitis (HP) (n=2), and corresponding densitometry of WNT-5A relative to Ponceau, Student's *t* test. Ponceau S staining was used for loading confirmation. *p<0.05.

The protein CD81 has been described as one of the most expressed surface markers in myofibroblasts (Akamatsu, Arai et al. 2013) and a marker of a specific EV subpopulation which is characterized by a specific protein composition as analysed by proteomics (Kowal, Arras et al. 2016). Of note, WNT-5A correlated with CD81 (Fig. 20A, r^2=0.4586, P=0.0156), as well as TSG101 (Fig. 20B, r^2=0.3762, P=0.0339). Collectively, these results suggest that WNT-5A expression is increased in EVs in IPF and that EV-bound WNT-5A has a potential role in intercellular communication during fibrogenesis.

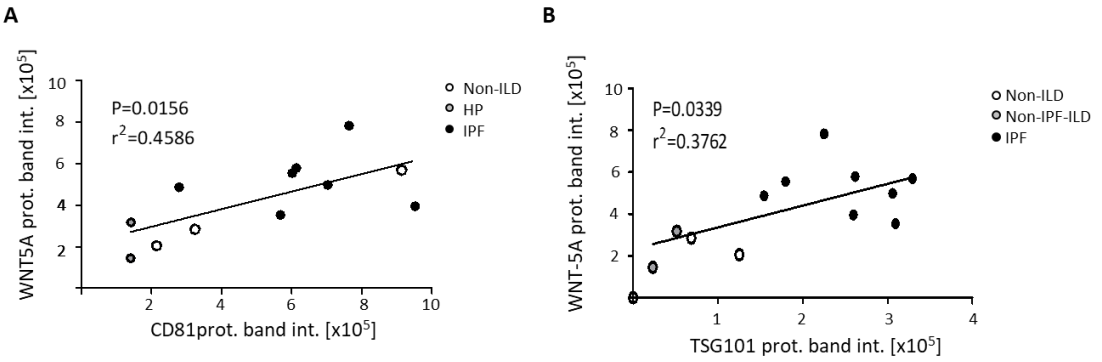

Figure 20. WNT-5A expression in BALF-EVs correlates with the EV-enriched markers CD81 and TSG101. (A) Correlation between WNT-5A and CD81 expression. (B) Correlation between WNT-5A and TSG101 expression Dots represent single values, linear regression test.

4.3. Lung fibroblasts are a source of EV-bound WNT-5A

The next aim was to find which cell type might be the source of WNT-5A secretion through EVs. WNT-5A has recently been found to be upregulated in lung fibroblasts in chronic lung disease (Baarsma and Konigshoff 2017), therefore highlighting fibroblasts as one source of EV-associated WNT-5A in IPF. To analyse if fibroblasts are indeed a major source of WNT5A secretion in the lung, EVs were isolated from cell culture supernatants from primary human lung fibroblasts (phLFs) and from alveolar epithelial type II (phATII) cells in comparison. EVs isolated from cell culture supernatants from both cell types showed the typical EV morphology and size (Fig. 21A). Notably, WNT-5A was found highly enriched in EVs from phLFs whereas it was almost undetectable in phATII cells (Fig. 21B), thus suggesting that phLFs are a major source of WNT-5A secretion via EVs in the lung.

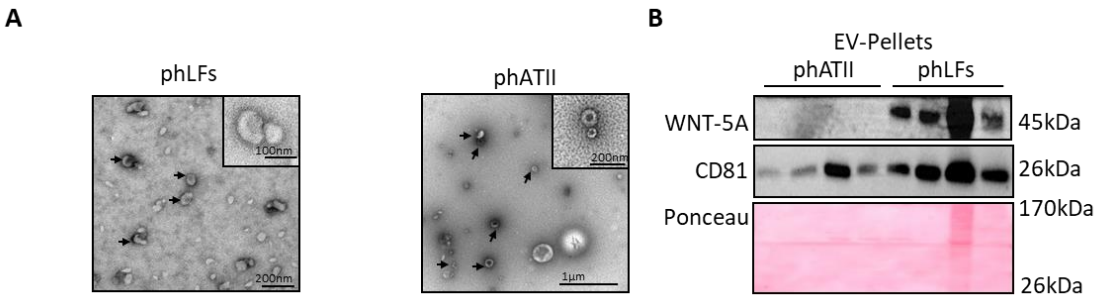

Figure 21. Lung fibroblasts are a major source of EV-bound WNT-5A. (A) Representative transmission electron microscopy images of EVs isolated from primary human lung fibroblasts (phLFBs) and primary human epithelial type II (phATII) cell culture supernatants. (B) Comparison of the EV-enriched proteins TSG101 and CD81, as well as WNT-5A, in equally loaded EV Pellets isolated from phLFBs or phATII cell culture supernatants. Ponceau S staining was used as loading control.

4.4. EVs induce lung fibroblast proliferation

Lung fibroblast proliferation has been linked to lung fibrosis (Vuga, Ben-Yehudah et al. 2009, Baarsma and Konigshoff 2017). To address the potential functional implications of EVs in IPF, EVs were collected from phLFs supernatant and used to treat phLFs in an autocrine fashion to analyse the proliferative effect.

4.4.1. Lung fibroblast-derived EVs induce proliferation in an autocrine manner

phLFs were stimulated with EVs from the same line at increasing concentrations to measure the proliferative response. Upon EV treatment, phLFs exhibited a significant increase in their metabolic activity compared to phLFs treated with EV-free-medium only (Fig. 22A, % increase in metabolic activity to control: 0.01µg EVs 19.7±10.4, P=0.0064, 0.5µg EVs 17.6±12.45, P=0.0199). Similarly, there was a significant increase in the number of cells upon EV treatment (Fig. 22B), indicating that EVs impact fibroblast proliferation in an autocrine manner.

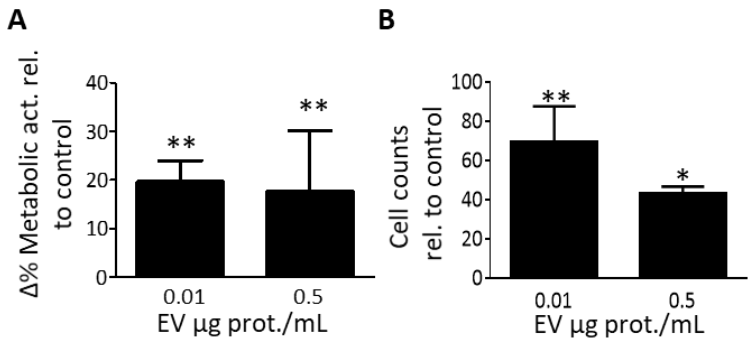

Figure 22. EVs induce lung fibroblast proliferation in an autocrine manner. Assessment of proliferation by WST-1 assay (A) or cell counting (B) of phLFs stimulated with EVs from the same cell type at the indicating concentrations for 48h (n=3 and n=6 respectively; 1way ANOVA; Dunnett´s post-test; *p<0.05)

4.4.2. Intact EVs are required for the induction of phLFs proliferation

To investigate if the structural integrity of EVs is really needed for the WNT-5A effect on lung fibroblast proliferation, EVs were pre-treated with a detergent which disrupts the EV membrane without affecting the protein content. The proliferative response was significantly decreased in those fibroblasts that received disrupted EVs when compared to intact EVs (Fig. 23). Therefore, structurally intact EVs containing WNT-5A are required for the observed effects on proliferation.

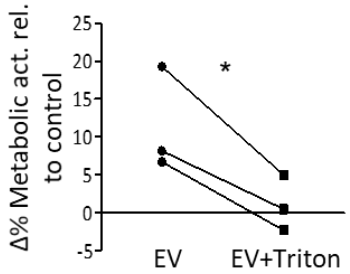

Figure 23. EV structure is needed for the proliferative effect of EV-bound WNT-5A. Proliferation analysis by WST-1 assay in phLFs stimulated with autocrine EVs alone (EV) or pre-treated with detergent (EV+triton). N=3 per group. Paired Student's *t* test; *p<0.05.

4.4.3. Lung fibroblast-EVs downregulate the expression of myofibroblast markers

Giving that activation of lung fibroblasts into myofibroblasts is another hallmark in IPF (White, Lazar et al. 2003), the expression of certain genes known as myofibroblast markers was next investigated as an additional functional readout of effects mediated by phLF-derived EVs. Next to an effect on proliferation, there was a decreased gene expression of the myofibroblast markers *FN1*, *ACTA2, COL1A1* and *TNC* upon EV treatment of lung fibroblasts (Fig. 24). These data indicate that EV-bound WNT-5A promotes a proliferative rather than a synthetic cellular phenotype of fibroblasts.

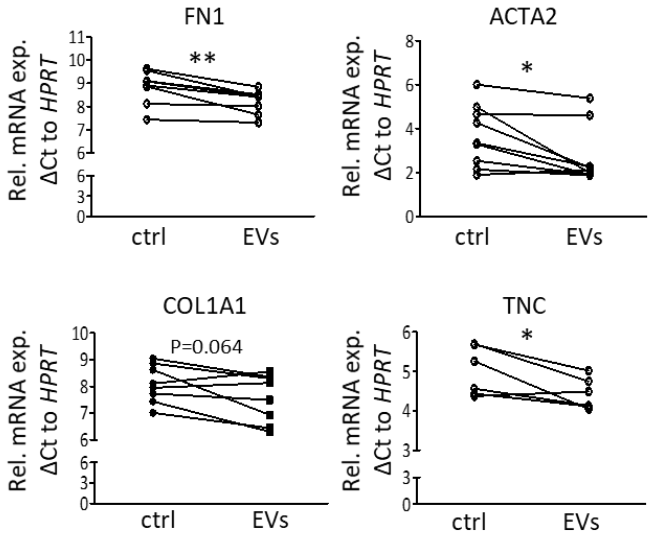

Figure 24. Effect of primary human lung fibroblasts derived EVs on (myo)fibroblast gene expression. phLFs were treated with EVs derived from the same patient at the concentration of 1.5µg EV prot/mL (n=6-9) and mRNA levels of *FN1*, *ACTA2, COL1A1* and *TNC* were assessed. Paired Student's *t* test; *P<0.05, **P<0.01.

4.5. EV-mediated proliferation of lung fibroblasts is dependent of WNT-5A

To investigate whether the effects of EVs on lung fibroblast proliferation were mediated by WNTs, overall inhibition of WNT protein secretion as well as specific inhibition of WNT-5A were next performed prior to phLF treatments.

4.5.1. EV-induced lung fibroblast proliferation is mediated by WNT proteins

To elucidate whether the effects of EVs on lung fibroblast proliferation were promoted by WNT proteins, the overall WNT secretion was inhibited by the inhibitor of WNT production molecule 2 (IWP2), which inactivates the O-acyltransferase Porcupine thus preventing the exit of WNT proteins from the endoplasmatic reticulum (Dodge, Moon et al. 2012). Pre-treatment of phLFs with IWP2 efficiently decreased WNT-5A secretion in phLFs supernatants (Fig. 25A). Moreover, the inhibition of WNT protein secretion in the EV-producing cells also reduced the capability of EVs to induce proliferation in the recipient phLFs when compared to the effect of EVs from vehicle-treated cells (Fig. 25B, % increase in metabolic activity to control: DMSO (vehicle)-EV 45.8±26.6 *vs*. IWP2-EV 27.0±12.3). This result indicates that EV-induced fibroblast proliferation is mediated, at least in part, by WNT proteins.

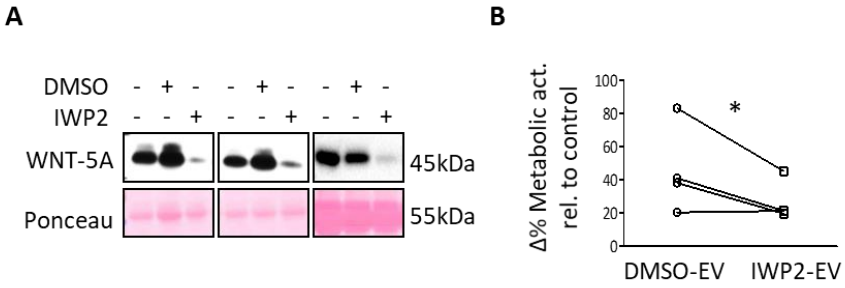

Figure 25. Human lung fibroblast derived EVs induce lung fibroblast proliferation through WNT proteins. (A) Detection of WNT-5A protein in phLFs supernatants after treatment with inhibitor of WNT protein secretion IWP2 or DMSO as control (data show n=3 independent experiments). (B) Proliferation analysis by WST1-assay after 48 h stimulation of phLFs with 0.5 µg prot./ml of autocrine EVs isolated in phLFs following treatment with IWP2 (IWP-EV) or DMSO control (DMSO-EV) (n=4 per group). Paired Student's *t* test; *P<0.05.

4.5.2. EV-mediated phLF proliferation is WNT-5A dependent

Given that the use of IWP2 is not exclusive to WNT-5A, and to further confirm that the effect of EVs on proliferation was mediated by WNT-5A, silencing and neutralizing experiments targeting specifically WNT-5A were performed. The siRNA-mediated silencing of WNT-5A in phLFs prior to EV-isolation efficiently inhibited WNT-5A secretion (26A). Importantly, silencing of WNT-5A didn't modify the EV secretion itself, since there were no significant changes on the expression of the secretion profile or the EV-enriched proteins CD81 and TSG101 (Fig. 26B and 26C).

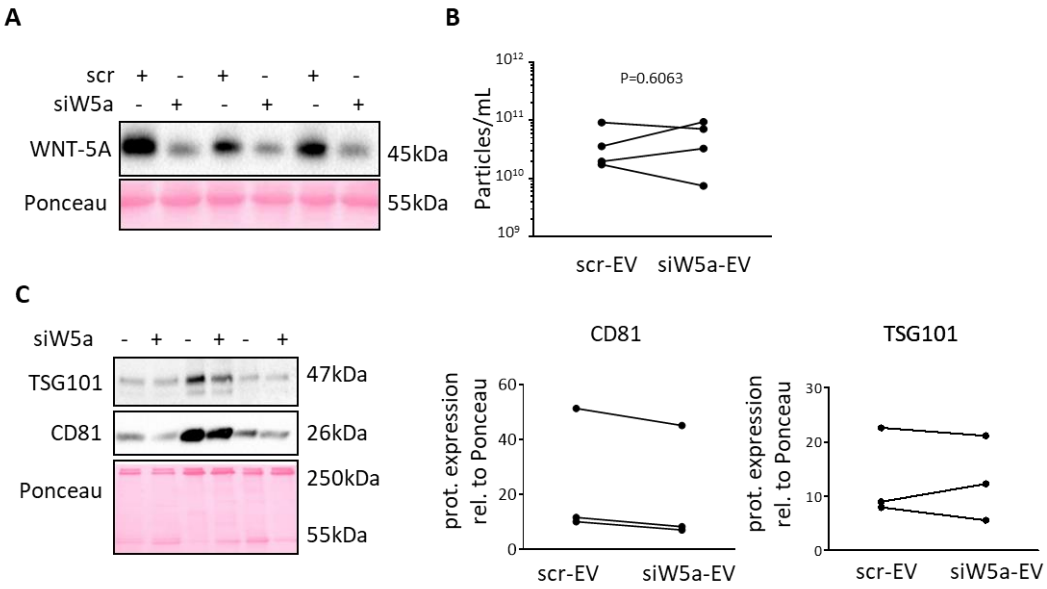

Figure 26. Human lung fibroblast-derived EVs drive lung fibroblast proliferation in a WNT-5A dependent manner. (A) Analysis of WNT-5A protein in supernatants from phLFs treated with WNT-5A siRNA (siW5A) or scrambled siRNA control (scr) for 24h. Ponceau S staining was used for loading confirmation of the supernatants. (B) Quantification by nanoparticle tracking analysis of EV secretion from phLF transfected with a siRNA targeting WNT-5A or a control siRNA. (C) Protein analysis of the EV-enriched proteins TSG101 and CD81 in EV-Pellets isolated from phLF transfected with a siRNA targeting WNT-5A or a control siRNA (left panel). Ponceau S staining was used as loading confirmation and to normalize protein expression. Densitometry of CD81 (middle) and TSG101 (right) relative to Ponceau are presented. Paired Student's *t* test for all.

In addition, WNT-5A-depleted EVs exhibited significant reduced potential to induce proliferation (Fig. 27, % increase in metabolic activity: scramble siRNA-EV 23.7±15.5 *vs*. WNT-5A siRNA-EV 4.2±9.1, P=0.0401), which demonstrates that the effect of phLF-EVs on lung fibroblast proliferation is mainly dependent on WNT-5A.

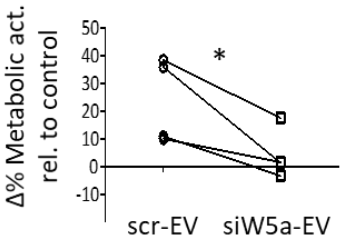

Figure 27. Silencing of WNT-5A produces EVs with reduced potential to induce lung fibroblast proliferation. Proliferation assay after 48 h stimulation of phLFs with 0.5 µg protein/ml of EVs isolated from phLFs after treatment with WNT-5A siRNA (siW5A-EV) or scrambled (scr-EV) (n=3 per group). Paired Student's *t* test. *P<0.05.

These results describing a WNT-5A-dependent proliferation were further supported by the finding that WNT-5A silencing in fibroblasts also decreased mRNA and protein expression of the cell cycle regulator Cyclin-D1 (Fig. 28A and 28B, respectively).

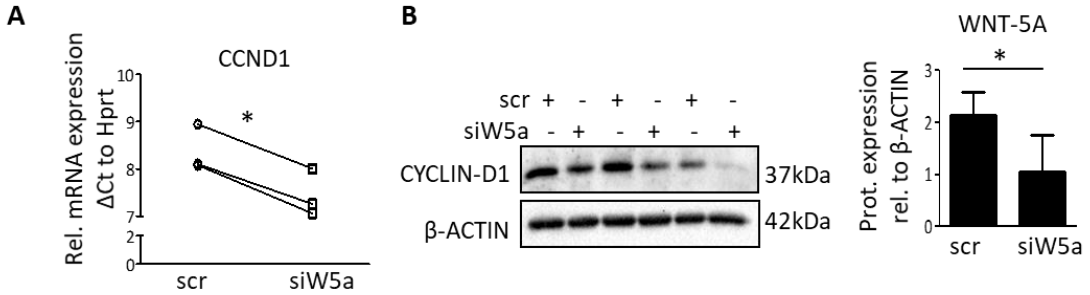

Figure 28. Silencing of WNT-5A in lung fibroblasts reduces the expression of the cell cycle regulator Cyclin-D1. (A) mRNA levels and (B) protein expression of cyclin D1 gene (CCND1) after 24 h stimulation of phLFs with siWNT-5A (siW5A) or scrambled siRNA (scr) as control. N=3 per group. Paired Student's *t* test for all; *P<0.05.

To further confirm these results and exclude any effects on EV composition that might be caused by the WNT-5A silencing, WNT-5A inhibition was also performed directly on phLF-EVs. For that, EVs obtained from non-treated phLFs were incubated with a WNT-5A neutralizing antibody (WNT-5A-AB) or with IgG control prior to phLFs stimulation. WNT-5A neutralization on EVs also decreased their potential to induce fibroblast proliferation (Fig. 29, % increased metabolic activity: EV+IgG 23.8±10.3 *vs*. EV+WNT-5A-AB 10±14.6, P=0.0449). In summary, these results provide evidence that it is mainly WNT-5A that mediates the pro-proliferative effect of EVs on lung fibroblasts.

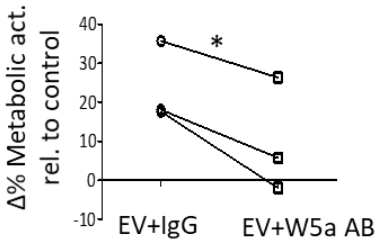

Figure 29. Neutralization of WNT-5A directly on EVs decreases their capability to induce lung fibroblast proliferation. Proliferation assay after 48 h stimulation of phLFs with 0.01 µg proein./ml of autocrine Evs that have been incubated with 1 µg of WNT-5A neutralizing antibody (EV+W5A AB) or IgG control (EV+IgG) (n=3 per group). Paired Student's *t* test; *P<0.05.

4.6. TGF-β increases WNT-5A secretion on EVs and exaggerates phLFs proliferation

Transforming growth factor (TGF-β) is a key profibrotic cytokine (Chambers and Mercer 2015) and has recently been reported to induce WNT-5A expression in lung fibroblasts (Newman, Sills et al. 2016). To elucidate whether a fibrotic stimulus would influence the potential of phLFs-EVs to induce WNT-5A-dependent proliferation, phLFs were treated with TGF-β and the EV production and response was studied.

4.6.1. The WNT-shuttle protein GPR177 is upregulated upon TGF-β stimulation

To investigate the effect of EVs derived from a fibrotic context, phLFs were treated with TGF-β before EV isolation. Fibrotic stimulation of phLFs by TGF-β led to an increased secretion of the WNT shuttle protein GPR177 in the supernatants when compared to control (Fig. 30), indicating an increased WNT secretion on EVs by phLFs under fibrotic conditions.

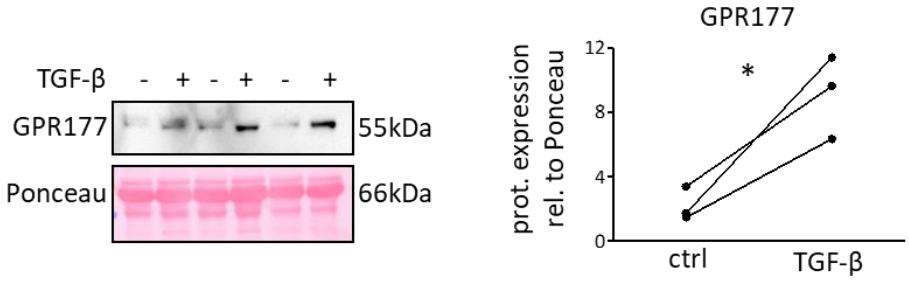

Figure 30. GPR177 secretion by phLFs is upregulated upon TGF-β treatment. (A) Protein levels of secreted GPR177 in the supernatants of phLFs after stimulation with TGF-β and subsequent densitometry relative to Ponceau. n=3 per group, paired Student's *t* test; *p<0.05.

4.6.2. TGF-β increases WNT-5A secretion on lung fibroblast EVs

Specific upregulation of WNT-5A secretion in phLFs EVs was observed upon TGF-β treatment (Fig. 31A, WNT-5A protein in EVs: ctrl 0.52±0.33, TGF-β 1.68±0.66, P=0.0262). Of

note, WNT-5A was particularly enriched in the EV fraction compared to the EV-free supernatant (Fig. 31B) meaning that WNT-5A is mostly secreted via EVs.

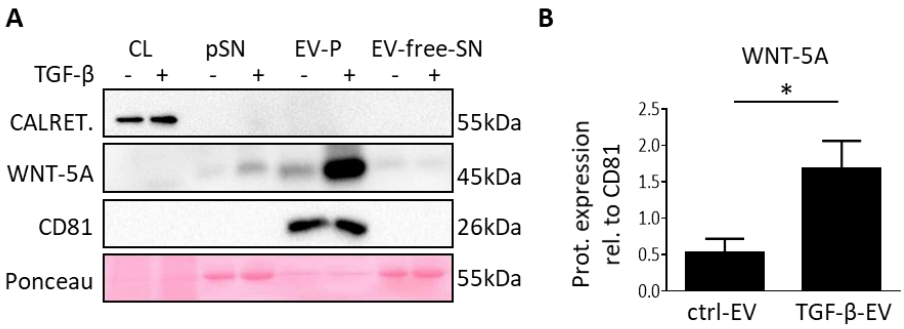

Figure 31. TGF-β treatment on lung fibroblasts leads to an increased WNT-5A secretion on Evs. (A) Protein expression analysis of endoplasmatic reticulum protein Calreticulin, the EV-enriched protein CD81 and WNT-5A in: cell lysates (CL), pure supernatants (pSN), EV-Pellets (EV-P) and EV-free-supernatants (EV-free-SN) from phLFBs treated with TGF-β (2ng/ml) for 48 h, and (B) respective densitometry analysis of WNT-5A relative to CD81 (graph represents 3 independent experiments). Paired Student's *t* test; *p<0.05.

4.6.3. TGF-β stimulation drives an increased proliferation response in lung fibroblasts, which is mediated by WNT-5A

EVs from TGF-β-treated phLFs were used to treat normal phLFs which responded with a increased proliferation when compared to those treated with control EVs (Fig. 32A). To investigate whether the proliferation mediated by TGF-β-derived EVs was indeed dependent on WNT-5A, EVs from control and TGF-β-treated phLFs were incubated with WNT-5A antibody before being used to treat the EV recipient cells. WNT-5A neutralization on TGF-β-derived EVs reduced their capability to promote proliferation in the recipient phLFs (Fig. 32B).

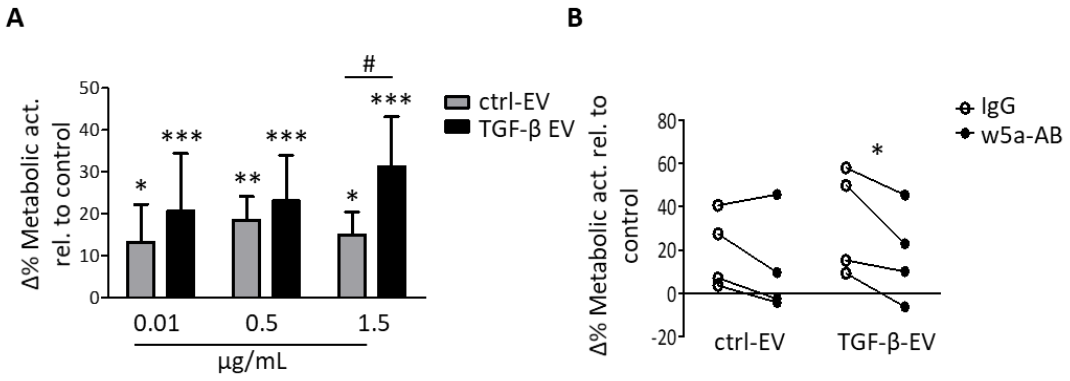

Figure 32. TGF-β-derived EVs induces increased proliferation of lung fibroblasts, which is dependent on WNT-5A. Assessment of proliferation by WST-1 assay of phLFs stimulated for 48h with (A) EVs from TGF-β-treated phLFs at the indicating concentrations (n=4; 1way ANOVA, Dunnett's post-test (*), Bonferroni post-test (#); $p<0.05$), and (B) same EVs incubated with WNT-5A antibody (w5a-AB) or IgG control (IgG), paired Student's *t* test; *$p<0.05$.

4.7. BALF-EVs from IPF patients promote lung fibroblast proliferation in a WNT-5A-dependent manner

Finally, to investigate the proliferative effect of EV-bound WNT-5A in the human disease, EVs were isolated from BALF of different IPF patients and were used to treat donor phLFs and study the proliferation response.

4.7.1 EVs from BALF of IPF patients significantly increase proliferation of phLFs

EVs from BALF of IPF patients were found to significantly increase phLF proliferation in a dose-dependent manner as measured by total metabolic activity (Fig. 33A; WST-1 assay). This proliferative effect was additionally confirmed by cell counting (Fig. 33B) and by a DNA-synthesis based method (Fig. 33C; BrdU assay).

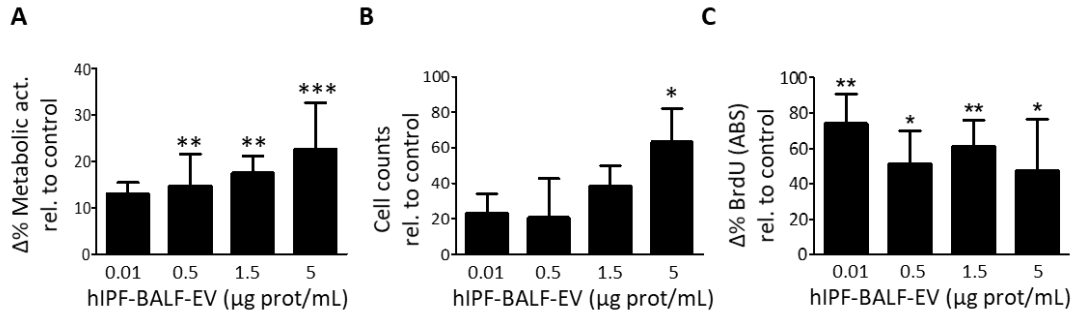

Figure 33. EVs from BALF of IPF patients induces lung fibroblast proliferation. Assessment of proliferation by (A) WST-1 assay, (B) cell counting or (C) BrdU assay of phLFs stimulated with EVs isolated from human IPF-BALF at the indicating concentrations for 48h (1way ANOVA, Dunnett´s post-test, n=7, n=3 and n=8; respectively).

To further confirm that the EV structure was required for the effect on proliferation, IPF-EVs were incubated with a detergent to disrupt the EV membrane and were used along with intact EVs to treat phLFs. Only intact EVs were able to induce proliferation on phLFs (Fig. 34) indicating the need of a structurally intact EV to exert the functional effect.

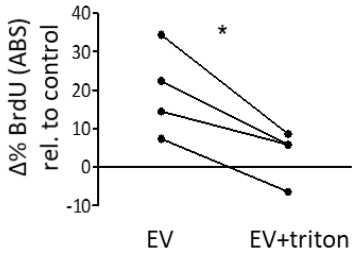

Figure 34. EV structure is required for IPF-derived EVs effect on lung fibroblast proliferation. Proliferation analysis by WST-1 assay in phLFs stimulated with IPF-EVs alone (EV) or pre-treated with detergent (EV+triton). N=4 per group. Paired Student's *t* test; p<0.05.

4.7.2 WNT-5A drives the proliferative effect of IPF-derived EVs

Finally, to elucidate if the proliferative response to IPF-EVs was mediated by WNT-5A, a neutralizing antibody against WNT-5A was used. The effect on proliferation was significantly decreased when IPF-EVs were pre-incubated with a WNT-5A-AB (Fig. 35, % increased metabolic activity: EV+IgG 19.3±10 vs EV+W5A-AB 8±13.9, P=0.0284), therefore indicating that the proliferation of phLFs in response to IPF-EVs was indeed due to EV-bound WNT-5A.

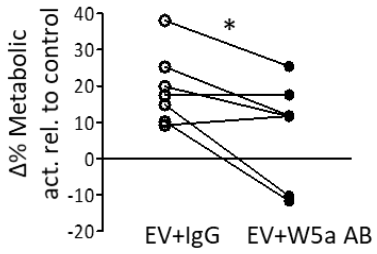

Figure 35. Lung fibroblast proliferation in response to EVs from IPF patients is dependent on WNT-5A. Proliferation assay by WST-1 of donor phLFs after 48h treatment with human IPF-BALF-EVs incubated with WNT-5A antibody (W5a AB) or IgG control (n=7 per group; paired Student's *t* test; p<0.05).

5. DISCUSSION

Extracellular vesicles (EVs) are secreted membranous vesicles of a diameter between 10-2000 nm that are known to transport a variety of proteins, nucleic acids or lipids, thus driving different biological processes depending on the cellular source and context (Yanez-Mo, Siljander et al. 2015). Increasing interest has been paid in the last decade into research of EVs as essential vehicles of both physiological and pathological processes by harboring specific mediators of a (diseased) cell of origin and communicating with other cellular compartments and tissues. Within the lung, our understanding and knowledge of EV function in disease has just recently begun to grow, with studies highlighting a potential role of EVs in particular in lung cancer and inflammatory lung disease (Schneider, Speth et al. 2016, Nana-Sinkam, Acunzo et al. 2017, Parimon, Brauer et al. 2018). However, besides an observational study that detected increased tissue factor activity in microparticles from BALF of ILD patients (Novelli, Neri et al. 2014), EV function in the context of IPF remains largely unknown. Active WNT proteins, which are known to play a role in idiopathic pulmonary fibrosis, have recently been discovered to be transported through EVs (Gross and Boutros 2013), nevertheless the presence and role of EV-associated WNT proteins have not been explored yet in IPF. This study focuses on characterizing the EV profile and functionality in the context of pulmonary fibrosis and demonstrates for the first time that 1) EVs, exosomes in particular, are increased in experimental and human pulmonary fibrosis, 2) that WNT-5A ligand can be detected on EVs in the fibrotic lung, and 3) that IPF-derived EVs, specifically via WNT-5A, contribute to fibroblast proliferation, and thus contribute to disease pathology. Therefore, this study proposes a new mechanism of intercellular communication in IPF pathogenesis, where the fibrotic context promotes secretion of EV-bound WNT-5A

by lung fibroblasts, which in turn increases fibroblast proliferation thereby contributing to disease progression (Fig. 36).

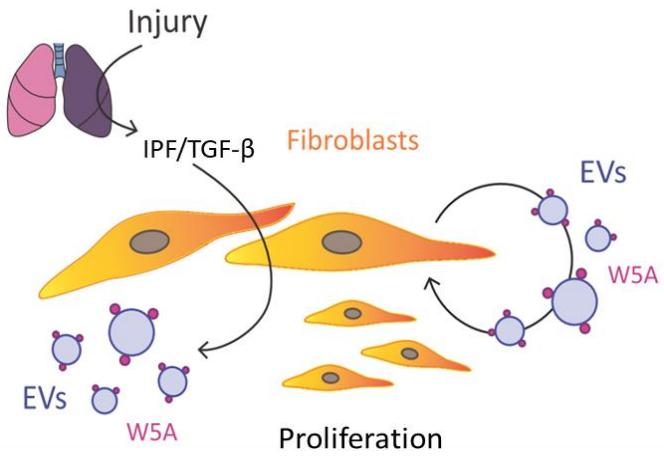

Figure 36. Proposed mechanism for EVs in IPF. Repetitive lung injury modifies the lung microenvironment and promotes increased WNT-5A secretion via extracellular vesicles (EVs) by lung fibroblasts. In turn, EV-derived WNT-5A enhances fibroblasts proliferation contributing to the progression of IPF. Abbreviations: Extracellular vesicles (EVs), WNT-5A (W5A), Idiopathic pulmonary fibrosis (IPF), Transforming grow factor beta (TGF-β).

5.1. The vesicle isolation and characterization: an imperative to study EVs

The growing field of EV biology has benefited from the efforts to standardize protocols for the isolation and characterization of EVs (Thery, Witwer et al. 2018). Nevertheless, all currently available isolation methods lead to distinct EV populations, thus highlighting the importance of a proper characterization in each study (Coumans, Brisson et al. 2017). In this study, serial ultracentrifugation has been generally used as a state-of-the-art method that does not modify the original sample, therefore being preferably used for quantification, characterization of human samples, and functional studies. Initially, ultracentrifugation was limited to a certain initial volume of sample, therefore, the EVs from murine BALF used for protein analysis purposes, were isolated by ExoQuick© which is a reagent that precipitates EVs. Despite the use of precipitation reagents such as ExoQuick© is acceptable for protein characterization, this method is known to pool down protein aggregates (usually in small fractions) that may interfere in the analysis. Further optimizations of the isolation protocol allowed later to use ultracentrifugation on murine BALF samples as well for the quantification of EVs. Furthermore, the vesicle population obtained in both murine and human biosamples has been comprehensively characterized by morphology, number, size, and expression of EV markers using transmission electron microscopy, nanoparticle tracking analysis, dynamic light scattering, and Western Blotting. This extensive characterization has demonstrated for the first time intact EVs from BALF, specially exosomes, that exhibit functional properties. The present study is the first to study EVs in BALF from IPF patients thus representing and initial proof-of-concept that BALF-EVs contribute to disease specially through WNT-5A. However, future studies would have to include larger number of human samples from IPF as well as other ILD cases

and include accurate tools such as proteomic analysis in order to address the heterogeneity of BALF samples.

5.2. Non-canonical WNT-5A protein as a main player in IPF

Disturbed WNT signaling has been implicated in the pathogenesis of several chronic lung diseases, including IPF (Baarsma and Konigshoff 2017). Thus far, most studies have focused on the canonical WNT/β-catenin pathway in IPF and it is well-established that canonical WNT signaling is upregulated mainly in alveolar type II cells in experimental and human lung fibrosis (Chilosi, Poletti et al. 2003, Konigshoff, Balsara et al. 2008, Aumiller, Balsara et al. 2013). The non-canonical WNT pathway, and its role in chronic lung diseases, however, is much less explored. In this regard, the non-canonical WNT-5A protein has been found upregulated in an unbiased microarray screen comparing primary human lung fibroblasts isolated from IPF and Donor lung tissue (Vuga, Ben-Yehudah et al. 2009). WNT-5A has also been linked to fibroblast survival and, more recently, WNT-5A was reported to be upregulated in early fibrotic-like changes in human 3D-LTCs (Vuga, Ben-Yehudah et al. 2009, Newman, Sills et al. 2016, Alsafadi, Staab-Weijnitz et al. 2017). Therefore, the present work was focused specifically on WNT-5A which was found upregulated in EVs from BALF of experimental and human lung fibrosis, as well as from supernatants of 3D-LTCs from fibrotic mouse lungs and in TGF-β-treated lung fibroblasts. EVs from fibrotic conditions were furthermore found to induce lung fibroblast proliferation through non-canonical WNT-5A ligand. Nevertheless, while WNT-5A has been largely reported to act β-catenin independent, also indirect β-catenin dependent functions can be observed. In this regard, Nabhan *et al*. recently

reported that WNT-5A expressing fibroblasts might induce WNT/β-catenin signaling in ATII cells (Nabhan, Brownfield et al. 2018), however, if this effect is mediated by EVs has not been investigated. Experiments showing the potential of fibroblasts-derived EVs on ATII cells inducing WNT/β-catenin signaling and their effects in mechanisms such as epithelial-to-mesenchymal transition (EMT), will be important to answer this question. In addition, since functional WNT-3A has also been found on EVs (Bartscherer, Pelte et al. 2006), the study of WNT-3A expression in lung fibroblasts or ATII cells from lung fibrosis and their autocrine/paracrine effects would give some insights into the potential canonical role of EVs in IPF.

5.3. EV-bound WNT-5A promotes lung fibroblast proliferation

Gross et al. discovered that active WNT ligands can be transported on EVs, which inspired the major aim of this work (Gross and Boutros 2013): to investigate the role of EVs carrying WNT ligands in lung fibrosis. WNT transport on EVs has important implications with respect to the signaling range of WNT proteins, which was thought to be rather short and limited to close neighboring cells. In this regard, EV-mediated transport can contribute to a larger signaling range of WNT proteins and thus determine the signaling outcome on other cells. In this study, EVs were found to affect lung fibroblasts proliferation which was mediated in a large extend by the non-canonical WNT ligand WNT-5A. Importantly, this effect could not only be attenuated by using siRNA-mediated knockdown, but further by antibody-mediated neutralization of WNT-5A on EVs and by detergent-mediated disruption of EV structure. These data corroborate that indeed EV-bound WNT-5A was responsible for the observed effects and that WNT-5A localizes on the EV membrane as

described in a previous study (Menck, Klemm et al. 2013). Recent data, although in a different organ, also demonstrates that EV-bound WNT-5A contribute to cardiac fibrosis by activating profibrotic WNT pathways on cardiac fibroblasts (Dzialo, Rudnik et al. 2019). Nevertheless, WNT-5A has also been reported to promote other processes in fibroblast such as adhesion (Kawasaki, Torii et al. 2007) or invasion (Waster, Rosdahl et al. 2011), as well as epithelial-mesenchymal transition (Gujral, Chan et al. 2014). Here, however, WNT-5A expressing EVs from lung fibroblasts were found to reduce myofibroblast activation genes Fibronectin, Collagen1a1 and Acta2, which needs to be further studied on a protein level. Nevertheless, this observation is indicating that the lung fibroblasts are probably downregulating their synthetic state in order to stablish a proliferative phenotype as found in response to EV-bound WNT-5A stimulus. In addition, to obtain a better picture of the role of WNT-5A expressing EVs in lung fibrosis, other processes such as adhesion and invasion could be analysed by a migration assay in which fibroblast would respond to EVs sender and recipient cells.

5.4. The cellular source of WNT-5A harbouring EVs

EVs are prime mediators for intercellular communication. In IPF pathogenesis, altered cellular crosstalk and communication is a key feature leading to aberrant epithelial wound healing and fibroblast activation, proliferation, and myofibroblast differentiation (Fernandez and Eickelberg 2012). A previous study based on gene expression patterns, found significantly increased WNT-5A in lung fibroblasts from unusual interstitial pneumonia (UIP) patients compared to controls with normal histology (Fernandez and Eickelberg 2012), which pointed at lung fibroblasts as a potential source of EV secretion of WNT-5A. In addition, a deep-tissue single cell study of the lung has detected WNT-5A significantly increased in interstitial lung fibroblasts in the aged mice (Angeledis et al. 2019) which is a risk factor for IPF. The hypothesis of lung fibroblasts as a source of EV-bound WNT-5A secretion in the lung, was confirmed by this study which describes primary human lung fibroblasts as an important source of EV-bound WNT-5A in comparison to primary human lung epithelial type II cells. Importantly, WNT-5A was found to be increased on lung fibroblast-derived EVs upon profibrotic stimulation with TGF-β. Moreover, lung fibroblast-derived EVs were found to induce an autocrine effect on fibroblast proliferation, which was enhanced when EVs were produced under fibrotic conditions. Interestingly, mesenchymal stem cell (MSC)-derived exosomes were also found to induce dermal fibroblast proliferation (McBride, Rodriguez-Menocal et al. 2017). In addition to lung fibroblast proliferation, differentiation of fibroblasts into a myofibroblast can be observed during lung remodelling (Chapman 2012). It is thought that fibroblasts exert different phenotypes within a fibrotic lung based upon their spatio-temporal distribution, for instance, it has been found that activated lung fibroblasts secrete prostaglandins in EVs in order to maintain

homeostasis (McBride, Rodriguez-Menocal et al. 2017). In this study, notably, fibroblast derived EVs did not promote myofibroblast differentiation, but rather decrease myofibroblast markers and as such promote a proliferative rather than a synthetic phenotype. Studies focusing on tumor associated fibroblasts have observed that EVs are able to promote myofibroblast differentiation (Webber, Spary et al. 2015); however, mesenchymal stem cell derived exosomes have also been reported to suppress myofibroblast differentiation (Fang, Xu et al. 2016). Importantly, EVs derived from cigarette smoked epithelium were able to promote myofibroblast differentiation too (Fujita, Araya et al. 2015). Among the BALF-EVs there are a mixture of different EVs from different cellular sources, which can lead to distinct cellular functions depending of their cargos. In the present study WNT-5A was undetectable in EVs from epithelial type II cells at a baseline level in comparison to lung fibroblast EVs, thus indicating that fibroblasts are a main source of WNT-5A secretion through EVs. Nevertheless, melanoma-derived macrophages have been also reported to harbour WNT-5A on EVs (Menck, Klemm et al. 2013). It will be important to further investigate EVs from other cellular sources, such as alveolar macrophages or lung epithelial cells, and study their effects on lung fibroblast phenotype. In addition, it will be highly interesting to sort different cell types from EVs from IPF-BALF and analyse their effects on normal lung fibroblast in order to see if the whole EV profile is changed in the different cell types of the fibrosis-derived BALF and what kind of effect do they mediate to drive disease.

5.5. The contribution of EVs to impaired cellular crosstalk in IPF

In IPF pathogenesis, aberrant wound healing of epithelium dysregulates the epithelial-to-mesenchymal cellular crosstalk thus altering lung fibroblasts and leading to disease. Here, lung fibroblasts are presented as an important source of EV-bound WNT-5A secretion which exert specific autocrine effects. Additionally, paracrine effects mediated by EVs likely contribute to impaired cellular crosstalk in disease (Williamson, Sadofsky et al. 2015). It has been suggested that epithelial cell injury impairs, interestingly, local secretion of IL-1β in response to an epithelial wound is capable of promoting WNT-5A secretion by myofibroblasts which induces migration and proliferation of epithelial cells in the intestinal epithelium (Raymond, Marchbank et al. 2012). Therefore, it is plausible that in IPF, injured lung epithelial cells signal to fibroblasts, which in turn increase WNT-5A secretion via EVs, thus promoting fibroblast proliferation and contributing to disease burden. Therefore, it will be interesting to analyse if stimulation with IL-1β is potentiating/contributing to the WNT-5A secretion on EVs in response to TGF-β stimulus and see the effect of those EVs on epithelial cell migration and proliferation. Additionally, an increase in WNT-5A in primary COPD fibroblasts has been reported to negatively affect alveolar epithelial cell function (Baarsma and Konigshoff 2017), suggesting that fibroblast-derived EV-bound WNT-5A might also influence epithelial cells which highlights the importance of defining the contribution of EVs to impaired cellular crosstalk in IPF between lung fibroblasts and lung epithelial cells more precisely.

5.6. The heterogeneity of BALF-derived EVs

This investigation has focused mainly on fibroblast derived EVs for functional studies and provides evidence that WNT-5A bound EVs in IPF BALF contributes to the functional effects. This suggests that WNT-5A harbouring EVs derived from fibroblast, which can be found in IPF BALF, may contribute largely to the observed phenotype. However, it is most likely that within the BALF from IPF patients also other cell derived EVs are included, such as epithelial cell or immune cell subpopulations, which thus might alter the functional outcome. The EV heterogeneity and the lack of markers for cell-specific origin, makes it difficult to elucidate the different cellular sources of the EVs present in biofluids such as BALF (Colombo, Moita et al. 2013). Tracing the cellular origin of EVs in biofluids could be possible with recent techniques like Multiplex Proximity Extension Assays (PEA) which performs a proteomic profile that allows the correlation of EVs with their originating cell type based on their protein profile (i.e. tissue-specific proteins or integrins present in EVs) (Larssen, Wik et al. 2017). Using a technique like this will be useful and important to further investigate EV heterogeneity in the BALF of IPF patients, to profile the EV secretion from different cellular sources into BALF and their distinct effects on the fibrotic lung cell phenotypes.

5.7. The WNT-5A EV receptor cells

In this study, WNT-5A protein expression was found highly upregulated, in particular on EVs, thus enabling WNT-5A transport and signaling between cells even upon larger distances. Furthermore, WNT-5A is described to act through EVs promoting lung fibroblast proliferation in an autocrine manner. Nevertheless, as WNT-5A has also been reported to promote other processes rather than fibroblast proliferation, it seems very likely that WNT-5A EVs from lung fibroblasts might also affect other cell types even distant to the EV source. Due to their location, the alveolar macrophages are potential candidates to be receptors of the EVs that are secreted into the lumen, nevertheless, EVs might also reach other parts of the organism through the blood circulation. The fact that WNT-5A secreted by primary fibroblasts has been recently described to affect alveolar epithelial cell function in COPD (Baarsma and Konigshoff 2017), highlights the need to further investigate EV-mediated WNT-5A signaling on different cell types other than fibroblast.

5.8. Disease-specific composition of EVs

It is described that same proteins, which can be found in EVs, might have different effects on the receptor cells depending on the disease context. For instance, whereas WNT-5A is known to promote lung fibroblast proliferation in IPF (Vuga et al. 2009), it is also able to inhibit WNT/β-catenin driven repair in epithelial cells in COPD (Kneidinger, Yildirim et al. 2011, Baarsma and Konigshoff 2017). These disease-specific effects on the cellular phenotype could be mediated by the distinct composition of EVs or a specific surface receptor profile on the recipient cell in the disease. As such, it has been demonstrated that EVs can be detected by specific cell types due to a distinct integrin expression pattern (Hoshino, Costa-Silva et al. 2015). Another intriguing hypothesis is based on the idea that depending on the microenvironment, EVs harbor diverse components of a specific pathway, including specific signaling receptors that enable the recipient cell to exert novel functions and phenotypes. For instance, a specific non-canonical receptor for WNT-5A could be shed together with the WNT-5A ligand to stablish a more efficient signal and response in the receptor cell. Therefore, EVs are more than a pure vehicle and can be able to modulate the cellular response in addition to their cargos. In order to decipher which additional receptors or proteins might be carried by EVs along with WNT-5A, an unbiased proteomics approach has been started to follow up this study using EVs from BALF of IPF and normal samples. To study the whole EV composition in the disease-specific context will help us to understand the role of EVs in the IPF pathogenesis.

5.9. Pathogenic versus protective role of EVs

This investigation reflects the relevance of WNT-5A ligand secretion through EVs and raises the more general question whether EVs, most likely as a mixture of EVs from different cellular sources, rather promote lung fibrosis development or might also have a protective role *in vivo*. Notably, several studies to date indicate that EVs appear to play versatile roles depending on the (disease) specific microenvironment. For instance, EVs have been reported to exhibit a protective role in facilitating tissue repair by fostering innate immune defense mechanisms (Kesimer, Scull et al. 2009), while others have suggested a proinflammatory role of EVs in asthma (Kulshreshtha, Ahmad et al. 2013, Haj-Salem, Plante et al. 2018), sarcoidosis (Qazi, Torregrosa Paredes et al. 2010) and LPS-induced lung inflammation (Speth, Bourdonnay et al. 2016). Moreover, several studies suggest that EVs derived from non-small cell lung cancer cells promote tumor development and metastasis in lung cancer (Zheng, Zhan et al. 2018, Wu, Yin et al. 2019) and EVs derived from serum from lung cancer patients induce epithelial-to-mesenchymal transition on recipient human bronchial epithelial cells (Rahman, Barger et al. 2016). On the other hand, exogenously administered MSC-derived EVs have demonstrated therapeutic potential in the injured lung (Katsuda and Ochiya 2015, Fang, Xu et al. 2016, Cruz and Rocco 2017, Bari, Ferrarotti et al. 2019) indicating that EVs alone are not pathogenic. Additional studies are needed to elucidate whether EVs play a role in promoting IPF pathogenesis or if they represent an attempt to resolve the damage. Inhibition of EV secretion or altering EV composition in vivo, ideally in a cell-specific manner would provide crucial insight into this question. The sphingomyelinase inhibitor GW4869 blocks the global production of exosomes (which are the main vesicle present in our EV isolations) (Essandoh, Yang et al.

2015) and could be a promising method to inhibit exosome-bound WNTs without affecting other WNT pools that might be needed for repair and regeneration. Targeting EVs for a potential therapy should be further explored as it might allow targeting a specific subset of profibrotic mediators that drive the disease.

5.10. Limitations and conclusive remarks

A limited amount of patient samples was investigated in this study to provide first evidence that EVs are increased in IPF and carry important functional mediators, such as WNT-5A. In part, this was due to the limitation of the amount of initial volume of the BALF required to perform EV isolations, however, the isolation method was optimized during the study and less amount of sample will be needed in future. Nevertheless, a comprehensive characterization of EVs requires large amount of biosamples, which restricted the overall number of patient samples that could be included in this study. While both independent cohorts showed similar results, future investigations of larger cohorts will be essential to further confirm the potential correlation of EVs with clinical parameters, such as lung function. These studies will need to consider the heterogeneity of the BALF samples (such as differential cell counts), include different ILDs, and allow adjustment for parameter as age and gender. Furthermore, it will be interesting to explore the potential role of EVs as blood biomarkers for ILDs (M, Bayraktar et al. 2017, Njock, Guiot et al. 2019), and other EV components such as DNA, mRNA or microRNAs that might contribute to disease (Schneider, Speth et al. 2016, Nana-Sinkam, Acunzo et al. 2017, Parimon, Brauer et al. 2018). Given that the EVs can enter the systemic circulation, it is possible that EVs secreted by lung cells will end up in other (distant) organs.

Tracking EVs along the organism would be possible using reporter mice in which cell specific tags can be found on EVs secreted by the different cell types (Gangadaran, Hong et al. 2018). The hypothesis that EVs originated by the cells of the fibrotic lung might travel to other organs to deliver their diseased-influenced message could explain the development of non-respiratory comorbidities associated with IPF such as ischaemic heart disease (IHD) and gastroesophageal reflux (GER) (Cano-Jimenez, Hernandez Gonzalez et al. 2018). Therefore, targeting EVs, not only in the lung but using a systemic approach, could be beneficial to improve patient survival.

In summary, our present study is the first to report that EVs can be found in experimental and human pulmonary fibrosis, carry fibrotic mediators such as WNT-5A, and contribute to fibrogenesis. Further investigations of EVs in this devastating disease are warranted to better understand the contribution to fibrotic pathomechanisms, as well as to elucidate their potential as therapeutic targets and biomarkers. Nevertheless, this work englobes for the first time a fine characterization of EVs in IPF and describes their role in the pathology by promoting lung fibroblast proliferation. Furthermore, the fact that EVs derived from the fibrotic lung might travel to other organs extends our view of IPF as a disease of the lung to a broader picture and opens a new window of therapeutic possibilities for the treatment of pulmonary fibrosis and IPF-associated comorbidities.

6. **REFERENCES**

Akamatsu, T., Y. Arai, I. Kosugi, H. Kawasaki, S. Meguro, M. Sakao, K. Shibata, T. Suda, K. Chida and T. Iwashita (2013). "Direct isolation of myofibroblasts and fibroblasts from bleomycin-injured lungs reveals their functional similarities and differences." Fibrogenesis Tissue Repair **6**(1): 15.

Alsafadi, H. N., C. A. Staab-Weijnitz, M. Lehmann, M. Lindner, B. Peschel, M. Konigshoff and D. E. Wagner (2017). "An ex vivo model to induce early fibrosis-like changes in human precision-cut lung slices." Am J Physiol Lung Cell Mol Physiol **312**(6): L896-L902.

Andreu, Z. and M. Yanez-Mo (2014). "Tetraspanins in extracellular vesicle formation and function." Front Immunol **5**: 442.

Antoniou, K. M., G. A. Margaritopoulos, S. Tomassetti, F. Bonella, U. Costabel and V. Poletti (2014). "Interstitial lung disease." Eur Respir Rev **23**(131): 40-54.

Aumiller, V., N. Balsara, J. Wilhelm, A. Gunther and M. Konigshoff (2013). "WNT/beta-catenin signaling induces IL-1beta expression by alveolar epithelial cells in pulmonary fibrosis." Am J Respir Cell Mol Biol **49**(1): 96-104.

Baarsma, H. A. and M. Konigshoff (2017). "'WNT-er is coming': WNT signalling in chronic lung diseases." Thorax **72**(8): 746-759.

Baarsma, H. A., M. Konigshoff and R. Gosens (2013). "The WNT signaling pathway from ligand secretion to gene transcription: molecular mechanisms and pharmacological targets." Pharmacol Ther **138**(1): 66-83.

Bari, E., I. Ferrarotti, M. L. Torre, A. G. Corsico and S. Perteghella (2019). "Mesenchymal stem/stromal cell secretome for lung regeneration: The long way through "pharmaceuticalization" for the best formulation." J Control Release **309**: 11-24.

Barnes, P. J. (2017). "Glucocorticosteroids." Handb Exp Pharmacol **237**: 93-115.

Bartscherer, K., N. Pelte, D. Ingelfinger and M. Boutros (2006). "Secretion of Wnt ligands requires Evi, a conserved transmembrane protein." Cell **125**(3): 523-533.

Burgy, O. and M. Konigshoff (2018). "The WNT signaling pathways in wound healing and fibrosis." Matrix Biol **68-69**: 67-80.

Cano-Jimenez, E., F. Hernandez Gonzalez and G. B. Peloche (2018). "Comorbidities and Complications in Idiopathic Pulmonary Fibrosis." Med Sci (Basel) **6**(3).

Chambers, R. C. and P. F. Mercer (2015). "Mechanisms of alveolar epithelial injury, repair, and fibrosis." Ann Am Thorac Soc **12 Suppl 1**: S16-20.

Chapman, H. A. (2011). "Epithelial-mesenchymal interactions in pulmonary fibrosis." Annu Rev Physiol **73**: 413-435.

Chapman, H. A. (2012). "Epithelial responses to lung injury: role of the extracellular matrix." Proc Am Thorac Soc **9**(3): 89-95.

Chilosi, M., A. Carloni, A. Rossi and V. Poletti (2013). "Premature lung aging and cellular senescence in the pathogenesis of idiopathic pulmonary fibrosis and COPD/emphysema." Transl Res **162**(3): 156-173.

Chilosi, M., V. Poletti, A. Zamo, M. Lestani, L. Montagna, P. Piccoli, S. Pedron, M. Bertaso, A. Scarpa, B. Murer, A. Cancellieri, R. Maestro, G. Semenzato and C. Doglioni (2003). "Aberrant Wnt/beta-catenin pathway activation in idiopathic pulmonary fibrosis." Am J Pathol **162**(5): 1495-1502.

Collard, H. R., L. Richeldi, D. S. Kim, H. Taniguchi, I. Tschoepe, M. Luisetti, J. Roman, G. Tino, R. Schlenker-Herceg, C. Hallmann and R. M. du Bois (2017). "Acute exacerbations in the INPULSIS trials of nintedanib in idiopathic pulmonary fibrosis." Eur Respir J **49**(5).

Colombo, M., C. Moita, G. van Niel, J. Kowal, J. Vigneron, P. Benaroch, N. Manel, L. F. Moita, C. Thery and G. Raposo (2013). "Analysis of ESCRT functions in exosome biogenesis, composition and secretion highlights the heterogeneity of extracellular vesicles." J Cell Sci **126**(Pt 24): 5553-5565.

Colombo, M., G. Raposo and C. Thery (2014). "Biogenesis, secretion, and intercellular interactions of exosomes and other extracellular vesicles." Annu Rev Cell Dev Biol **30**: 255-289.
Coumans, F. A. W., A. R. Brisson, E. I. Buzas, F. Dignat-George, E. E. E. Drees, S. El-Andaloussi, C. Emanueli, A. Gasecka, A. Hendrix, A. F. Hill, R. Lacroix, Y. Lee, T. G. van Leeuwen, N. Mackman, I. Mager, J. P. Nolan, E. van der Pol, D. M. Pegtel, S. Sahoo, P. R. M. Siljander, G. Sturk, O. de Wever and R. Nieuwland (2017). "Methodological Guidelines to Study Extracellular Vesicles." Circ Res **120**(10): 1632-1648.
Cruz, F. F. and P. R. M. Rocco (2017). "Stem-cell extracellular vesicles and lung repair." Stem Cell Investig **4**: 78.
Dela Cruz, C. S., M. J. Kang, W. K. Cho and C. G. Lee (2011). "Transgenic modelling of cytokine polarization in the lung." Immunology **132**(1): 9-17.
Deng, Z., Y. Rong, Y. Teng, X. Zhuang, A. Samykutty, J. Mu, L. Zhang, P. Cao, J. Yan, D. Miller and H. G. Zhang (2017). "Exosomes miR-126a released from MDSC induced by DOX treatment promotes lung metastasis." Oncogene **36**(5): 639-651.
Dodge, M. E., J. Moon, R. Tuladhar, J. Lu, L. S. Jacob, L. S. Zhang, H. Shi, X. Wang, E. Moro, A. Mongera, F. Argenton, C. M. Karner, T. J. Carroll, C. Chen, J. F. Amatruda and L. Lum (2012). "Diverse chemical scaffolds support direct inhibition of the membrane-bound O-acyltransferase porcupine." J Biol Chem **287**(27): 23246-23254.
Dzialo, E., M. Rudnik, R. I. Koning, M. Czepiel, K. Tkacz, M. Baj-Krzyworzeka, O. Distler, M. Siedlar, G. Kania and P. Blyszczuk (2019). "WNT3a and WNT5a Transported by Exosomes Activate WNT Signaling Pathways in Human Cardiac Fibroblasts." Int J Mol Sci **20**(6).
Eickelberg, O. and M. Selman (2010). "Update in diffuse parenchymal lung disease 2009." Am J Respir Crit Care Med **181**(9): 883-888.
Essandoh, K., L. Yang, X. Wang, W. Huang, D. Qin, J. Hao, Y. Wang, B. Zingarelli, T. Peng and G. C. Fan (2015). "Blockade of exosome generation with GW4869 dampens the sepsis-induced inflammation and cardiac dysfunction." Biochim Biophys Acta **1852**(11): 2362-2371.
Fang, S., C. Xu, Y. Zhang, C. Xue, C. Yang, H. Bi, X. Qian, M. Wu, K. Ji, Y. Zhao, Y. Wang, H. Liu and X. Xing (2016). "Umbilical Cord-Derived Mesenchymal Stem Cell-Derived Exosomal MicroRNAs Suppress Myofibroblast Differentiation by Inhibiting the Transforming Growth Factor-beta/SMAD2 Pathway During Wound Healing." Stem Cells Transl Med **5**(10): 1425-1439.
Fernandez, I. E. and O. Eickelberg (2012). "The impact of TGF-beta on lung fibrosis: from targeting to biomarkers." Proc Am Thorac Soc **9**(3): 111-116.
Fisher, M., S. D. Nathan, C. Hill, J. Marshall, F. Dejonckheere, P. O. Thuresson and T. M. Maher (2017). "Predicting Life Expectancy for Pirfenidone in Idiopathic Pulmonary Fibrosis." J Manag Care Spec Pharm **23**(3-b Suppl): S17-S24.
Flaherty, K. R. and F. J. Martinez (2000). "The role of pulmonary function testing in pulmonary fibrosis." Curr Opin Pulm Med **6**(5): 404-410.
Fleetwood, K., R. McCool, J. Glanville, S. C. Edwards, S. Gsteiger, M. Daigl and M. Fisher (2017). "Systematic Review and Network Meta-analysis of Idiopathic Pulmonary Fibrosis Treatments." J Manag Care Spec Pharm **23**(3-b Suppl): S5-S16.
Fujita, Y., J. Araya, S. Ito, K. Kobayashi, N. Kosaka, Y. Yoshioka, T. Kadota, H. Hara, K. Kuwano and T. Ochiya (2015). "Suppression of autophagy by extracellular vesicles promotes myofibroblast differentiation in COPD pathogenesis." J Extracell Vesicles **4**: 28388.
Fujita, Y., N. Kosaka, J. Araya, K. Kuwano and T. Ochiya (2015). "Extracellular vesicles in lung microenvironment and pathogenesis." Trends Mol Med **21**(9): 533-542.
Galli, J. A., A. Pandya, M. Vega-Olivo, C. Dass, H. Zhao and G. J. Criner (2017). "Pirfenidone and nintedanib for pulmonary fibrosis in clinical practice: Tolerability and adverse drug reactions." Respirology **22**(6): 1171-1178.
Gangadaran, P., C. M. Hong and B. C. Ahn (2018). "An Update on in Vivo Imaging of Extracellular Vesicles as Drug Delivery Vehicles." Front Pharmacol **9**: 169.

Goldstein, R. A., P. K. Rohatgi, E. H. Bergofsky, E. R. Block, R. P. Daniele, D. R. Dantzker, G. S. Davis, G. W. Hunninghake, T. E. King, Jr., W. J. Metzger and et al. (1990). "Clinical role of bronchoalveolar lavage in adults with pulmonary disease." Am Rev Respir Dis **142**(2): 481-486.
Gould, S. J. and G. Raposo (2013). "As we wait: coping with an imperfect nomenclature for extracellular vesicles." J Extracell Vesicles **2**.
Greco, V., M. Hannus and S. Eaton (2001). "Argosomes: a potential vehicle for the spread of morphogens through epithelia." Cell **106**(5): 633-645.
Gross, J. C. and M. Boutros (2013). "Secretion and extracellular space travel of Wnt proteins." Curr Opin Genet Dev **23**(4): 385-390.
Gujral, T. S., M. Chan, L. Peshkin, P. K. Sorger, M. W. Kirschner and G. MacBeath (2014). "A noncanonical Frizzled2 pathway regulates epithelial-mesenchymal transition and metastasis." Cell **159**(4): 844-856.
Haj-Salem, I., S. Plante, A. S. Gounni, M. Rouabhia and J. Chakir (2018). "Fibroblast-derived exosomes promote epithelial cell proliferation through TGF-beta2 signalling pathway in severe asthma." Allergy **73**(1): 178-186.
Harding, C. and P. Stahl (1983). "Transferrin recycling in reticulocytes: pH and iron are important determinants of ligand binding and processing." Biochem Biophys Res Commun **113**(2): 650-658.
Hessvik, N. P. and A. Llorente (2018). "Current knowledge on exosome biogenesis and release." Cell Mol Life Sci **75**(2): 193-208.
Hoshino, A., B. Costa-Silva, T. L. Shen, G. Rodrigues, A. Hashimoto, M. Tesic Mark, H. Molina, S. Kohsaka, A. Di Giannatale, S. Ceder, S. Singh, C. Williams, N. Soplop, K. Uryu, L. Pharmer, T. King, L. Bojmar, A. E. Davies, Y. Ararso, T. Zhang, H. Zhang, J. Hernandez, J. M. Weiss, V. D. Dumont-Cole, K. Kramer, L. H. Wexler, A. Narendran, G. K. Schwartz, J. H. Healey, P. Sandstrom, K. J. Labori, E. H. Kure, P. M. Grandgenett, M. A. Hollingsworth, M. de Sousa, S. Kaur, M. Jain, K. Mallya, S. K. Batra, W. R. Jarnagin, M. S. Brady, O. Fodstad, V. Muller, K. Pantel, A. J. Minn, M. J. Bissell, B. A. Garcia, Y. Kang, V. K. Rajasekhar, C. M. Ghajar, I. Matei, H. Peinado, J. Bromberg and D. Lyden (2015). "Tumour exosome integrins determine organotropic metastasis." Nature **527**(7578): 329-335.
Janowska-Wieczorek, A., M. Wysoczynski, J. Kijowski, L. Marquez-Curtis, B. Machalinski, J. Ratajczak and M. Z. Ratajczak (2005). "Microvesicles derived from activated platelets induce metastasis and angiogenesis in lung cancer." Int J Cancer **113**(5): 752-760.
Johannson, K. A., E. Vittinghoff, K. Lee, J. R. Balmes, W. Ji, G. G. Kaplan, D. S. Kim and H. R. Collard (2014). "Acute exacerbation of idiopathic pulmonary fibrosis associated with air pollution exposure." Eur Respir J **43**(4): 1124-1131.
Jones, M. G., A. Fabre, P. Schneider, F. Cinetto, G. Sgalla, M. Mavrogordato, S. Jogai, A. Alzetani, B. G. Marshall, K. M. O'Reilly, J. A. Warner, P. M. Lackie, D. E. Davies, D. M. Hansell, A. G. Nicholson, I. Sinclair, K. K. Brown and L. Richeldi (2016). "Three-dimensional characterization of fibroblast foci in idiopathic pulmonary fibrosis." JCI Insight **1**(5).
Katsuda, T. and T. Ochiya (2015). "Molecular signatures of mesenchymal stem cell-derived extracellular vesicle-mediated tissue repair." Stem Cell Res Ther **6**: 212.
Kawasaki, A., K. Torii, Y. Yamashita, K. Nishizawa, K. Kanekura, M. Katada, M. Ito, I. Nishimoto, K. Terashita, S. Aiso and M. Matsuoka (2007). "Wnt5a promotes adhesion of human dermal fibroblasts by triggering a phosphatidylinositol-3 kinase/Akt signal." Cell Signal **19**(12): 2498-2506.
Kesimer, M., M. Scull, B. Brighton, G. DeMaria, K. Burns, W. O'Neal, R. J. Pickles and J. K. Sheehan (2009). "Characterization of exosome-like vesicles released from human tracheobronchial ciliated epithelium: a possible role in innate defense." FASEB J **23**(6): 1858-1868.
King, C. S. and S. D. Nathan (2017). "Idiopathic pulmonary fibrosis: effects and optimal management of comorbidities." Lancet Respir Med **5**(1): 72-84.

King, T. E., Jr., A. Pardo and M. Selman (2011). "Idiopathic pulmonary fibrosis." Lancet **378**(9807): 1949-1961.
Klee, S., M. Lehmann, D. E. Wagner, H. A. Baarsma and M. Konigshoff (2016). "WISP1 mediates IL-6-dependent proliferation in primary human lung fibroblasts." Sci Rep **6**: 20547.
Kneidinger, N., A. O. Yildirim, J. Callegari, S. Takenaka, M. M. Stein, R. Dumitrascu, A. Bohla, K. R. Bracke, R. E. Morty, G. G. Brusselle, R. T. Schermuly, O. Eickelberg and M. Konigshoff (2011). "Activation of the WNT/beta-catenin pathway attenuates experimental emphysema." Am J Respir Crit Care Med **183**(6): 723-733.
Koles, K., J. Nunnari, C. Korkut, R. Barria, C. Brewer, Y. Li, J. Leszyk, B. Zhang and V. Budnik (2012). "Mechanism of evenness interrupted (Evi)-exosome release at synaptic boutons." J Biol Chem **287**(20): 16820-16834.
Konigshoff, M., N. Balsara, E. M. Pfaff, M. Kramer, I. Chrobak, W. Seeger and O. Eickelberg (2008). "Functional Wnt signaling is increased in idiopathic pulmonary fibrosis." PLoS One **3**(5): e2142.
Konigshoff, M. and O. Eickelberg (2010). "WNT signaling in lung disease: a failure or a regeneration signal?" Am J Respir Cell Mol Biol **42**(1): 21-31.
Konigshoff, M., M. Kramer, N. Balsara, J. Wilhelm, O. V. Amarie, A. Jahn, F. Rose, L. Fink, W. Seeger, L. Schaefer, A. Gunther and O. Eickelberg (2009). "WNT1-inducible signaling protein-1 mediates pulmonary fibrosis in mice and is upregulated in humans with idiopathic pulmonary fibrosis." J Clin Invest **119**(4): 772-787.
Korkut, C. and V. Budnik (2009). "WNTs tune up the neuromuscular junction." Nat Rev Neurosci **10**(9): 627-634.
Kottmann, R. M., C. M. Hogan, R. P. Phipps and P. J. Sime (2009). "Determinants of initiation and progression of idiopathic pulmonary fibrosis." Respirology **14**(7): 917-933.
Kowal, J., G. Arras, M. Colombo, M. Jouve, J. P. Morath, B. Primdal-Bengtson, F. Dingli, D. Loew, M. Tkach and C. Thery (2016). "Proteomic comparison defines novel markers to characterize heterogeneous populations of extracellular vesicle subtypes." Proc Natl Acad Sci U S A **113**(8): E968-977.
Kowal, J., M. Tkach and C. Thery (2014). "Biogenesis and secretion of exosomes." Curr Opin Cell Biol **29**: 116-125.
Kubo, H. (2018). "Extracellular Vesicles in Lung Disease." Chest **153**(1): 210-216.
Kuhn, C. and J. A. McDonald (1991). "The roles of the myofibroblast in idiopathic pulmonary fibrosis. Ultrastructural and immunohistochemical features of sites of active extracellular matrix synthesis." Am J Pathol **138**(5): 1257-1265.
Kulshreshtha, A., T. Ahmad, A. Agrawal and B. Ghosh (2013). "Proinflammatory role of epithelial cell-derived exosomes in allergic airway inflammation." J Allergy Clin Immunol **131**(4): 1194-1203, 1203 e1191-1114.
Lakkaraju, A. K., C. Mary, A. Scherrer, A. E. Johnson and K. Strub (2008). "SRP keeps polypeptides translocation-competent by slowing translation to match limiting ER-targeting sites." Cell **133**(3): 440-451.
Larssen, P., L. Wik, P. Czarnewski, M. Eldh, L. Lof, K. G. Ronquist, L. Dubois, E. Freyhult, C. J. Gallant, J. Oelrich, A. Larsson, G. Ronquist, E. J. Villablanca, U. Landegren, S. Gabrielsson and M. Kamali-Moghaddam (2017). "Tracing Cellular Origin of Human Exosomes Using Multiplex Proximity Extension Assays." Mol Cell Proteomics **16**(8): 1547.
Lehmann, M., H. A. Baarsma and M. Konigshoff (2016). "WNT Signaling in Lung Aging and Disease." Ann Am Thorac Soc **13 Suppl 5**: S411-S416.
Lehmann, M., M. Korfei, K. Mutze, S. Klee, W. Skronska-Wasek, H. N. Alsafadi, C. Ota, R. Costa, H. B. Schiller, M. Lindner, D. E. Wagner, A. Gunther and M. Konigshoff (2017). "Senolytic drugs target alveolar epithelial cell function and attenuate experimental lung fibrosis ex vivo." Eur Respir J **50**(2).
Ley, B. and H. R. Collard (2013). "Epidemiology of idiopathic pulmonary fibrosis." Clin Epidemiol **5**: 483-492.

Li, X. Q., J. T. Liu, L. L. Fan, Y. Liu, L. Cheng, F. Wang, H. Q. Yu, J. Gao, W. Wei, H. Wang and G. P. Sun (2016). "Exosomes derived from gefitinib-treated EGFR-mutant lung cancer cells alter cisplatin sensitivity via up-regulating autophagy." Oncotarget **7**(17): 24585-24595.
Lorena, D., K. Uchio, A. M. Costa and A. Desmouliere (2002). "Normal scarring: importance of myofibroblasts." Wound Repair Regen **10**(2): 86-92.
Lozano, R., M. Naghavi, K. Foreman, S. Lim, K. Shibuya, V. Aboyans, J. Abraham, T. Adair, R. Aggarwal, S. Y. Ahn, M. Alvarado, H. R. Anderson, L. M. Anderson, K. G. Andrews, C. Atkinson, L. M. Baddour, S. Barker-Collo, D. H. Bartels, M. L. Bell, E. J. Benjamin, D. Bennett, K. Bhalla, B. Bikbov, A. Bin Abdulhak, G. Birbeck, F. Blyth, I. Bolliger, S. Boufous, C. Bucello, M. Burch, P. Burney, J. Carapetis, H. Chen, D. Chou, S. S. Chugh, L. E. Coffeng, S. D. Colan, S. Colquhoun, K. E. Colson, J. Condon, M. D. Connor, L. T. Cooper, M. Corriere, M. Cortinovis, K. C. de Vaccaro, W. Couser, B. C. Cowie, M. H. Criqui, M. Cross, K. C. Dabhadkar, N. Dahodwala, D. De Leo, L. Degenhardt, A. Delossantos, J. Denenberg, D. C. Des Jarlais, S. D. Dharmaratne, E. R. Dorsey, T. Driscoll, H. Duber, B. Ebel, P. J. Erwin, P. Espindola, M. Ezzati, V. Feigin, A. D. Flaxman, M. H. Forouzanfar, F. G. Fowkes, R. Franklin, M. Fransen, M. K. Freeman, S. E. Gabriel, E. Gakidou, F. Gaspari, R. F. Gillum, D. Gonzalez-Medina, Y. A. Halasa, D. Haring, J. E. Harrison, R. Havmoeller, R. J. Hay, B. Hoen, P. J. Hotez, D. Hoy, K. H. Jacobsen, S. L. James, R. Jasrasaria, S. Jayaraman, N. Johns, G. Karthikeyan, N. Kassebaum, A. Keren, J. P. Khoo, L. M. Knowlton, O. Kobusingye, A. Koranteng, R. Krishnamurthi, M. Lipnick, S. E. Lipshultz, S. L. Ohno, J. Mabweijano, M. F. MacIntyre, L. Mallinger, L. March, G. B. Marks, R. Marks, A. Matsumori, R. Matzopoulos, B. M. Mayosi, J. H. McAnulty, M. M. McDermott, J. McGrath, G. A. Mensah, T. R. Merriman, C. Michaud, M. Miller, T. R. Miller, C. Mock, A. O. Mocumbi, A. A. Mokdad, A. Moran, K. Mulholland, M. N. Nair, L. Naldi, K. M. Narayan, K. Nasseri, P. Norman, M. O'Donnell, S. B. Omer, K. Ortblad, R. Osborne, D. Ozgediz, B. Pahari, J. D. Pandian, A. P. Rivero, R. P. Padilla, F. Perez-Ruiz, N. Perico, D. Phillips, K. Pierce, C. A. Pope, 3rd, E. Porrini, F. Pourmalek, M. Raju, D. Ranganathan, J. T. Rehm, D. B. Rein, G. Remuzzi, F. P. Rivara, T. Roberts, F. R. De Leon, L. C. Rosenfeld, L. Rushton, R. L. Sacco, J. A. Salomon, U. Sampson, E. Sanman, D. C. Schwebel, M. Segui-Gomez, D. S. Shepard, D. Singh, J. Singleton, K. Sliwa, E. Smith, A. Steer, J. A. Taylor, B. Thomas, I. M. Tleyjeh, J. A. Towbin, T. Truelsen, E. A. Undurraga, N. Venketasubramanian, L. Vijayakumar, T. Vos, G. R. Wagner, M. Wang, W. Wang, K. Watt, M. A. Weinstock, R. Weintraub, J. D. Wilkinson, A. D. Woolf, S. Wulf, P. H. Yeh, P. Yip, A. Zabetian, Z. J. Zheng, A. D. Lopez, C. J. Murray, M. A. AlMazroa and Z. A. Memish (2012). "Global and regional mortality from 235 causes of death for 20 age groups in 1990 and 2010: a systematic analysis for the Global Burden of Disease Study 2010." Lancet **380**(9859): 2095-2128.
Luga, V., L. Zhang, A. M. Viloria-Petit, A. A. Ogunjimi, M. R. Inanlou, E. Chiu, M. Buchanan, A. N. Hosein, M. Basik and J. L. Wrana (2012). "Exosomes mediate stromal mobilization of autocrine Wnt-PCP signaling in breast cancer cell migration." Cell **151**(7): 1542-1556.
M, H. R., E. Bayraktar, K. H. G, M. F. Abd-Ellah, P. Amero, A. Chavez-Reyes and C. Rodriguez-Aguayo (2017). "Exosomes: From Garbage Bins to Promising Therapeutic Targets." Int J Mol Sci **18**(3).
Magro, C. M., J. Allen, A. Pope-Harman, W. J. Waldman, P. Moh, S. Rothrauff and P. Ross, Jr. (2003). "The role of microvascular injury in the evolution of idiopathic pulmonary fibrosis." Am J Clin Pathol **119**(4): 556-567.
Makiguchi, T., M. Yamada, Y. Yoshioka, H. Sugiura, A. Koarai, S. Chiba, N. Fujino, Y. Tojo, C. Ota, H. Kubo, S. Kobayashi, M. Yanai, S. Shimura, T. Ochiya and M. Ichinose (2016). "Serum extracellular vesicular miR-21-5p is a predictor of the prognosis in idiopathic pulmonary fibrosis." Respir Res **17**(1): 110.
Marmai, C., R. E. Sutherland, K. K. Kim, G. M. Dolganov, X. Fang, S. S. Kim, S. Jiang, J. A. Golden, C. W. Hoopes, M. A. Matthay, H. A. Chapman and P. J. Wolters (2011). "Alveolar epithelial cells express mesenchymal proteins in patients with idiopathic pulmonary fibrosis." Am J Physiol Lung Cell Mol Physiol **301**(1): L71-78.

McBride, J. D., L. Rodriguez-Menocal, W. Guzman, A. Candanedo, M. Garcia-Contreras and E. V. Badiavas (2017). "Bone Marrow Mesenchymal Stem Cell-Derived CD63(+) Exosomes Transport Wnt3a Exteriorly and Enhance Dermal Fibroblast Proliferation, Migration, and Angiogenesis In Vitro." Stem Cells Dev **26**(19): 1384-1398.
Meiners, S., O. Eickelberg and M. Konigshoff (2015). "Hallmarks of the ageing lung." Eur Respir J **45**(3): 807-827.
Menck, K., F. Klemm, J. C. Gross, T. Pukrop, D. Wenzel and C. Binder (2013). "Induction and transport of Wnt 5a during macrophage-induced malignant invasion is mediated by two types of extracellular vesicles." Oncotarget **4**(11): 2057-2066.
Mikels, A. J. and R. Nusse (2006). "Wnts as ligands: processing, secretion and reception." Oncogene **25**(57): 7461-7468.
Mutze, K., S. Vierkotten, J. Milosevic, O. Eickelberg and M. Konigshoff (2015). "Enolase 1 (ENO1) and protein disulfide-isomerase associated 3 (PDIA3) regulate Wnt/beta-catenin-driven trans-differentiation of murine alveolar epithelial cells." Dis Model Mech **8**(8): 877-890.
Nabhan, A. N., D. G. Brownfield, P. B. Harbury, M. A. Krasnow and T. J. Desai (2018). "Single-cell Wnt signaling niches maintain stemness of alveolar type 2 cells." Science **359**(6380): 1118-1123.
Nakatani, Y., K. Masudo, Y. Miyagi, Y. Inayama, N. Kawano, Y. Tanaka, K. Kato, T. Ito, H. Kitamura, Y. Nagashima, S. Yamanaka, N. Nakamura, J. Sano, N. Ogawa, N. Ishiwa, K. Notohara, M. Resl and E. J. Mark (2002). "Aberrant nuclear localization and gene mutation of beta-catenin in low-grade adenocarcinoma of fetal lung type: up-regulation of the Wnt signaling pathway may be a common denominator for the development of tumors that form morules." Mod Pathol **15**(6): 617-624.
Nalysnyk, L., J. Cid-Ruzafa, P. Rotella and D. Esser (2012). "Incidence and prevalence of idiopathic pulmonary fibrosis: review of the literature." Eur Respir Rev **21**(126): 355-361.
Nana-Sinkam, S. P., M. Acunzo, C. M. Croce and K. Wang (2017). "Extracellular Vesicle Biology in the Pathogenesis of Lung Disease." Am J Respir Crit Care Med **196**(12): 1510-1518.
Nathan, S. D., C. Albera, W. Z. Bradford, U. Costabel, I. Glaspole, M. K. Glassberg, D. R. Kardatzke, M. Daigl, K. U. Kirchgaessler, L. H. Lancaster, D. J. Lederer, C. A. Pereira, J. J. Swigris, D. Valeyre and P. W. Noble (2017). "Effect of pirfenidone on mortality: pooled analyses and meta-analyses of clinical trials in idiopathic pulmonary fibrosis." Lancet Respir Med **5**(1): 33-41.
Newman, D. R., W. S. Sills, K. Hanrahan, A. Ziegler, K. M. Tidd, E. Cook and P. L. Sannes (2016). "Expression of WNT5A in Idiopathic Pulmonary Fibrosis and Its Control by TGF-beta and WNT7B in Human Lung Fibroblasts." J Histochem Cytochem **64**(2): 99-111.
Njock, M. S., J. Guiot, M. A. Henket, O. Nivelles, M. Thiry, F. Dequiedt, J. L. Corhay, R. E. Louis and I. Struman (2019). "Sputum exosomes: promising biomarkers for idiopathic pulmonary fibrosis." Thorax **74**(3): 309-312.
Novelli, F., T. Neri, L. Tavanti, C. Armani, C. Noce, F. Falaschi, M. L. Bartoli, F. Martino, A. Palla, A. Celi and P. Paggiaro (2014). "Procoagulant, tissue factor-bearing microparticles in bronchoalveolar lavage of interstitial lung disease patients: an observational study." PLoS One **9**(4): e95013.
Oda, K., K. Yatera, H. Izumi, H. Ishimoto, S. Yamada, H. Nakao, T. Hanaka, T. Ogoshi, S. Noguchi and H. Mukae (2016). "Profibrotic role of WNT10A via TGF-beta signaling in idiopathic pulmonary fibrosis." Respir Res **17**: 39.
Ota, C., J. P. Ng-Blichfeldt, M. Korfei, H. N. Alsafadi, M. Lehmann, W. Skronska-Wasek, M. D. S. M, A. Guenther, D. E. Wagner and M. Konigshoff (2018). "Dynamic expression of HOPX in alveolar epithelial cells reflects injury and repair during the progression of pulmonary fibrosis." Sci Rep **8**(1): 12983.
Pan, B. T. and R. M. Johnstone (1983). "Fate of the transferrin receptor during maturation of sheep reticulocytes in vitro: selective externalization of the receptor." Cell **33**(3): 967-978.
Panakova, D., H. Sprong, E. Marois, C. Thiele and S. Eaton (2005). "Lipoprotein particles are required for Hedgehog and Wingless signalling." Nature **435**(7038): 58-65.

Papiris, S. A., K. Kagouridis, L. Kolilekas, A. I. Papaioannou, A. Roussou, C. Triantafillidou, K. Baou, K. Malagari, S. Argentos, A. Kotanidou, A. Karakatsani and E. D. Manali (2015). "Survival in Idiopathic pulmonary fibrosis acute exacerbations: the non-steroid approach." BMC Pulm Med **15**: 162.
Parimon, T., R. Brauer, S. Y. Schlesinger, T. Xie, D. Jiang, L. Ge, Y. Huang, T. P. Birkland, W. C. Parks, D. M. Habiel, C. M. Hogaboam, S. A. Gharib, N. Deng, Z. Liu and P. Chen (2018). "Syndecan-1 Controls Lung Tumorigenesis by Regulating miRNAs Packaged in Exosomes." Am J Pathol **188**(4): 1094-1103.
Port, F. and K. Basler (2010). "Wnt trafficking: new insights into Wnt maturation, secretion and spreading." Traffic **11**(10): 1265-1271.
Qazi, K. R., P. Torregrosa Paredes, B. Dahlberg, J. Grunewald, A. Eklund and S. Gabrielsson (2010). "Proinflammatory exosomes in bronchoalveolar lavage fluid of patients with sarcoidosis." Thorax **65**(11): 1016-1024.
Raghu, G. (2017). "Pharmacotherapy for idiopathic pulmonary fibrosis: current landscape and future potential." Eur Respir Rev **26**(145).
Raghu, G., H. R. Collard, J. J. Egan, F. J. Martinez, J. Behr, K. K. Brown, T. V. Colby, J. F. Cordier, K. R. Flaherty, J. A. Lasky, D. A. Lynch, J. H. Ryu, J. J. Swigris, A. U. Wells, J. Ancochea, D. Bouros, C. Carvalho, U. Costabel, M. Ebina, D. M. Hansell, T. Johkoh, D. S. Kim, T. E. King, Jr., Y. Kondoh, J. Myers, N. L. Muller, A. G. Nicholson, L. Richeldi, M. Selman, R. F. Dudden, B. S. Griss, S. L. Protzko, H. J. Schunemann and A. E. J. A. C. o. I. P. Fibrosis (2011). "An official ATS/ERS/JRS/ALAT statement: idiopathic pulmonary fibrosis: evidence-based guidelines for diagnosis and management." Am J Respir Crit Care Med **183**(6): 788-824.
Raghu, G., M. Remy-Jardin, J. M. Myers, L. Richeldi and K. C. Wilson (2019). "The 2018 Diagnosis of IPF Guidelines: Surgical Lung Biopsy in Probable UIP is Not Mandatory." Am J Respir Crit Care Med.
Rahman, M. A., J. F. Barger, F. Lovat, M. Gao, G. A. Otterson and P. Nana-Sinkam (2016). "Lung cancer exosomes as drivers of epithelial mesenchymal transition." Oncotarget **7**(34): 54852-54866.
Raposo, G., H. W. Nijman, W. Stoorvogel, R. Liejendekker, C. V. Harding, C. J. Melief and H. J. Geuze (1996). "B lymphocytes secrete antigen-presenting vesicles." J Exp Med **183**(3): 1161-1172.
Ratajczak, J., K. Miekus, M. Kucia, J. Zhang, R. Reca, P. Dvorak and M. Z. Ratajczak (2006). "Embryonic stem cell-derived microvesicles reprogram hematopoietic progenitors: evidence for horizontal transfer of mRNA and protein delivery." Leukemia **20**(5): 847-856.
Raymond, M., T. Marchbank, M. P. Moyer, R. J. Playford, I. R. Sanderson and L. Kruidenier (2012). "IL-1beta stimulation of CCD-18co myofibroblasts enhances repair of epithelial monolayers through Wnt-5a." Am J Physiol Gastrointest Liver Physiol **303**(11): G1270-1278.
Routledge, D. and S. Scholpp (2019). "Mechanisms of intercellular Wnt transport." Development **146**(10).
Sauleda, J., B. Nunez, E. Sala and J. B. Soriano (2018). "Idiopathic Pulmonary Fibrosis: Epidemiology, Natural History, Phenotypes." Med Sci (Basel) **6**(4).
Schafer, M. J., T. A. White, K. Iijima, A. J. Haak, G. Ligresti, E. J. Atkinson, A. L. Oberg, J. Birch, H. Salmonowicz, Y. Zhu, D. L. Mazula, R. W. Brooks, H. Fuhrmann-Stroissnigg, T. Pirtskhalava, Y. S. Prakash, T. Tchkonia, P. D. Robbins, M. C. Aubry, J. F. Passos, J. L. Kirkland, D. J. Tschumperlin, H. Kita and N. K. LeBrasseur (2017). "Cellular senescence mediates fibrotic pulmonary disease." Nat Commun **8**: 14532.
Schneider, D. J., J. M. Speth and M. Peters-Golden (2016). "Signed, Sealed, Delivered: Microenvironmental Modulation of Extracellular Vesicle-Dependent Immunoregulation in the Lung." Front Cell Dev Biol **4**: 94.
Selman, M. and A. Pardo (2002). "Idiopathic pulmonary fibrosis: an epithelial/fibroblastic cross-talk disorder." Respir Res **3**: 3.

Selman, M., A. Pardo and N. Kaminski (2008). "Idiopathic pulmonary fibrosis: aberrant recapitulation of developmental programs?" PLoS Med **5**(3): e62.
Spagnolo, P., J. Grunewald and R. M. du Bois (2014). "Genetic determinants of pulmonary fibrosis: evolving concepts." Lancet Respir Med **2**(5): 416-428.
Speth, J. M., E. Bourdonnay, L. R. Penke, P. Mancuso, B. B. Moore, J. B. Weinberg and M. Peters-Golden (2016). "Alveolar Epithelial Cell-Derived Prostaglandin E2 Serves as a Request Signal for Macrophage Secretion of Suppressor of Cytokine Signaling 3 during Innate Inflammation." J Immunol **196**(12): 5112-5120.
Staab-Weijnitz, C. A., I. E. Fernandez, L. Knuppel, J. Maul, K. Heinzelmann, B. M. Juan-Guardela, E. Hennen, G. Preissler, H. Winter, C. Neurohr, R. Hatz, M. Lindner, J. Behr, N. Kaminski and O. Eickelberg (2015). "FK506-Binding Protein 10, a Potential Novel Drug Target for Idiopathic Pulmonary Fibrosis." Am J Respir Crit Care Med **192**(4): 455-467.
Strieter, R. M. and B. Mehrad (2009). "New mechanisms of pulmonary fibrosis." Chest **136**(5): 1364-1370.
Takahashi, T., S. Kobayashi, N. Fujino, T. Suzuki, C. Ota, M. He, M. Yamada, S. Suzuki, M. Yanai, S. Kurosawa, M. Yamaya and H. Kubo (2012). "Increased circulating endothelial microparticles in COPD patients: a potential biomarker for COPD exacerbation susceptibility." Thorax **67**(12): 1067-1074.
Tanaka, K., K. Okabayashi, M. Asashima, N. Perrimon and T. Kadowaki (2000). "The evolutionarily conserved porcupine gene family is involved in the processing of the Wnt family." Eur J Biochem **267**(13): 4300-4311.
Thery, C., K. W. Witwer, E. Aikawa, M. J. Alcaraz, J. D. Anderson, R. Andriantsitohaina, A. Antoniou, T. Arab, F. Archer, G. K. Atkin-Smith, D. C. Ayre, J. M. Bach, D. Bachurski, H. Baharvand, L. Balaj, S. Baldacchino, N. N. Bauer, A. A. Baxter, M. Bebawy, C. Beckham, A. Bedina Zavec, A. Benmoussa, A. C. Berardi, P. Bergese, E. Bielska, C. Blenkiron, S. Bobis-Wozowicz, E. Boilard, W. Boireau, A. Bongiovanni, F. E. Borras, S. Bosch, C. M. Boulanger, X. Breakefield, A. M. Breglio, M. A. Brennan, D. R. Brigstock, A. Brisson, M. L. Broekman, J. F. Bromberg, P. Bryl-Gorecka, S. Buch, A. H. Buck, D. Burger, S. Busatto, D. Buschmann, B. Bussolati, E. I. Buzas, J. B. Byrd, G. Camussi, D. R. Carter, S. Caruso, L. W. Chamley, Y. T. Chang, C. Chen, S. Chen, L. Cheng, A. R. Chin, A. Clayton, S. P. Clerici, A. Cocks, E. Cocucci, R. J. Coffey, A. Cordeiro-da-Silva, Y. Couch, F. A. Coumans, B. Coyle, R. Crescitelli, M. F. Criado, C. D'Souza-Schorey, S. Das, A. Datta Chaudhuri, P. de Candia, E. F. De Santana, O. De Wever, H. A. Del Portillo, T. Demaret, S. Deville, A. Devitt, B. Dhondt, D. Di Vizio, L. C. Dieterich, V. Dolo, A. P. Dominguez Rubio, M. Dominici, M. R. Dourado, T. A. Driedonks, F. V. Duarte, H. M. Duncan, R. M. Eichenberger, K. Ekstrom, S. El Andaloussi, C. Elie-Caille, U. Erdbrugger, J. M. Falcon-Perez, F. Fatima, J. E. Fish, M. Flores-Bellver, A. Forsonits, A. Frelet-Barrand, F. Fricke, G. Fuhrmann, S. Gabrielsson, A. Gamez-Valero, C. Gardiner, K. Gartner, R. Gaudin, Y. S. Gho, B. Giebel, C. Gilbert, M. Gimona, I. Giusti, D. C. Goberdhan, A. Gorgens, S. M. Gorski, D. W. Greening, J. C. Gross, A. Gualerzi, G. N. Gupta, D. Gustafson, A. Handberg, R. A. Haraszti, P. Harrison, H. Hegyesi, A. Hendrix, A. F. Hill, F. H. Hochberg, K. F. Hoffmann, B. Holder, H. Holthofer, B. Hosseinkhani, G. Hu, Y. Huang, V. Huber, S. Hunt, A. G. Ibrahim, T. Ikezu, J. M. Inal, M. Isin, A. Ivanova, H. K. Jackson, S. Jacobsen, S. M. Jay, M. Jayachandran, G. Jenster, L. Jiang, S. M. Johnson, J. C. Jones, A. Jong, T. Jovanovic-Talisman, S. Jung, R. Kalluri, S. I. Kano, S. Kaur, Y. Kawamura, E. T. Keller, D. Khamari, E. Khomyakova, A. Khvorova, P. Kierulf, K. P. Kim, T. Kislinger, M. Klingeborn, D. J. Klinke, 2nd, M. Kornek, M. M. Kosanovic, A. F. Kovacs, E. M. Kramer-Albers, S. Krasemann, M. Krause, I. V. Kurochkin, G. D. Kusuma, S. Kuypers, S. Laitinen, S. M. Langevin, L. R. Languino, J. Lannigan, C. Lasser, L. C. Laurent, G. Lavieu, E. Lazaro-Ibanez, S. Le Lay, M. S. Lee, Y. X. F. Lee, D. S. Lemos, M. Lenassi, A. Leszczynska, I. T. Li, K. Liao, S. F. Libregts, E. Ligeti, R. Lim, S. K. Lim, A. Line, K. Linnemannstons, A. Llorente, C. A. Lombard, M. J. Lorenowicz, A. M. Lorincz, J. Lotvall, J. Lovett, M. C. Lowry, X. Loyer, Q. Lu, B. Lukomska, T. R. Lunavat, S. L. Maas, H. Malhi, A. Marcilla, J. Mariani, J. Mariscal, E. S. Martens-Uzunova, L. Martin-Jaular, M. C. Martinez, V. R. Martins, M. Mathieu, S. Mathivanan, M. Maugeri, L. K.

McGinnis, M. J. McVey, D. G. Meckes, Jr., K. L. Meehan, I. Mertens, V. R. Minciacchi, A. Moller, M. Moller Jorgensen, A. Morales-Kastresana, J. Morhayim, F. Mullier, M. Muraca, L. Musante, V. Mussack, D. C. Muth, K. H. Myburgh, T. Najrana, M. Nawaz, I. Nazarenko, P. Nejsum, C. Neri, T. Neri, R. Nieuwland, L. Nimrichter, J. P. Nolan, E. N. Nolte-'t Hoen, N. Noren Hooten, L. O'Driscoll, T. O'Grady, A. O'Loghlen, T. Ochiya, M. Olivier, A. Ortiz, L. A. Ortiz, X. Osteikoetxea, O. Ostergaard, M. Ostrowski, J. Park, D. M. Pegtel, H. Peinado, F. Perut, M. W. Pfaffl, D. G. Phinney, B. C. Pieters, R. C. Pink, D. S. Pisetsky, E. Pogge von Strandmann, I. Polakovicova, I. K. Poon, B. H. Powell, I. Prada, L. Pulliam, P. Quesenberry, A. Radeghieri, R. L. Raffai, S. Raimondo, J. Rak, M. I. Ramirez, G. Raposo, M. S. Rayyan, N. Regev-Rudzki, F. L. Ricklefs, P. D. Robbins, D. D. Roberts, S. C. Rodrigues, E. Rohde, S. Rome, K. M. Rouschop, A. Rughetti, A. E. Russell, P. Saa, S. Sahoo, E. Salas-Huenuleo, C. Sanchez, J. A. Saugstad, M. J. Saul, R. M. Schiffelers, R. Schneider, T. H. Schoyen, A. Scott, E. Shahaj, S. Sharma, O. Shatnyeva, F. Shekari, G. V. Shelke, A. K. Shetty, K. Shiba, P. R. Siljander, A. M. Silva, A. Skowronek, O. L. Snyder, 2nd, R. P. Soares, B. W. Sodar, C. Soekmadji, J. Sotillo, P. D. Stahl, W. Stoorvogel, S. L. Stott, E. F. Strasser, S. Swift, H. Tahara, M. Tewari, K. Timms, S. Tiwari, R. Tixeira, M. Tkach, W. S. Toh, R. Tomasini, A. C. Torrecilhas, J. P. Tosar, V. Toxavidis, L. Urbanelli, P. Vader, B. W. van Balkom, S. G. van der Grein, J. Van Deun, M. J. van Herwijnen, K. Van Keuren-Jensen, G. van Niel, M. E. van Royen, A. J. van Wijnen, M. H. Vasconcelos, I. J. Vechetti, Jr., T. D. Veit, L. J. Vella, E. Velot, F. J. Verweij, B. Vestad, J. L. Vinas, T. Visnovitz, K. V. Vukman, J. Wahlgren, D. C. Watson, M. H. Wauben, A. Weaver, J. P. Webber, V. Weber, A. M. Wehman, D. J. Weiss, J. A. Welsh, S. Wendt, A. M. Wheelock, Z. Wiener, L. Witte, J. Wolfram, A. Xagorari, P. Xander, J. Xu, X. Yan, M. Yanez-Mo, H. Yin, Y. Yuana, V. Zappulli, J. Zarubova, V. Zekas, J. Y. Zhang, Z. Zhao, L. Zheng, A. R. Zheutlin, A. M. Zickler, P. Zimmermann, A. M. Zivkovic, D. Zocco and E. K. Zuba-Surma (2018). "Minimal information for studies of extracellular vesicles 2018 (MISEV2018): a position statement of the International Society for Extracellular Vesicles and update of the MISEV2014 guidelines." J Extracell Vesicles **7**(1): 1535750.

Torregrosa Paredes, P., J. Esser, C. Admyre, M. Nord, Q. K. Rahman, A. Lukic, O. Radmark, R. Gronneberg, J. Grunewald, A. Eklund, A. Scheynius and S. Gabrielsson (2012). "Bronchoalveolar lavage fluid exosomes contribute to cytokine and leukotriene production in allergic asthma." Allergy **67**(7): 911-919.

Uhl, F. E., S. Vierkotten, D. E. Wagner, G. Burgstaller, R. Costa, I. Koch, M. Lindner, S. Meiners, O. Eickelberg and M. Konigshoff (2015). "Preclinical validation and imaging of Wnt-induced repair in human 3D lung tissue cultures." Eur Respir J **46**(4): 1150-1166.

Valadi, H., K. Ekstrom, A. Bossios, M. Sjostrand, J. J. Lee and J. O. Lotvall (2007). "Exosome-mediated transfer of mRNAs and microRNAs is a novel mechanism of genetic exchange between cells." Nat Cell Biol **9**(6): 654-659.

Vuga, L. J., A. Ben-Yehudah, E. Kovkarova-Naumovski, T. Oriss, K. F. Gibson, C. Feghali-Bostwick and N. Kaminski (2009). "WNT5A is a regulator of fibroblast proliferation and resistance to apoptosis." Am J Respir Cell Mol Biol **41**(5): 583-589.

Waster, P., I. Rosdahl, B. F. Gilmore and O. Seifert (2011). "Ultraviolet exposure of melanoma cells induces fibroblast activation protein-alpha in fibroblasts: Implications for melanoma invasion." Int J Oncol **39**(1): 193-202.

Webber, J. P., L. K. Spary, A. J. Sanders, R. Chowdhury, W. G. Jiang, R. Steadman, J. Wymant, A. T. Jones, H. Kynaston, M. D. Mason, Z. Tabi and A. Clayton (2015). "Differentiation of tumour-promoting stromal myofibroblasts by cancer exosomes." Oncogene **34**(3): 290-302.

White, E. S., M. H. Lazar and V. J. Thannickal (2003). "Pathogenetic mechanisms in usual interstitial pneumonia/idiopathic pulmonary fibrosis." J Pathol **201**(3): 343-354.

Willert, K. and R. Nusse (2012). "Wnt proteins." Cold Spring Harb Perspect Biol **4**(9): a007864.

Williamson, J. D., L. R. Sadofsky and S. P. Hart (2015). "The pathogenesis of bleomycin-induced lung injury in animals and its applicability to human idiopathic pulmonary fibrosis." Exp Lung Res **41**(2): 57-73.

Wolf, P. (1967). "The nature and significance of platelet products in human plasma." Br J Haematol **13**(3): 269-288.
Wolters, P. J., H. R. Collard and K. D. Jones (2014). "Pathogenesis of idiopathic pulmonary fibrosis." Annu Rev Pathol **9**: 157-179.
Wu, F., Z. Yin, L. Yang, J. Fan, J. Xu, Y. Jin, J. Yu, D. Zhang and G. Yang (2019). "Smoking Induced Extracellular Vesicles Release and Their Distinct Properties in Non-Small Cell Lung Cancer." J Cancer **10**(15): 3435-3443.
Yanez-Mo, M., P. R. Siljander, Z. Andreu, A. B. Zavec, F. E. Borras, E. I. Buzas, K. Buzas, E. Casal, F. Cappello, J. Carvalho, E. Colas, A. Cordeiro-da Silva, S. Fais, J. M. Falcon-Perez, I. M. Ghobrial, B. Giebel, M. Gimona, M. Graner, I. Gursel, M. Gursel, N. H. Heegaard, A. Hendrix, P. Kierulf, K. Kokubun, M. Kosanovic, V. Kralj-Iglic, E. M. Kramer-Albers, S. Laitinen, C. Lasser, T. Lener, E. Ligeti, A. Line, G. Lipps, A. Llorente, J. Lotvall, M. Mancek-Keber, A. Marcilla, M. Mittelbrunn, I. Nazarenko, E. N. Nolte-'t Hoen, T. A. Nyman, L. O'Driscoll, M. Olivan, C. Oliveira, E. Pallinger, H. A. Del Portillo, J. Reventos, M. Rigau, E. Rohde, M. Sammar, F. Sanchez-Madrid, N. Santarem, K. Schallmoser, M. S. Ostenfeld, W. Stoorvogel, R. Stukelj, S. G. Van der Grein, M. H. Vasconcelos, M. H. Wauben and O. De Wever (2015). "Biological properties of extracellular vesicles and their physiological functions." J Extracell Vesicles **4**: 27066.
Yoshioka, Y., Y. Konishi, N. Kosaka, T. Katsuda, T. Kato and T. Ochiya (2013). "Comparative marker analysis of extracellular vesicles in different human cancer types." J Extracell Vesicles **2**.
Zheng, H., Y. Zhan, S. Liu, J. Lu, J. Luo, J. Feng and S. Fan (2018). "The roles of tumor-derived exosomes in non-small cell lung cancer and their clinical implications." J Exp Clin Cancer Res **37**(1): 226.
Zuo, G. W., C. D. Kohls, B. C. He, L. Chen, W. Zhang, Q. Shi, B. Q. Zhang, Q. Kang, J. Luo, X. Luo, E. R. Wagner, S. H. Kim, F. Restegar, R. C. Haydon, Z. L. Deng, H. H. Luu, T. C. He and Q. Luo (2010). "The CCN proteins: important signaling mediators in stem cell differentiation and tumorigenesis." Histol Histopathol **25**(6): 795-806.

7. ACKNOWLEGMENTS

I would like to thank my parents, Carmen and Angel, in the first place for their love and constant support during my PhD and my whole carrier. I am also very thankful to my husband, Vlady, for following and sharing with me this amazing experience in Munich as well as cheering me every day. I want to thank my mentor, Melanie Königshoff for her leadership, support and enthusiasm on this project and for encourage me to present this topic worldwide. This work would not have been possible without the unstoppable support, collaboration, and fruitful discussions of the MK lab members, specially Mareike Lehmann for her mentoring and guidance through my PhD, and for her advice and friendship. Special thanks go to Sarah Vierkotten for having the idea of introducing me in the amazing field of extracellular vesicles and troubleshooting the start-up of the techniques. I am grateful to my colleagues and friends Carolina, Flavia, Nina, Rita, Raphael, Stephan, Martina and Wiola, for all the fun and for sharing with me both good and tough moments. I will never forget this experience, so thanks everybody that have made it possible, it was such a ride and so much fun and now, finally, I am glad that it's over so I can call myself Dr. Aina Martin-Medina!

Affidavit

Martin-Medina, Aina

Surname, first name

Street

Zip code, town

Country

I hereby declare, that the submitted thesis entitled

The role of WNT ligand secretion in idiopathic pulmonary fibrosis

is my own work. I have only used the sources indicated and have not made unauthorised use of services of a third party. Where the work of others has been quoted or reproduced, the source is always given.

I further declare that the submitted thesis or parts thereof have not been presented as part of an examination degree to any other university.

Palma, 11.09.2019

Place, date

Aina Martin-Medina

Signature doctoral candidate

LMU LUDWIG-MAXIMILIANS-UNIVERSITÄT MÜNCHEN

Dean's Office
Medical Faculty

MMRS

Confirmation of congruency between printed and electronic version of the doctoral thesis

Martin-Medina, Aina

Surname, first name

Street

Zip code, town

Country

I hereby declare that the electronic version of the submitted thesis, entitled

The role of WNT ligand secretion in idiopathic pulmonary fibrosis

is congruent with the printed version both in content and format.

Palma, 11.09.2019

Place, date

Aina Martin-Medina

Signature doctoral candidate

LIST OF PUBLICATIONS

1. Increased extracellular vesicles mediate WNT5A signaling in idiopathic pulmonary fibrosis. *Am J Respir Crit Care Med. 2018 Jul 25. doi: 10.1164/rccm.201708-1580OC*
Martin-Medina A, Lehmann M, Herman S, Burgury O, Baarsma HA, Wagner DE, De Santis M, Ciolek F, Hofer T, Frankenberger M, Aichler M, Lidner M, Gesierich W, Günther A, Walch A, Behr J, Königshoff M.